AVANCES EN SISTEMAS INTERACTIVOS PARA PERSONAS CON PARÁLISIS CEREBRAL

Marc Comí Bonachí

UNIVERSITAT ROVIRA i VIRGILI

Biobased Polyurethanes with Tunable Properties through Covalent and Non-Covalent Approaches

MARC COMÍ BONACHÍ

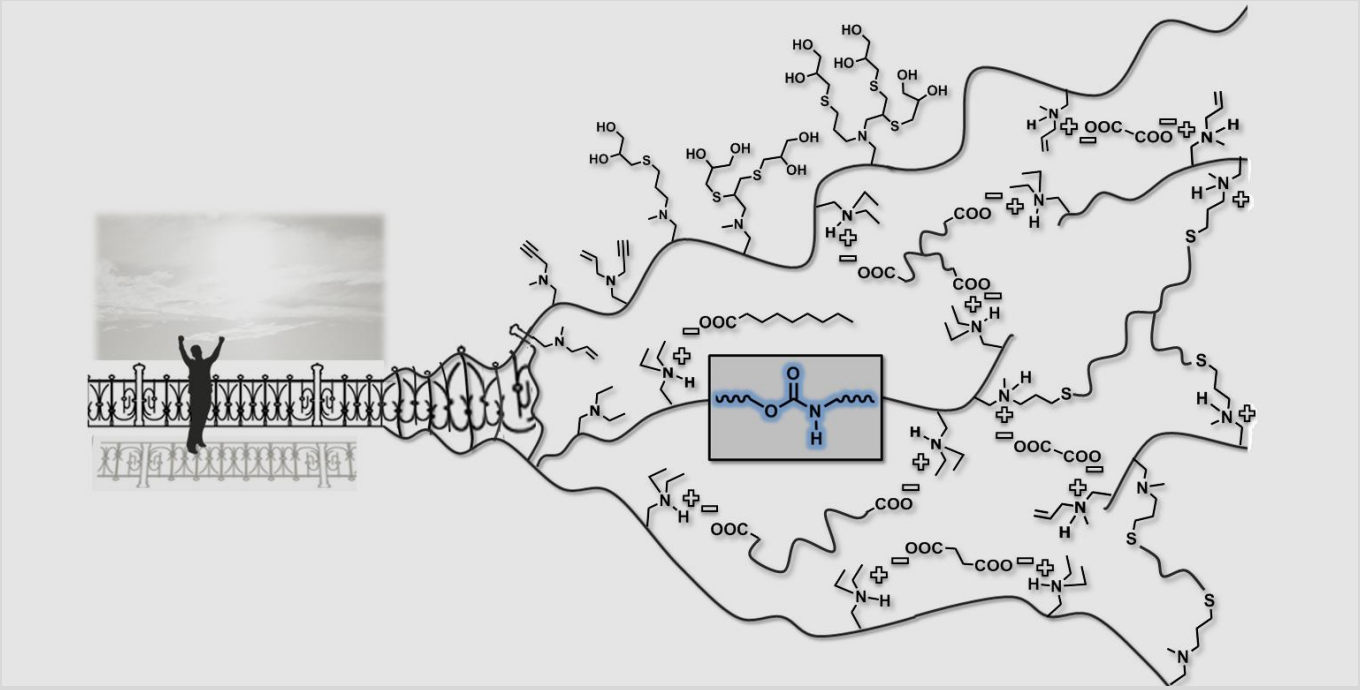

DOCTORAL THESIS
2017

Marc Comí Bonachí

Biobased polyurethanes with tunable properties through covalent and non-covalent approaches

DOCTORAL THESIS

Supervised by

Dra. Virginia Cádiz and Dr. Gerard Lligadas

Departament de Química Analítica i Química Orgànica

UNIVERSITAT ROVIRA i VIRGILI

Tarragona
2017

UNIVERSITAT ROVIRA I VIRGILI
AVANCES EN SISTEMAS INTERACTIVOS PARA PERSONAS CON PARÁLISIS CEREBRAL
Marc Comí Bonachí

UNIVERSITAT ROVIRA i VIRGILI

Departament de Química Analítica
i Química Orgànica
c/ Marcel·li Domingo, 1
Campus Sescelades
43007, Tarragona

Virginia Cádiz Deleito, Catedràtica d'Universitat, i Gerard Lligadas Puig, Professor Agregat, ambdós del Departament de Química Analítica i Química Orgànica de la Universitat Rovira i Virgili,

Fem constar:

Que aquest treball, titulat "Biobased polyurethanes with tunable properties through covalent and non-covalent approaches", que presenta Marc Comí Bonachí per a l'obtenció del títol de Doctor, ha estat realitzat sota la nostra direcció en el Departament de Química Analítica i Química Orgànica de la Universitat Rovira i Virgili.

Tarragona, 3 de març de 2017

El/s director/s de la tesi doctoral

V. Cádiz

Dra. Virginia Cádiz

Dr. Gerard Lligadas

Abstract

This Thesis is addressed to the development of side-chain functionalized polyurethanes (FPUs), with enhanced properties, made from fatty acid-based functional diols and two different diisocyanates; isophorone diisocyanate (IPDI) and hexamethylene diisocyanate (HDI). The novel FPUs present tertiary amine and alkyl, allyl, propargyl moieties or the combination of these, as side-chain positions groups. The FPUs were further modified via two post-polymerization mechanisms based on covalent or non-covalent bonds.

In the first case, photoinitiated thiol-ene/yne coupling reaction between allyl, propargyl-functionalized PUs (based on IPDI) and thioglycerol was carried out. Obtained hydroxyl-PUs exhibit different thermal and mechanical properties in comparison with precursor PUs. Moreover, the incorporation of hydroxyl groups lead to PUs with enhanced hydrophilicity. Alternatively, the FPU (based on IPDI) containing only tertiary amine pendant group was mixed with different carboxylic acids in an acid-base reaction. Supramolecular ionic PUs were characterized by spectroscopic tools to verify the presence of ionic hydrogen bond as ionic interaction. Correlation between structure and thermal and mechanical properties was demonstrated. Samples show rapid thermal reversibility and recyclability thanks to the reversible bonds.

In addition, elastomeric supramolecular PUs networks were prepared from HDI and aminodiol. The resulting materials exhibit some promising adaptive material properties such as effective energy dissipation upon deformation through unzipping the ionic hydrogen bonding network, combined with good shape-regeneration property and recycling/reshaping capability arising from their recoverable nature. More importantly, the resulting biobased elastomers possess the inherent self-healing ability, which can be seen as an upgrade of their sustainability.

A novel shape-memory polyurethane network is constructed by the thiol-ene functionalized polyurethane *via* dynamic ionic hydrogen bonds and covalent cross-links. By varying the covalent cross-linking density, the mechanical properties and the stimuli-responsive behaviour can be systematically tuned. This synthesis demonstrates a simple and effective pathway to fabricate multifunctional polyurethanes with desired functions, and the strategy can also be extended to exploring other types of dynamic non-covalent or covalent interactions to access a new range of multi-responsive properties.

Key words: bio-based polyurethanes, fatty acid, tertiary amine-containing diols monomers, side-chain functionalization, supramolecular interactions, hydrophilicity, self-healing properties, shape-memory properties.

Table of content

Chapter 1

Aim, Outline and Structure

UNIVERSITAT ROVIRA I VIRGILI
AVANCES EN SISTEMAS INTERACTIVOS PARA PERSONAS CON PARÁLISIS CEREBRAL
Marc Comí Bonachí

1.1. Aim and outline

In this Thesis, the potential use of vegetable oil-based monomers to prepare polyurethanes (PUs) is highlighted. PUs are extremely versatile materials allowing a huge variety of applications in automotive, building and construction, flooring and packaging or in the medical field. They are synthesized from polyol and poly(isocyanate) reactants producing carbamate (urethane) bonds. It is worth noting that most of PUs come from the petroleum-based feedstocks, therefore, there is a growing interest in the use of natural reagents to replace petroleum based PUs. The preparation of PUs from renewable feedstock is currently receiving increasing attention in the industry and academia. In point of fact, there are more than 20 different polyols which are currently available commercially, and all of them coming from vegetable oils.

For many high-tech applications PU materials should bear functionalities enabling tuning final material properties. The functionalization of PUs can be accomplished by introducing functional groups into oligodiols and further polymerization, post-polymerization modification, or by combining both strategies. Although the former approach is more experimentally feasible for the ease of incorporating functional groups into low or medium molecular weight oligodiol, in practice the functionalization is achieved by a variety of methods including the synthesis of polyols bearing reactive pendant groups to prepare novel comb-type, grafted structural functional polymers through post-modification. So far, there have been a few reports focusing on the preparation of novel functional bio-based PUs bearing reactive pendant groups.

Over the past few years, several approaches have been used to enhance the properties of PUs, in this way the synthesis of supramolecular PUs (SPUs) can receive relevant attention. These reversible behaviours endow supramolecular systems with versatile functions, such as facile processing/recycling, self-healing, shape memory and high stimuli-response. Several features make supramolecular chemistry particularly attractive when comes to self-healing: reversibility and speed, directionality, and sensitivity. In contrast to covalent bonding, these networks can be remodelled rapidly

and reversibly form from fluid-like to solid-like states. The possibility to repeatedly conduct the healing process even after multiple damages have occurred is the most important benefit of supramolecular self-healing materials. Supramolecular shape-memory PUs based on thermal-reversible non-covalent bonding recently have been another new kind of shape-memory polymers. In these systems, the reversible non-covalent interactions are used to stabilize mechanically strain stated in polymer elastomers; and shape recovery is achieved upon heating due to the dissociation of non-covalent bonds.

This Thesis is specifically addressed to prepare renewable PUs from castor oil and to develop functionalized monomer and polymer synthesis strategies to introduce different reactive side-chain points. Further the post-polymerization modification by different reactivity strategies result in, PUs systems with new properties. To achieve this goal, the experimental work was focused in 10-undecen-1-ol derived from the catalytic reduction of the 10-undedenoic carboxylic acid group, which is obtained from the pyrolysis of castor oil.

The specific objectives are:

- To prepare renewable monomers from castor oil derivatives containing different side-chain functional groups inert in front to isocyanate groups.
- To develop new side-chain functionalized PUs with isophorone (IPDI) and hexamethylene diisocyanate (HDI) respectively.
- To carry out the post-polymerization modification in mild conditions by using thiol-ene/yne coupling reactions.
- To prepare a family of supramolecular side-chain PUs using a PU which contains tertiary amine as pendant group and carboxylic acids.
- To combine the post-polymerization modification by photoinitiation thiol-ene/yne coupling reactions and supramolecular chemistry to synthetize supramolecular PU networks
- To analyse the new acquired properties of the modified PUs.

1.2. Structure of the Thesis

The work presented in this Thesis consists of eight chapters including aim and outline, experimental part and conclusions.

Chapter 1 is a general introduction of the Thesis which includes its aims and organization.

Chapter 2 is an introduction which reviews some aspects of polymers from renewable resources, especially from vegetable oils, such as their main synthetic methods, types and applications, with emphasis on the polymer functionalization. PUs partially synthesized from vegetable oils are contemplated together with the functionalized PUs.

In the following chapters, relevant aspects in the synthesis of functionalized PUs from vegetable oils, using covalent and non-covalent PU modifications are studied, and the new properties that have these obtained PUs. The chapters 3, 4, 5 and 6 describe each one of studies in chronologic order taking advantage of previous chapter's synthesis or results.

Chapter 3 explores the feasibility of synthesizing monomers with alkene/yne pendant groups derived from 10-undecen-1-ol and subsequently polymerization with IPDI to obtain alkene- alkyne side-chain PUs. These functionalized PUs have been further modified with thioglycerol via thiol-ene/yne coupling reaction resulting hydrophilic PUs. Thermal and mechanical properties are evaluated.

In **Chapter 4** we aim at exploiting the potential of supramolecular chemistry in the synthesis of new PUs with supramolecular interactions based on fatty acid derivatives. The tertiary amine pendant group of PU has been used in the acid-base reaction with different carboxylic acids. Correlation between chemical structure and physical properties of the obtained PUs with ionic interactions is analyzed.

Taking advantage of the previously synthesized supramolecular PUs, our aim in **Chapter 5** was to use the same strategy to prepare dynamic ionic PU networks. The chapter describes the preparation of new elastomeric PUs interpenetrating with di- and triacids by ionic hydrogen bonds. Mechanical properties of the obtained networks have thoroughly been analyzed. In addition, the potential application of the resulting materials as self-repairing materials is studied

Chapter 6 deals with the modification of PUs by introduction of two different groups by orthogonal post-polymerization modification process. Thus, the synthesis of ionic-covalent PU networks which present covalent and non-covalent modifications is described. Shape memory properties to develop materials with new potential applications are evaluated.

In **Chapter 7** collects the experimental part of this Thesis including raw materials, chemical methodologies and instrumentation.

Finally, **Chapter 8** presents the conclusions drawn from the results obtained in this Thesis.

Chapter 2

Introduction

Renewable resources

Polymers from natural resources

Vegetable oils

Polyurethanes from vegetable oils

Polyurethanes functionalization

UNIVERSITAT ROVIRA I VIRGILI
AVANCES EN SISTEMAS INTERACTIVOS PARA PERSONAS CON PARÁLISIS CEREBRAL
Marc Comí Bonachí

2.1. Renewable resources

The world's human population has increased near fourfold in the past 100 years, it is projected to increase from 9,2 billion by 2050. The median age of the world's population increases from 26.6 years in 2000 to 37.3 years in 2050. In 1960, roughly three billion people inhabited the planet; some 50 years later, in 2016, it was seven billion - with almost one billion people being added in the last decade 2005-15. This dramatically dates indicate that the Earth will suffer overpopulation.[1-3]

The main problem associated with overpopulation is the increased demand for natural resources faster than the rate of regeneration. In this case non-renewable resources, either form slowly or do not naturally form in the environment, actually naturally depletes and some cannot be recycled. Fossil fuels are created by the decomposition of dead plant and animal life that existed in the Earth millions of years ago.

The simple fact that it takes millions of years for fossil fuels to accumulate while the deposits are extracted rapidly, making it impossible for the rate of creation to keep up with the rate of extraction.[1] More generally, if the extraction rate is faster than replenishment rate the resource will be finite in the sense that it will eventually be depleted.[4,5]

The fossil fuels include petroleum, coal and natural gas and they represent more than 75% of resources were consumed by human are shown in Figure 2.1. In fact, nowadays the whole world is dependent on fossil fuels to fulfil their daily energy needs and a wide range of industrial materials such as solvents, fuels, synthetic fibers, and chemical products are being manufactured from petroleum resources.[6]

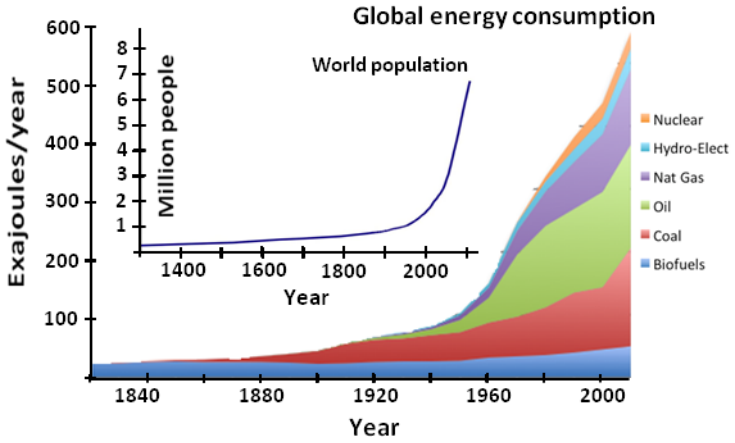

Figure 2.1. Graphic of world population and global energy consumption.

The utilization of renewable resources in energy and material applications is receiving increasing attentions in both industrial and academic settings, due to concerns regarding environmental sustainability.[7] In the last 50 years, the global energy demand has tripled due to the number of developing countries and innovations in technology. It is projected to triple again over the next 30 years. In Europe, many in such developing areas recognize that the need for renewable energy sources, as the present course of energy usage cannot be sustained indefinitely.

The demand for polymer is driven by growth in end use markets, such as packaging, automotive, infrastructure, transport rails, and telecommunication mainly from emerging economies. Polymers are continuously substituting metals, glass, paper, and other traditional materials in various applications due to its lightweight and strength and the design flexibility they offer brand owners along with low-cost. Polymers segment is expected to witness the highest growth over the next five years, increasing application of engineered plastics in various fields such as construction, automotive, and industrial manufacturing equipment.

2.2. Polymers from renewable resources

The polymer revolution was indeed one of the most significant feats of the petrochemical boom. Nowadays, most commercially available polymers are derived from non-renewable resources and account worldwide for approximately 7% of all oil and gas used.[8] Nature offers an abundance of opportunities for designing novel monomers and shaping structural and functional polymers in its wide variety of raw materials. Presently, their relative use for synthesis of monomers and polymers compared to petrochemicals is small.[9]

Nowadays, the strategy consists of developing systems capable of valorising in an optimized fashion all the components in terms to technical, economic and green issues, of a given vegetable or animal resource, without going to the detriment of food and feed production.[10] The compounds from renewable resources most used in the synthesis of polymers derived from vegetable resources and the compounds extracted from plants are shown in Figure 2.2, such as carbohydrates, lignins, terpens, sugars, polycarboxylic acids and triglycerides, gained relevancy in the last decade.[11,12]

The vegetable polysaccharides probably are the most important family of renewable resource in terms of abundance and its vast potential to provide a remarkable variety of macromolecular materials, such as cellulose and starch. Cellulose as the most abundant biopolymer on the Earth, which some 1 billion tons in essentially vegetable biomass, readily renewed thanks to solar energy and is essential in the novel strategies that comply with the realization of the biorefinery concept.[13] The first production of continuous cellulose materials like fibres and films dates back to the end of the 19th century.

The knowledge of its highly hidrophilicity property and biodegrability character are promoted numerous studies where combine cellulose nanofibres or nanocrystalls with other polymers to make novel materials.[14,15]

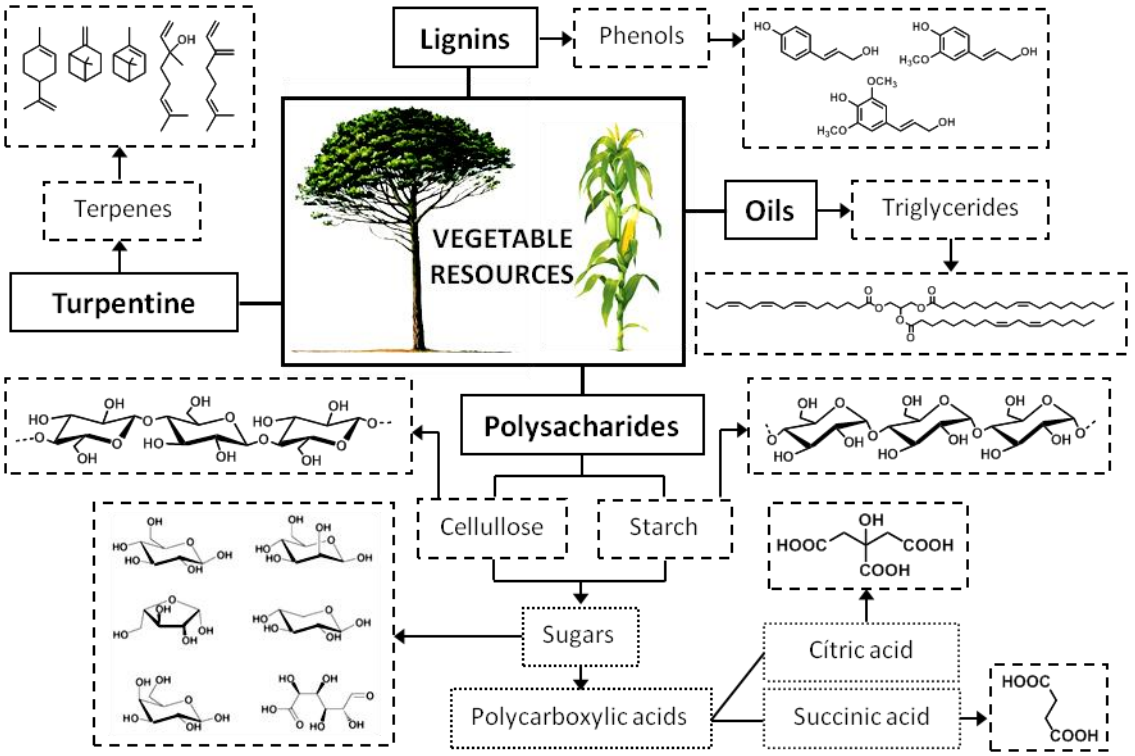

Figure 2.2. Some compounds from vegetable resource more used in chemical

Starch plays the fundamental role of the reinforcement element in the some plants structure such as potato, rice and corn. The starch appears in the nature in form of granules. The use of starch-based macromolecular materials has been assessed in the last years in literature.[16] Usually the starch in polymers synthesis is in form to thermoplastic starch. This is obtained by submitting starch granules to a thermo-mechanical destructing in the presence of water and a plasticizer, a process known as gelatinization, which renders the material amorphous. Their incorporation into different polymer matrices is providing a novel family of composites, such as for packaging applications.[17]

In addition other family of renewable resources provide from lignin that defines a vegetable biopolymers characterized by complex macromolecular structures containing of highly branched aromatic-aliphatic moieties. The lignin in the woody composites of vegetables is playing the role of barrier to moisture.[18] Only about the 2% of the some 70 Mt of lignin thus extracted throughout the world is presently exploited as a chemical commodity.[19] Much has been done in both fundamental and applied research to find novel ways to exploit these lignin fragments, particularly in the field of

macromolecular materials derived from small molecules like phenols, such as the synthesis of polibenzoxazines resins.[20]

The sugars are a very important renewable source of building blocks for the preparation of a variety of polymers which find valuable application, especially in the biomedical field, thanks to their biocompatibility and biodegradability.[21] This type of compounds are natural diols and can be used directly to prepare polyesters, polyurethanes, polycarbonates and polyethers, and after appropriate modifications, polyamides and polyimides. Such as, the synthesis of a new family of polyurethanes and poly(ester-urethanes), prepared from both aliphatic and aromatic diisocyanates and isorbide.[22,23]

Terpenes are a family of compounds that in mixture formed turpentine, the volatile fraction of pine resin and others conifer trees. The resin of these vegetables has been thoroughly exploited for millennia for a variety of useful applications. The global production of terpenes is nearly to 350.000 Tn per year. The polymer production from terpenes is related with the development of cationic initiators and is based in cationic polymerization of pinenes or limonenes, because they can be readily isolated in viable amounts.[24] Recently studies have shown original alternative mode of preparing polymeric materials from terpenes, makes use of ring-opening metathesis mechanism.[25] Also the chemical modification of these molecules aimed at preparing others different and attractive polymeric materials. These polymers find applications in paper sizing, adhesion and tack, emulsifications, coatings, drug delivery and printing inks.[26]

Other molecules derived from natural procedures and that offers a large range in the synthesis of polymers used as monomer or additive, are the polycarboxylic acids such as citric or succinic acid. These carboxylic acids are obtained from sugar cane, cellulosic or starch materials. Citric acid is a low cost commodity prepared industrially by a fermentation process producing about 70000 Tn annually. This triacid is used in synthesis of oligoesters with diol mixture,[27] or is introducing into a polyesterification

systems favouring their crosslinking in order to prepare high-tech coatings. While succinic acid is obtained from the fermentation of glucose and it can be exploited in the synthesis of polyesters, polyamides, copolymers and monomeric structures.[28,29]

2.3. Vegetable oils

Vegetable oils are considered to be one of the most important groups of renewable resources for the production of biobased polymers.[30,31,32] This used as raw materials offers numerous benefits, such as important purity, inherent biodegradability, low toxicity, high availability, versatile applications and relatively low price compared to others renewable resources and petroleum-based chemicals. The main constituents of vegetable oils are triglycerides, which are the product of esterification of glycerol with three fatty acids. Fatty acids account for 95% of the total weight of triglycerides and a general molecular structure of triglycerides is demonstrated in Figure 2.3.

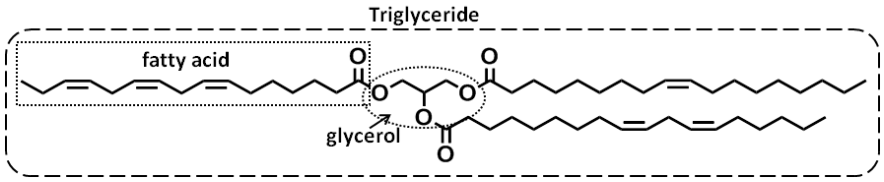

Figure 2.3. General structure of trygliceride.

The fatty acid mainly determines the physical and chemical properties of vegetable oils, these it depends on chain length and the numbers and locations of functional groups in the fatty acid chains. Usually, the length of the fatty chain is between 12 to 22 carbons and the number of double bonds is between 0 to 3 per fatty acid, as well as their positions within the aliphatic chain, also strongly affects the oil properties.[33]

Moreover, there are fatty acids with more functionalities than double bond, such as hydroxyl or epoxy group. In Figure 2.4, are shown some of the most significant fatty acids due to either their abundance or their functionality.[31]

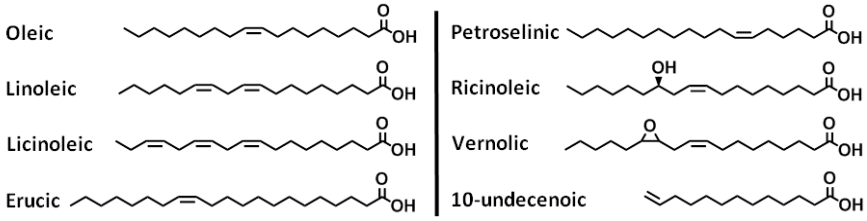

Figure 2.4. Structure of some important fatty acids.

The fatty acid composition of triglycerides diversifies depending on the crop, the plant, the season and the growing conditions. The average number of double bonds per triglyceride varies in different oils, the fatty acid content is placed in Table 2.1.

Table 2.1. Fatty acid percentage in various plant oils.

Fatty acid	C:DB [a]	Canola	Corn	Castor	Linseed	Olive	Palm	Soybean	Sunflower	High oleic
Myristic	14:0	0,1	0,1	0	0	0	0,1	0,1	0	0
Myristoleic	14:1	0	0	0	0	0	0	0	0	0
Palmitic	16:0	4,1	10,9	1	5,5	13,7	44,4	11	6,1	6,4
Palmitoleic	16:1	0,3	0,2	0	0	1,2	0,2	0,1	0	0,1
Margaric	17:0	0,1	0,1	0	0	0	0,1	0	0	0
Margaroleic	17:1	0	0	0	0	0	0	0	0	0
Stearic	18:0	1,8	2	1	3,5	2,5	4,1	4	3,9	3,1
Oleic	18:1	60,9	25,4	3	19,1	71,1	39,3	23,4	42,6	82,6
Linoleic	18:2	21	59,6	4,2	15,3	10	10	53,2	46,4	2,3
Linolenic	18:3	8,8	1,2	0,3	56,6	0,6	0,4	7,8	1	3,7
Arachidic	20:0	0,7	0,4	0	0	0,9	0,3	0,3	0	0,2
Gadoleic	20:1	1	0	0	0	0	0	0	0	0,4
Eicosadienoico	20:2	0	0	0,3	0	0	0	0	0	0
Behenic	22:0	0,3	0,1	0	0	0	0,1	0,1	0	0,3
Erucic	22:1	0,7	0	0	0	0	0	0	0	0,1
Lignoceric	24:0	0,2	0	0	0	0	0	0	0	0
Ricinoleic	18:1	0	0	89,5	0	0	0	0	0	0
Dihydroxystearic	18:0	0	0	0,7	0	0	0	0	0	0
DB/Triglyceride		3,9	4,5	3,1	6,6	2,8	1,8	4,6	4,5	3

[a] C, number of carbon atoms; BD, number of C=C doble bonds.

Particular attention has been paid to investigating the suitability of vegetable-oil-based polymers as future biomaterials. Vegetable oils such as soy, palm, linseed, sunflower and castor are valuable resources for the preparation of a variety of polymers.

In general, there are three main routes for the preparation of polymers from plant oils are shown in Figure 2.5. The first is the direct polymerization through the double

bonds or other reactive functional groups present in the fatty acid chain. The second route consists of the chemical modification of the double bonds, introducing functional groups which are easier to polymerize, and the third is the chemical transformation of plant oils to produce platform chemicals which can be used to produce monomers for the polymer synthesis.[34]

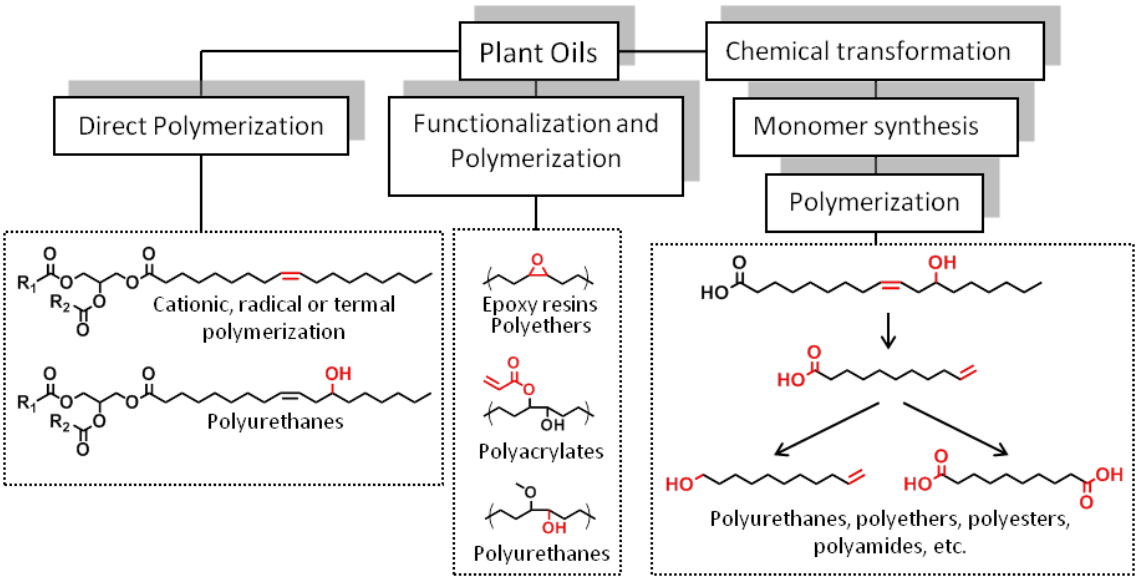

Figure 2.5. General routes to syntetize polymers from plant oils.

2.3.1. Direct polymerization

During the last decade, a variety of vegetable oil-based polymeric systems have been developed.[35] The direct polymerization of vegetable oils is generally considered difficult due to their lack of active functional groups. Unmodified vegetable oils have been polymerized by thermal[36] or cationic[37] polymerization methods. Vegetable oils such as linseed and tung oils have been classically exploited as drying oils. Drying oils can undergo auto-oxidation with the help of oxygen atmosphere to form peroxides,[38] which undergo crosslinking through radical recombination to form highly branched or crosslinked polymeric materials.[39] This polymerization is used mostly in paints and coatings, but also in inks and resins.

Apart from conjugated double bonds, internal double bonds in vegetable oils are not very reactive to be polymerized directly by radical polymerization because of the presence of allyl hydrogen, which are good radical trap.[38] In spite of that, the uses of olefinic monomers such as styrene, divinylbenzene, norbornadiene or dicloropentadiene are usually copolymerized by cationic polymerization of double bonds (Scheme 2.1) by cationic polymerization with vegetable oils such as soybean,[40,41] corn,[37] linseed[42] or sunflower[43] oil. The presence of this olefinic monomers increase the properties of the final material.

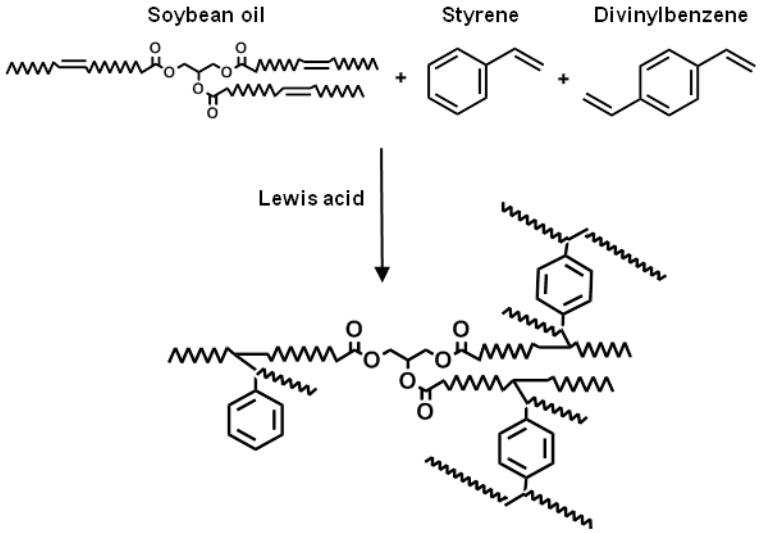

Scheme 2.1. Cationic copolymerization of soybean oils with styrene and divinylbenzene.

Castor oil, with high content in ricinoleic acid, has been directly polymerized by reaction between its hydroxyl groups with dicarboxylates to obtain thermosetting polyesters, as well as by reacting with diisocyanates to yield polyurethanes.[44]

2.3.2. Functionalization and polymerization

Generally, the reactive sites within vegetable oils, such as carbon-carbon double bonds and the ester functionality, allow for the introduction of such groups. The functionalization of triglyceride double bonds to introduce readily polymerizable

functional groups is a common strategy for obtaining high performance polymeric materials.

Epoxidation has been one of the most commonly used methods for the functionalization of carbon-carbon double bonds.[45] The epoxidation of vegetable oils can be conducted either in bulk or in solution with preformed or in situ prepared peracids, i.e. an active oxygen provider, under either homogenous or heterogeneous catalysis.[46] The epoxidation is usually conducted at a temperature between 30 and 80 °C for a reaction time of 10–20 h, depending on the types of feedstocks and ratios of reactants involved in the reaction. Under optimized conditions, conversion yields higher than 90 % can be achieved.[47-49] The undesirable side reactions of oxirane ring-opening during epoxidation can be largely minimized by conducting the reaction in a solution and at low temperature as well as under acidic ion exchange resin or lipase catalysis.[46,48,50,51] Other route is the use of peroxyacetic or peroxyformic acid formed "in situ" by reacting hydrogen peroxide with acetic or formic acids in the presence of sulphuric acid or acidic ion exchange resins as catalysts.[52] Epoxidation can be also achieved through a chemo-enzymatic process that involves the formation of peracid catalyzed by lipase followed by a Prilezhaev epoxidation.[53]

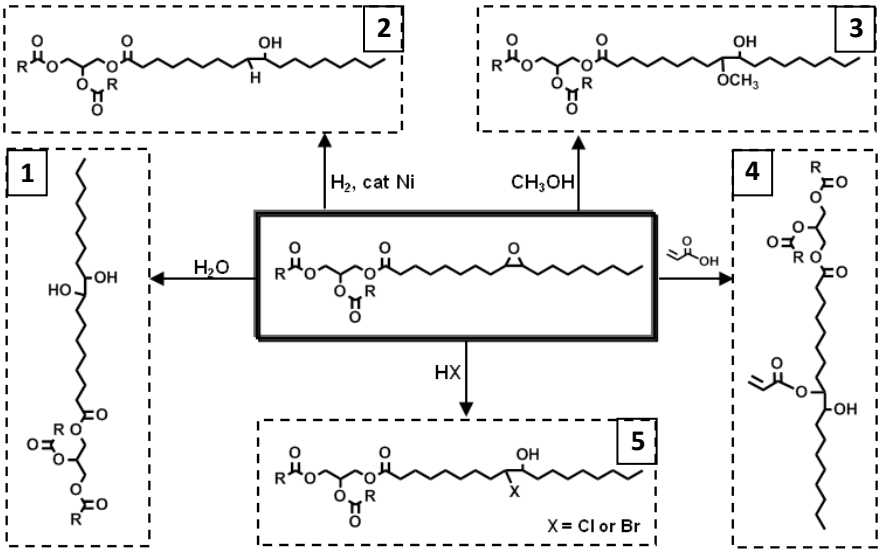

Scheme 2.2. Ring-opening products of epoxidized triglycerides.

Polyols are produced from epoxidized vegetable oil by oxirane ring-opening reactions using a broad range of active hydrogen containing compounds such as alcohols, inorganic and organic acids, amines, water, and hydrogen.[45,51,54,55] A schematic representation of the production of polyols from vegetable oils by epoxidation followed by oxirane ring-opening is shown in Scheme 2.2. The properties of polyols produced by epoxidation and subsequent oxirane ring-opening depend on several production variables including feedstock characteristics and the types of ring-opening agents. Vegetable oils with a higher degree of unsaturation produce polyols with higher hydroxyl functionalities, resulting in PUs with higher crosslinking density and higher tensile strength.[56] Oxirane ring-opening agents are divided into following major categories:

1) Water is the cheapest ring-opening reagent.[57] The epoxy rings could be hydrolyzed by water in the presence of formic acid, acetic acid and perchloric acid. One epoxy group would theoretically generate two hydroxyl groups upon reacting with one molecule of water. Epoxidation and water ring-opening could be conducted in one pot. When hydrogen peroxide (30% in water) and acetic acid were applied to epoxidize vegetable oils, subsequent hydrolysis of epoxy groups by water could be realized by increasing the temperature when epoxidation was completed.[58,59,60]

2) Hydrogen. Polyols from ring-opening of epoxidized vegetable oils by hydrogen under Raney nickel catalysis are grease at room temperature, which has limited their applications.[61]

3) Alcohols. When monoalcohols are used for ring-opening, each epoxy moiety only generates one secondary hydroxyl group, which are much less reactive than primary hydroxyl groups.[62] Methanol is the common choice of monoalcohols for ring-opening due to its low cost, low molecular weight, and low boiling point. In order to produce polyols with higher functionalities and with primary hydroxyl groups, diols such as 1,2-propanediol and ethylene glycol have also been used for

oxirane ring-opening reactions.[54,63] However, the produced polyols tend to possess high viscosities due to their increased hydroxyl numbers.

4) Carboxylic acids such as formic and acetic acids have been used for ring-opening of epoxidized vegetable oils to produce polyester polyols, which have been shown to have potential for anti-wear applications.[45,55,64] Thus, the introduction of acrylic acid exhibits higher reactivity and can undergoes free radical polymerization to afford thermosets with good thermal and mechanical properties.[65]

5) Inorganic acids such as HCl, HBr, and H_3PO_4 have also been reported as ring-opening agents.[61,66] Due to the incompatibility between inorganic acids and epoxidized vegetable oils, polar organic solvents such as acetone and t-butyl alcohol are typically added into the reactor to facilitate reactions. There are some drawbacks associated with the polyols from oxirane ring-opening reactions of epoxidized vegetable oils by inorganic acids. Polyols produced from oxirane ring-opening by HCl and HBr are waxes at room temperature,[61] while those produced by H_3PO_4 contain significant fractions of oligomers because of the oligomerizations that occur between oxirane groups.[66]

Simultaneous oxirane ring-opening and transesterification[67] of epoxidized canola oil was achieved by using a strong acid catalyst (e.g., sulfuric acid) and excess amounts of diols (e.g., 1,2-propanediol or 1,3-propanediol). Because transesterification effectively removed the glycerol backbone from polyols, the produced polyols had lower molecular weights (ca. 433 g/mol) and viscosities (about 3 Pa.s), and higher hydroxyl numbers (about 270 and 320 mg KOH/g) than polyols obtained by oxirane ring-opening alone.[47] In a more recent study, polyols with similar properties have also been produced from epoxidized soybean oil through simultaneous ring-opening and amidation reactions.[68]

2.3.3. Polymerization of oil-derived platform monomers

The most recent contributions show a growing interest in the use of fatty acids as precursors of monomers; not only because of their renewability, but also because of the properties they can provide to the final polymers. In this way, monomers can be achieved for the synthesis of linear polymers. The triglycerides from vegetable oils can be subjected to hydrolysis or methanolysis to obtain the fatty acids and their esters as well as glycerol. The ozonolysis and reduction reaction or the pyrolysis of some fatty acids, such as ricinoleic acid,[69] can be useful to isolate new coumpounds. In this way, monomers can be achieved for the synthesis of linear polymers as is shown in Scheme 2.3. For the last years, thiol-ene coupling has been applied to the synthesis of monomers derived from vegetable oils such as, diacids, diols and hydroxyl-acids for the synthesis of linear polyesters and polyurethanes, as well as monomers for branched structures have been described.[70]

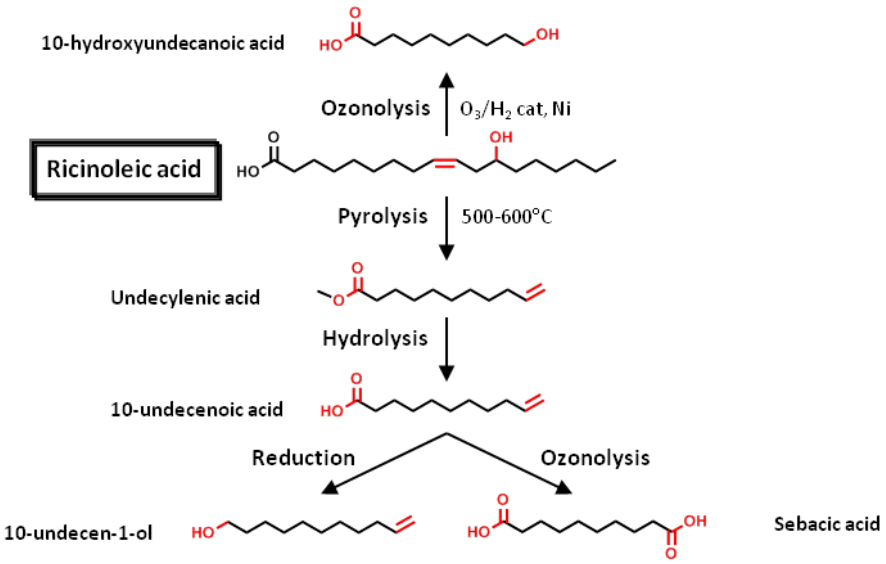

Scheme 2.3. Common monomers from ricinoleic acid.

In addition, acyclic metathesis polymerization (ADMET)[71] and ring-opening metathesis polymerization (ROMP)[72] are important reactions applied recently to the transformation of fatty acids into monomers and polymers and they are shown in Scheme 2.4. The development of new highly active catalysts which are tolerant to a wide range of functionalities opens new possibilities for this chemistry.

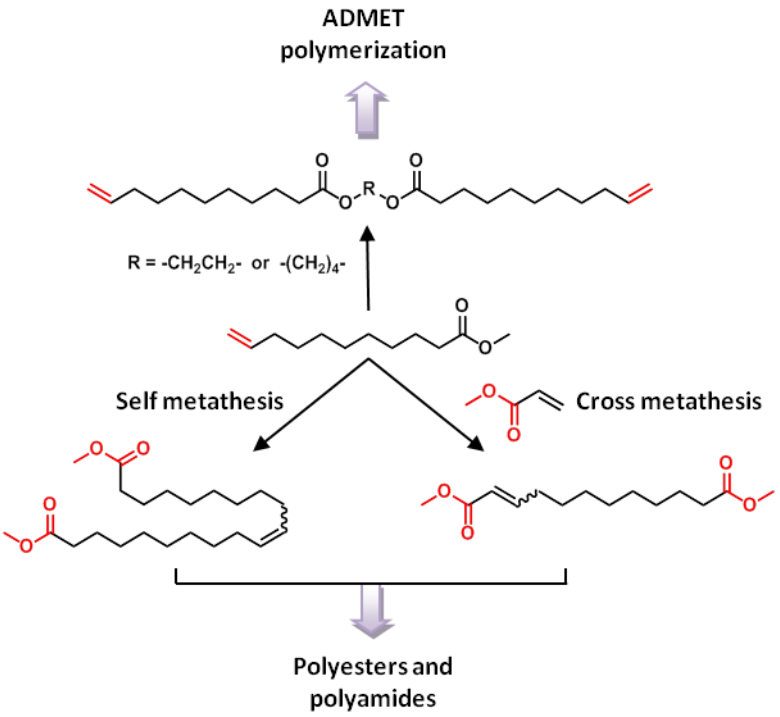

Scheme 2.4. Synthesis of monomers from vegetable oils by metathesis reaction.

2.4. Polyurethanes from vegetable oils

The polymeric materials known as polyurethanes (PUs) form a general family of polymers that contain the urethane group (Figure 2.6) in their chemical repeating unit. The relatively short history of PUs; of slightly more than 75 years, begins with their discovery on the year 1937 by Otto Bayer and his co-workers. PUs account for nearly 5 wt% of total worldwide polymer production and constitute one of the most important classes of polymeric materials due to their extreme utility and relatively low cost.[73-75] It is worth noting that most of PUs come from the petroleum-based feedstock,

therefore, there is a growing interest in the use of natural reagents to replace petroleum based PUs.[76] The high versatility has allowed the synthesis of different materials with diverse properties such as, elastomers, thermoplastics, foams, adhesives, coatings, fibers and sealants. Nowadays PUs have become one of the most usual polymers due to their wide range of applications such as, automotive, footwear, construction, engineering, wiring and most recently in medical devices.

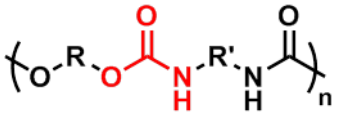

Figure 2.6. Urethane functional group.

PUs are formed by chemical reaction between a di/poly isocyanate and a diol or polyol, forming repeating urethane groups, depending on the functionality of the raw materials one can obtain linear or cross-linked polymers.

The reactivity of isocyanates is not exclusively for a hydroxyl group, there are others compounds that can affect in the production of polyurethanes, such as water, amines, carboxylic acids and ureas. In Scheme 2.5 are represented the isocyanates side reactions involved in the synthesis of polyurethanes. Probably the presence of water in the reaction is one of the most relevant drawbacks, because it is deblocked other undesired reactions. The isocyanate group is so active and reacts with active or acidic hydrogen almost instantly. This basic reaction produces the hydrolysis of isocyanate and forms carbon dioxide and amine groups. The carbon dioxide formed can be used to synthesise PU foams while the amine group will further react in a nucleophilic addition reaction with remaining isocyanate to produce urea groups. This last reaction can be exploited in the synthesis of polyureas.

In addition, isocyanate group not only reacts with primary amines, can also react with urea or urethane groups, even though the rate of reaction is much lower compared with that of the primary amine. The biurets and allophanates groups are the products

of nucleophilic reaction between isocyanate and urea or urethane group respectively. Moreover, other reactions that can be possible occurs when the isocyante is in presence of carboxylic acid groups or an high excess of the same or other isocyanate, in the first case, carbon dioxide and amide are produced while in the second case it can be formed dimers or trimers.[77]

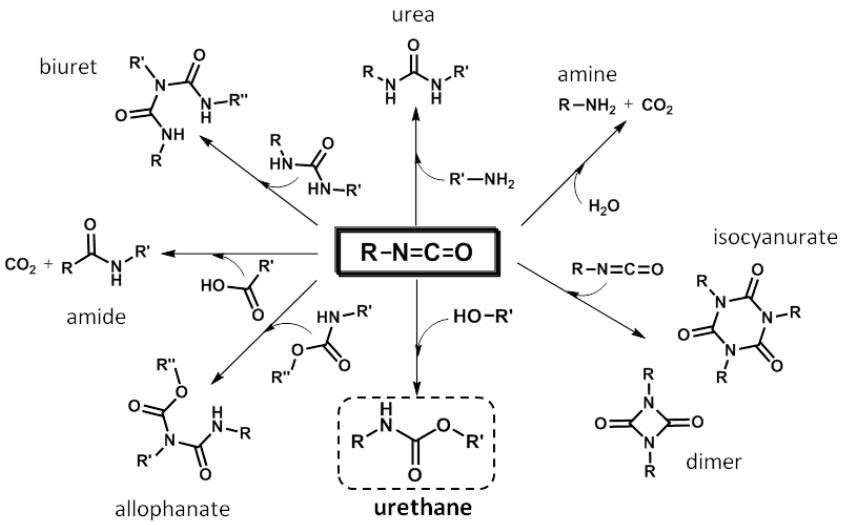

Scheme 2.5. Isocyanates side reactions involved in the synthesis of PUs.

Along with a fuctional group hydroxy or isocyanate, some additives may also be required during polyurethane production, primarily to control the reaction, modify the reaction conditions, and also to finish or modify the final product. One of these additives in polyurethane production are the catalysts. There are two with most relevancy basic catalysts such as tertiary amines or metal compound catalysts such as organotin. These are added to promote the reaction to occur at enhanced reaction rates, at lower temperatures, for deblocking the blocked isocyanates, for decreasing the deblocking and curing temperatures and times.

In case of tertiary amines, their catalytic activity is determined by their structure as well as their basicity; they promote their catalytic action by complex formation between amine and isocyanate, by donating the electrons on nitrogen atom of tertiary amine to the positively charged carbon atom of the isocyanate. On the other hand,

metals catalyse the isocyanate-hydroxyl reaction by complex formation with both isocyanate and hydroxyl groups. The positive metal centre interacts with electron rich oxygen atom of both the isocyanate and hydroxyl groups forming an intermediate complex, which by further rearrangement results in the formation of urethane bonds.

The diisocyanates with two isocyanates group per molecule are the most important isocyanate compounds in the PUs fabricated. These two functional groups react together with two molecules containing hydroxyl groups, to form a linear chain. The synthesis of diisocyanates is more complex than that the polyols for this reason usually chemists tend to work with commercially available diisocyanates, the most common are represented in Figure 2.6. Although the properties of the final material depends more on the polyol, the choice between one and other isocyanate for the same polyol also becomes enoguh high important for modulate the final PUs properties.

In the past, all of polyols used in the PUs production are derived from petroleum resources, but nowadays is increasing the interest to synthesize diols or polyols from renewable resources such as vegetable oils. Castor oil, which is rich in ricinoleic acid, has been historically the first and almost the only vegetable oil used in the synthesis of PUs and in interpenetrating polymer networks.[44]

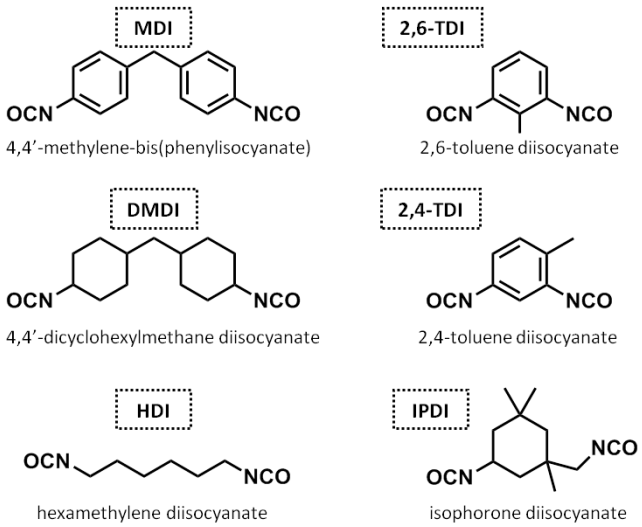

Figure 2.6. Typical diisocyanate used in the synthesis of PUs.

With the exception of castor oil, nearly all vegetable oils do not naturally contain the hydroxyl groups necessary to produce PUs. On account of that, many methods were developed to incorporate hydroxyl groups in the triglycerides from vegetable oils to produce polyols for polyurethanes production. The main routes to obtain vegetable oil-based polyols are represented in Scheme 2.6.

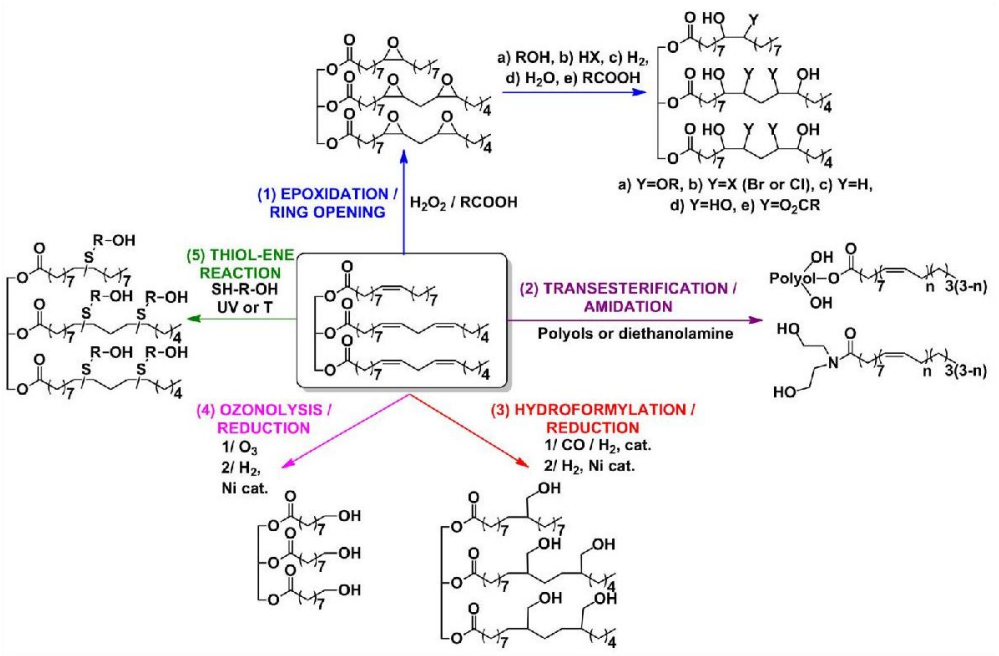

Scheme 2.6. The main routes to obtain vegetable oil-based polyols

(1) Epoxidation / oxirane ring-opening

Epoxidized polyols, as can be seen in the previous section (*Vegetable oils – Funtionalization and Polymerization*), are polyols derived from epoxidation and subsequent oxirane ring-opening. Epoxidized polyols have been used for the preparation of many PU products such as resins, foams, and coatings. By controlling factors such as vegetable oil composition, ring-opening agent, and degree of epoxidation, polyols and PUs with varying properties have been produced. A close relationship between the properties of epoxidized polyols from vegetable oils and their derived PUs has been observed: the higher the hydroxyl number and functionality of

the polyol, the higher the crosslinking density, the Tg, and the tensile strength of the PUs.[56,63,78]

It was been reported that halogenated (chlorinated and brominated) PUs possessed higher mechanical properties, higher Tg, and lower linear thermal expansion coefficients than non-halogenated ones (such as, methoxylated and hydrogenated PUs), which could be attributed to their stronger intermolecular attractions, higher crosslinking densities, and lower free volumes resulted from large halogen atoms; however, compared to non-halogenated PUs, halogenated ones showed lower thermal stability and higher initial weight loss as a result of the dissociation of bromine or chlorine.[79]

Much more examples of epoxidized polyols can be found in the synthesis of PU foams. Several strategies, such as addition of a crosslinker,[80] post-modifications by alcoholysis,[81] and mixing with commercial petroleum-derived polyols,[82,83] have been developed to produce rigid PU foams from epoxidized polyols. In view of its high hydroxyl number and compact backbone, glycerol has been proven to be an excellent crosslinker to increase the rigidity of epoxidized polyol-based PU foams. Under preferred glycerol addition (10–25 wt% of soy polyol) and optimized foam formulation conditions, the produced rigid PU foams exhibited mechanical and thermal-insulating properties comparable to analogues prepared from commercial polyether polyols. However, the epoxidized polyol-derived PU foams had the drawback of higher aging rates, i.e. an increase of thermal conductivity with time due to its higher N_2 permeation, than petroleum-derived foams, which may be alleviated by the addition of a crosslinker, such as glycerol.[82] Flexible PU foams from epoxidized polyols have also been prepared by this blending method. Mixing epoxidized polyols (up to 50 % by weight) with petroleum-derived polyols was found to increase the compressive strength and modulus of the resulting foams.[84-86]

Waterborne PU dispersions, including anionic and cationic PU or hybrid dispersions, have been synthesized from methoxylated soybean oil polyols.[87-92] As the polyol functionality and/or hard segment increased, PU films exhibited increased crosslinking density, Tg, and tensile strength. By employing polyols with increasing functionalities ranging from 2.4 to 4.0, PU films ranged from elastomers to ductile plastics to rigid plastics.[87,90]

Urethane-acrylic and urethane-styrene-acrylic hybrid latexes have been prepared from soybean oil-based epoxidized polyols by emulsion polymerization. Generally, these hybrid latex films showed improved tensile strength, Young's modulus, and thermal stability, compared to non-hybrid PU films.[88,91,92]

(2) Transesterification / amidation.

Usually, the discussed pathways for the production of vegetable oil-based polyols take place at the double bond moieties of vegetable oils. Transesterification and amidation use a different approach that makes use of the ester moieties in the structures of vegetable oils to produce polyols. Glycerol is the most predominantly used alcohol for the transesterification of vegetable oils, but the use of other alcohols, such as pentaerythritol[93] and triethanolamine,[94] has also been reported. During transesterification, the addition of a small amount of soap acts as an emulsifier that can improve the compatibility between glycerol and triglycerides and thus increase the production efficiency of monoglycerides. Transesterification reactions are mostly catalyzed by organic and inorganic bases such as methoxides of sodium, calcium, and postassium;[93,95] sodium hydroxide; and calcium hydroxide,[94] and by metal oxides such as lead and calcium oxides.[96] Polyols produced from vegetable oils by transesterification with glycerol (i.e., glycerolysis) are a mixture of mono-, di-, and tri-glycerides and residual glycerol. Among these components, monoglycerides, which contain two hydroxyl groups per molecule, play an important role for PU production. Polyols produced by the transesterification of vegetable oils can be partially or completely substituted for petroleum-derived polyols for the preparation of PU foams

and coatings.[94] Similar to the above transesterification processes, amidation with amines, usually diethanolamine, can also convert vegetable oils into diethanol fatty acid amides for producing PU foams and coatings. Compared to commonly used transesterification with glycerol at 230–250 °C [94,96] the amidation of vegetable oils with diethanolamine are carried out at a lower temperature, usually at 110 °C.[94,97,98] Amidation-derived polyols from vegetable oils, such as linseed, soybean, rapeseed, sunflower, coconut, Nahar, and cottonseed oils, have been used for the development of PU foams and coatings with satisfactory physical and mechanical properties.[94,99,100]

(3) Hydroformilation / reduction.

The hydroformylation/reduction of vegetable oils involves the addition of hydroxymethyl groups to the carbon-carbon double bonds in the fatty acid chains using a two-step procedure. In the first step, the vegetable oil is treated with syngas (a mixture of CO and H_2) in the presence of a catalyst to give aldehydes, which are then reduced with H_2 in the second step to yield hydroxyl groups. The most commonly used catalysts are simple cobalt carbonyl complexes, cobalt carbonyl complexes modified by tertiary phosphine/phosphite ligands, and tertiary phosphine/phosphite rhodium carbonyl species. With hydroformylation/reduction, the hydroxyl functionality of the vegetable oil-based polyol is dependent on the number of carbon-carbon double bonds in the vegetable oil. Because of this, soybean oil is most commonly used as the starting material, but other oils, including safflower and linseed oils, have also been used. [101,102] When reacted with isocyanates for PUs, hydroformylated polyols showed shorter gel time and better curing efficiency, compared to epoxidized polyols. PU foams with enhanced rigidity can be produced from hydroformylated polyols when mixed with a crosslinker such as glycerol. Hydroformylated polyols with narrowest functionality distribution resulted in PU coatings with the best balance of hardness, flexibility, and abrasion resistance.

(4) Ozonolysis / reduction

The ozonolysis/reduction of vegetable oils results in terminal primary hydroxyl groups. This method involves the efficient cleavage of the carbon-carbon double bonds present in the fatty acid chains to give, under the right conditions, shorter chain alcohols. In the first step, an ozonide is formed by treating a vegetable oil with ozone, which is then reduced by zinc to give an aldehyde, and further reduced with Raney nickel to the corresponding primary alcohol. The ozonide can also be treated with sodium borohydride to afford the primary alcohol directly. The ozonolysis procedure essentially removes half of each fatty acid chain, which is advantageous, because these dangling chains are not incorporated into the polyurethane and act as plasticizers to weaken the materials.

Zero or low volatile organic content (VOC) PU coatings from soybean oil glyceride polyols prepared by one-step ozonolysis with glycerol exhibited high hardness, gloss, and chemical resistance as well as excellent adhesion to metal surfaces. They are suitable for industrial, automotive and architectural applications. Rigid PU foams prepared from a mixture of glycerol and the above soybean oil glyceride polyol at a 1:3 weight ratio also showed satisfactory mechanical and thermal properties, which were comparable to those of PU analogues from a commercial polyol. Ozonolysis-derived polyols combined with poly(methyl methacrylate) (PMMA) have also been used to prepare sequential interpenetrating polymer networks (IPNs) with satisfactory mechanical properties.[103]

(5) Thiol-ene reaction

Thiol-ene coupling reactions involve a free radical chain mechanism by which thiols are grafted onto double bonds. They are not sensitive to oxygen and can be carried out in the absence of photoinitiators through a photoreaction.[104] Due to its high conversion yield and fast reaction rate, a UV-initiated thiol-ene coupling reaction is generally used for preparing polyols from vegetable oils and their derivatives with 2-mercaptoethanol

as a common thiol monomer. Soybean oil-based polyols have also been prepared via heat-initiated thiol-ene coupling which required longer reaction time than UV-initiated thiol-ene coupling.[105] During the thiol-ene coupling process of vegetable oils and their derivatives, side reactions occurred, including disulfide formation, double bond isomerization, and inter- and intra-molecular bond formation.[106] Despite these side reactions, most byproducts contained hydroxyl functional groups and could participate in PU formation.

Similar to polyols from epoxidation followed by oxirane ring-opening and from hydroformylation followed by hydrogenation, polyols from the thiol-ene coupling pathway also contain hydroxyl groups located in the middle of fatty acid chains, leaving part of the fatty acid chains as dangling components in PU structures. Currently, most thiol-ene coupling-derived polyols have been prepared from fatty acids or fatty acid esters (Scheme 2.7). Methyl-10-undecenoate from ricin oil,[107] oleic acid[108], and rapeseed oil[106] and diols from ricin or sunflower oils[109] have been successfully reacted with mercaptoethanol and other thiols under UV irradiation, to yield natural oils polyols. This simple, one-step reaction scheme makes it possible to introduce a new heteroatom into the triglyceride structure.[110] However, it has the drawback of being accompanied by secondary reactions (disulfide formation, esterification) generating by products, many of which are hydroxylated.

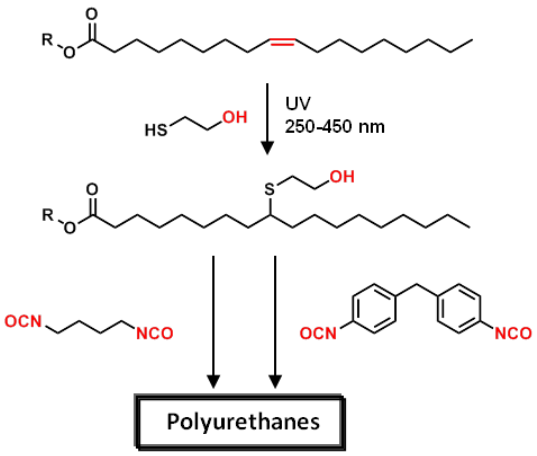

Scheme 2.7. Synthesis of polyurethanes from thiol-ene coupling modification of vegetable oils

2.5. Functionalized polyurethanes

The exploration of new methods for the preparation of functionalized polymers with unique structures is of vital importance to polymer science. Functionalized polymers may be considered in broad terms as those polymers whose are incorporated a functional group that it can be used as a reactive point. A specific functional group is usually carefully designed and located at a proper place on the polymer chain.

There are three locations in the functionalized polymers: the functional groups can be dispersed along the polymer main-chain, including chain ends, also the functional groups can be attached to the main-chain either directly or located in branched chains as observed in Figure 2.7.

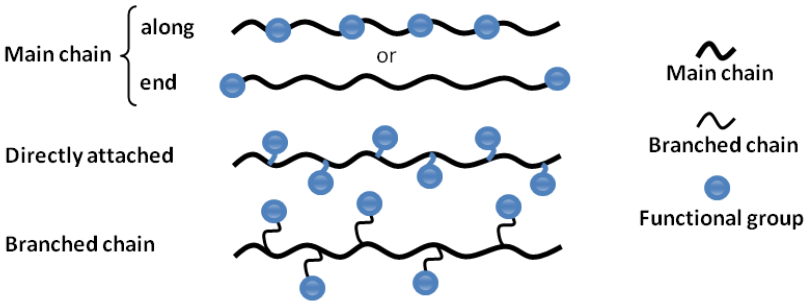

Figure 2.7. Positions of functional groups in functionalized polymers

The main objective of the introduction of special functional groups into the polymer backbone or side chains is to give the polymers special features. Functional groups are, therefore, typically chemical units that are chemically reactive, biologically active, electroactive, mesogenic, photoactive, and, more commonly, ionic, polar, or optically active.[111] However, pendent functionalization provides a unique opportunity to alter physical and chemical properties by distributing functionality along the polymer backbone. Pendent functionalization of aliphatic polyesters can be achieved by polymerization of functionalized monomers, postpolymerization modification, or a combination of the two approaches.[112]

In general, the properties of PUs are easily tailored by the appropriate selection of the individual monomeric units, many of which are commercially available.[113,114] Conversely, developing new methods for synthesizing PUs with modifiable reactive groups along their backbone remains an open challenge. [115,116] Different functional monomer incorporating hydroxyl,[117,118] amine,[119] maleimide,[120] alkyne,[121-126] alkene[123,127-129] or non-active/active ester[130,131] were reported. Nevertheless, careful attention should be paid toward the inertness of the introduced functional groups during the polymerization process to avoid secondary reactions (Scheme 5) making the materials unusable for the desired final applications. In order to this, the use of protection/deprotection strategies prior to polymerization is mandatory. For instance, the synthesis of functionalized PUs from protected hydroxyl groups by benzyl ether was reported. The study used O-protected L-threitol, L-arabinitol, and xylitol as monomers (Scheme 2.8) for the preparation of a series of linear [m,n]-type PUs by polycondensation in solution with HDI or MDI. Fully O-benzylated PUs showed high resistance to hydrolytic degradation, whereas the PUs obtained by removing the O-protecting groups, having free hydroxyl side groups, degraded significantly in saline buffer at pH 10 and 37 °C.

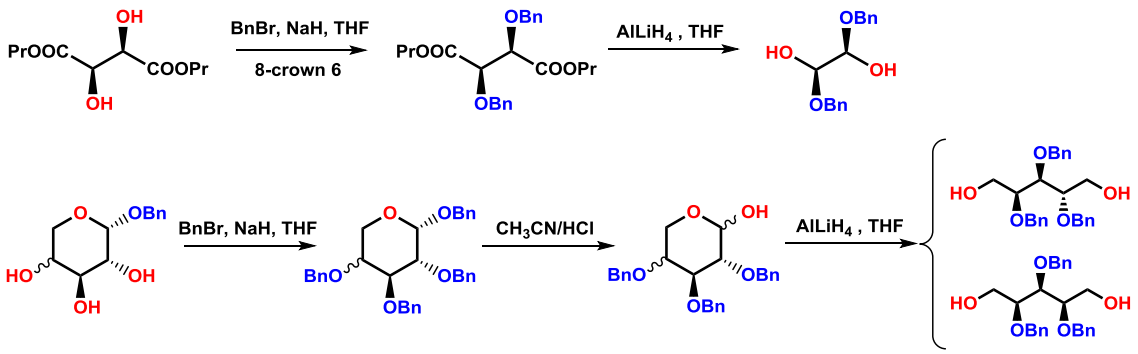

Scheme 2.8. Synthesis of carbohydrated based diols.

In addition, the introduction of amino groups into PU also requires protection/deprotection steps. Recently, the preparation of PUs bearing pendant amino groups starting from HDI, poly(ϵ-caprolactone) (PCL), and a modified poly(ethylene glycol) (PEG) has been described. The approach consists in the reaction of dihydroxyl PEG with NH_2-protected aspartic acid (Asp) leading to a prepolymer PEG−Asp−PEG. Then, the consequent reaction between HDI, PCL and the amino-protected PEG−Asp−PEG (Scheme 2.9) allowed for the formation of PU with a low loading of pendant amino groups after an ultimate deprotection step.[119]

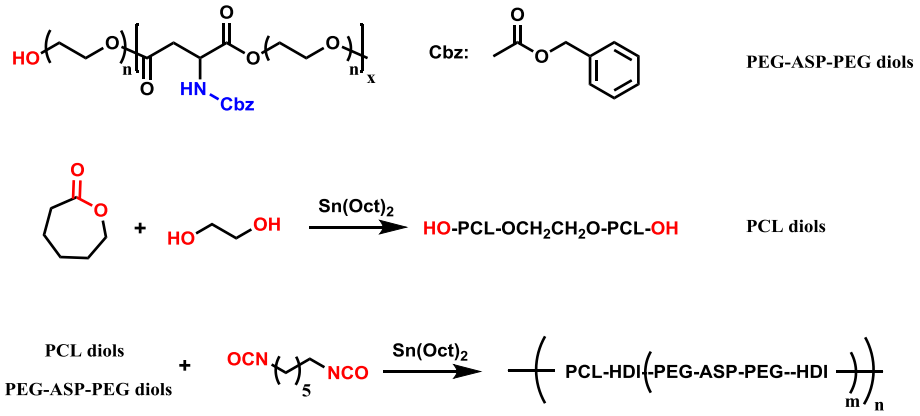

Scheme 2.9. Synthesis of PCL diol and coupling reaction of PCL diols with PEG-Asp-PEG.

Moreover, it was reported the synthesis of functionalized linear PUs with maleimide group. In this case, the design of functionalized linear PUs with maleimide side-chain group was carried out from a furan-protected maleimide-containing diol monomer, 1,4-butandiol and equimolar amounts of HDI. Resulting linear PU containing furan-protected maleimide was deprotected by retro-Diels-Alder reaction at 100 °C, yielding aliphatic PU's with pendant maleimide functions as is shown in Scheme 2.10.[120]

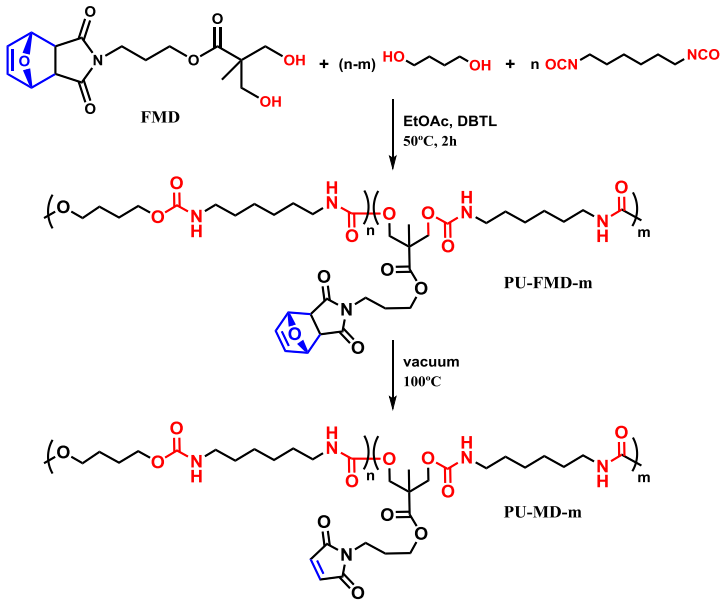

Scheme 2.10. Synthesis sequence of protected/deprotected maleimide-containig PU.

Apart from the incorporation of functionality using isocyanate chemistry, there are some strategies for the synthesis of functionalized polyurethanes more environmentally attractive isocyanate-free methods. These strategies permit the introduction of some functional groups into PU without protected/deprotected process. Recently, two relevant isocyanate-free strategies based on amine-thiol-ene conjugation[115] or cyclic carbonates[132] are reported (Scheme 2.11).

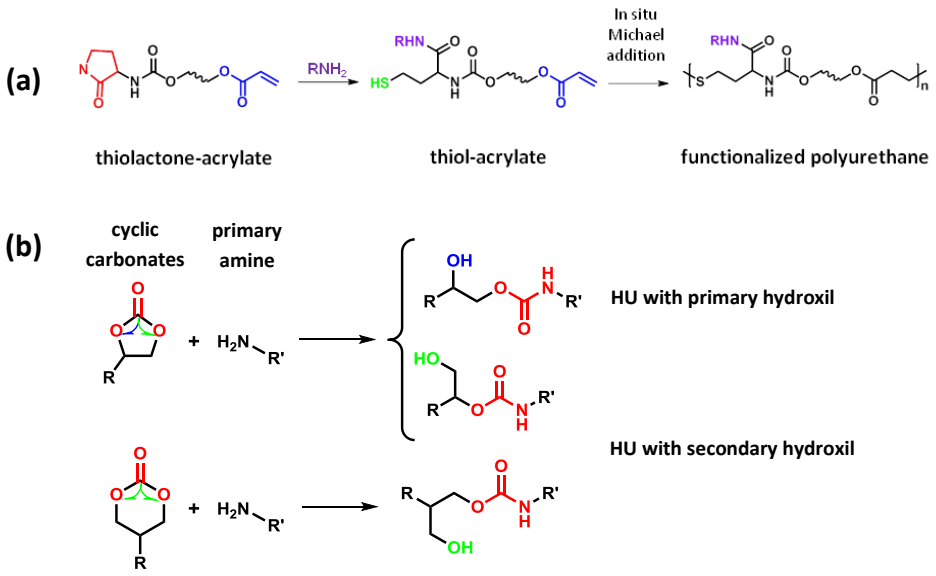

Scheme 2.11. (a) Synthesis of PUs functionalization based on amine-thiol-ene conjugation and (b) model reaction on 5- and 6-membered cyclic carbonates leading to hydroxyurethanes (HU).

Otherwise, an ideal synthesis of functionalized PUs approach is one that directly incorporates pendant functional group, from a functional monomer, during the polymerization reaction, but does not interfere with the polymerization process. The main strategy used during the polymerization process is the incorporation of functional groups in the diol moiety without previous protection. In this case, PUs containing pendant esters groups (Scheme 2.12) in side-chain derived from ester-containing diol was reported.[130] The resulting monomers were then polymerized with MDI to produce the corresponding functionalized PUs. The biocompatibilities of the synthesized ester-functionalized PUs with human osteoblast-like cell line have been evaluated for tissue engineering purposes. Furthermore, a method for the synthesis of high molecular weight functionalized PUs from pentafluorophenyl ester-containing diol precursor is reported.[131] Specifically, PUs containing the activated ester sidechains were synthesized via triflic acid-catalyzed polyaddition of the above diol with diisocyanates.

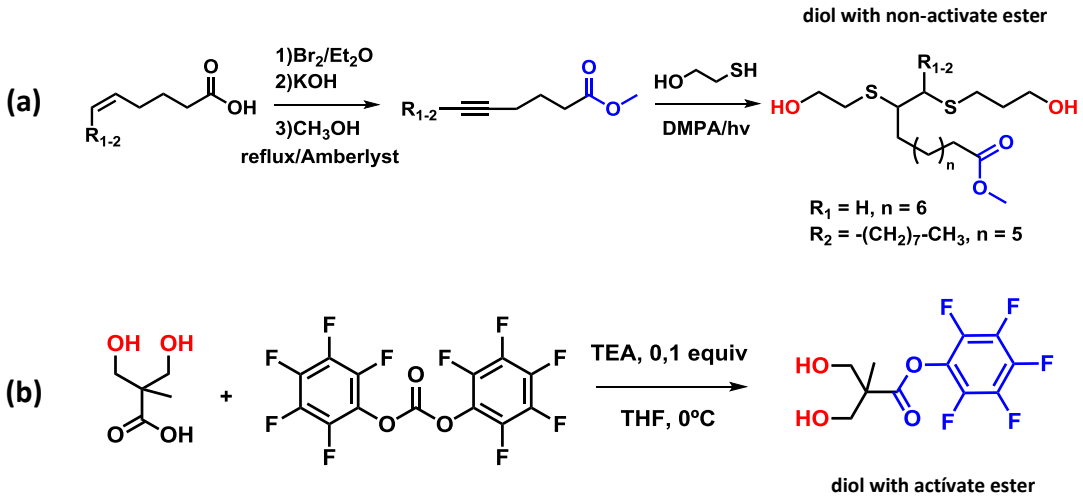

Scheme 2.12. Synthesis of diols contining non-activate (a) and actívate (b) esters groups.

Other compounds that can be used in the synthesis of functionalized PUs due to the inert behaviour of their functional groups during the polymerization process are the alkene/yne-containing diols. Thus, it was reported the preparation of alkyne and alkene-functionalized PUs using the bulk polymerization method. PUs with pendant sugar-moieties are capable of undergoing either copper catalyzed Huisgen 1,3-dipolar cycloaddition or thiol-ene click reactions.[123]

In this way, the functionalization of PUs can be accomplished also after the step-growth polymerization, using the reactive points introduced by the functional monomers polymerization as can be seen in above procedures. The process of change or introduce new functional groups thanks to previous functional groups presents in PU is called post-polymerization modification.

The modification of polymers after the successful achievement of a polymerization process is an important task in macromolecular science. Click chemistry may serve as a powerful strategy in its search. Click chemistry has emerged as a widespread approach that uses only the most-practical and -reliable chemical transformations, with an explosive growth in publications in recent years.[133-135] Although fitting the requirements of a click reaction is a tall order, several processes did so. Thus, the thiol-ene/yne coupling reaction is a well-established click reaction that combines a thiol moiety and an alkene/alkyne group in a robust, efficient, and orthogonal method for the functionalization of different compounds.[136] Allyl and alkynil groups can be used in thiol-ene/yne coupling reactions as the unsaturation part with great success.[137-139]

The tremendous potential of the click chemistry in post-polymerization modification of functionalized PU have specifically been developed for high-tech applications by applying modern methods of chemical biological, physical and technological material science.[117-139] These developments have resulted in available functional polymers with tailor-made properties.

2.6. References

[1] W. Lutz, W. Sanderson, S. Scherbov. The coming acceleration of global population ageing. *Nature*. **2008**, *451*, 7179, 716-719.

[2] T. B. Johansson, A. P. Patwardhan, N. Nakićenović, L. Gomez-Echeverri (Eds). *Global energy assessment: toward a sustainable future*. Cambridge University Press. **2012**. 8-10.

[3] M. Brueckner, H. Schwandt. Income and population growth. *The Economic Journal.* **2015**, 125, 589, 1653-1676.

[4] S. H. Mohr, J. Wang, G. Ellem, J. Ward, D. Giurco. Projection of world fossil fuels by country. *Fuel*. **2015**, *141*, 120-135.

[5] M. Höök, X. Tang. Depletion of fossil fuels and anthropogenic climate change-A review. *Energy Policy*. **2013**, *52*, 797-809.

[6] S. Paltsev. Energy Scenarios: The Value and Limits of Scenario Analysis. *MIT Center for Energy and Environmental Policy Research*. **2016**.

[7] J. J. Bozell. Topical Issue: Feedstocks for the Future: Renewables in Green Chemistry Edited by: Joseph J. Bozell. **2008**.

[8] C. K. Williams, M. A. Hillmyer. Polymers from renewable resources: a perspective for a special issue of polymer reviews. *Polymer Reviews*. **2008***,* 48, 1, 1-10.

[9] Y. Zhu, C. Romain, C. K. Williams. Sustainable polymers from renewable resources. *Nature*. **2016**, 540, 7633, 354-362.

[10] A. Gandini. The irruption of polymers from renewable resources on the scene of macromolecular science and technology. *Green Chemistry.* **2011**, 13, 5, 1061-1083.

[11] A. Gandini, T. M. Lacerda. From monomers to polymers from renewable resources: Recent advances. *Progress in Polymer Science*. **2015**, 48, 1-39.

[12] A. Gandini, T. M. Lacerda, A. J. Carvalho, E. Trovatti. Progress of polymers from renewable resources: furans, vegetable oils, and polysaccharides. *Chemical reviews*. **2015**, 116, 3, 1637-1669.

[13] A. V. Bridgwater. Review of fast pyrolysis of biomass and product upgrading. *Biomass and bioenergy*. **2012**, 38, 68-94.

[14] K. Benhamou, H. Kaddami, A. Magnin, A. Dufresne, A. Ahmad. Bio-based polyurethane reinforced with cellulose nanofibers: a comprehensive investigation on the effect of interface. *Carbohydrate polymers*. **2015**, 122, 202-211.

[15] C. Tan, J. Peng, W. Lin, Y. Xing, K. Xu, J. Wu, M. Chen. Role of surface modification and mechanical orientation on property enhancement of cellulose nanocrystals/polymer nanocomposites. *European Polymer Journal*. **2015**, 62, 186-197.

[16] A. Gandini. Polymers from renewable resources: a challenge for the future of macromolecular materials. *Macromolecules.* **2008**, 41, 24, 9491-9504.

[17] F. P. La Mantia, M. Morreale. Green composites: A brief review. *Composites Part A: Applied Science and Manufacturing*. **2011**, 42, 6, 579-588.

[18] R. A. Burton, J. B. Michael, G. B. Fincher. Heterogeneity in the chemistry, structure and function of plant cell walls. *Nature Chemical Biology.* **2010**, 6, 10, 724-732.

[19] J. Lora, B. M. Naceur, A. Gandini. Industrial commercial lignins: sources, properties and applications. Elsevier, Amsterdam. **2008**, 225-241.

[20] M. Comí, G. Lligadas, J. C. Ronda, M. Galià, V. Cádiz. Renewable benzoxazine monomers from "lignin-like" naturally occurring phenolic derivatives. *Journal of Polymer Science Part A: Polymer Chemistry.* **2013**, 51, 22, 4894-4903.

[21] F. Fenouillot, A. Rousseau, G. Colomines, R. Saint-Loup, J. P. Pascault. Polymers from renewable 1, 4: 3, 6-dianhydrohexitols (isosorbide, isomannide and isoidide): A review. *Progress in Polymer Science.* **2010**, 35, 5, 578-622.

[22] C-H. Lee, H. Takagi, H. Okamoto, M. Kato, A. Usuki. Synthesis, characterization, and properties of polyurethanes containing 1, 4:3, 6-dianhydro-D-sorbitol. *Journal of Polymer Science Part A: Polymer Chemistry.* **2011**, 47, 22, 6025-6031.

[23] R. Marin, S. Muñoz-Guerra. Carbohydrate-based poly (ester-urethane) s: A comparative study regarding cyclic alditols extenders and polymerization procedures. *Journal of Applied Polymer Science.* **2009**, 114, 6, 3723-3736.

[24] A. J. D. Silvestre, A. Gandini. Terpenes: major sources, properties and applications. *Monomers, Polymers and Composites from Renewable Resources* 1. **2008**, 2, 17-38.

[25] M. Winnacker, B. Rieger. Recent progress in sustainable polymers obtained from cyclic terpenes: synthesis, properties, and application potential. *ChemSusChem*. **2015**, 8, 15, 2455-2471..

[26] K. Satoh. Controlled/living polymerization of renewable vinyl monomers into bio-based polymers. *Polymer Journal*. **2015**, *47*(8), 527-536..

[27] P. A. de Jongh, P. K. Paul, E. Khoshdel, P. Wilson, K. Kempe, D. M. Haddleton. Thermal study of polyester networks based on renewable monomers citric acid and gluconolactone. *Polymer International*. **2017**, 66, 1, 59-63..

[28] E. Jäger, R. K. Donato, M. Perchacz, A. Jäger, F. Surman, A. Höcherl, H. S. Schrekker. Biocompatible succinic acid-based polyesters for potential biomedical applications: fungal biofilm inhibition and mesenchymal stem cell growth. *RSC Advances*. **2015**, 5, 104, 85756-85766..

[29] J. Xu, B. H. Guo. Microbial succinic acid, its polymer poly (butylene succinate), and applications. In *Plastics from Bacteria.* Springer Berlin Heidelberg. **2010**, 347-388.

[30] Y. Xia, R. C. Larock. Vegetable oil-based polymeric materials: synthesis, properties, and applications. *Green Chemistry.* **2010**, *12*, 11, 1893-1909.

[31] L. Montero de Espinosa, M. A. Meier. Plant oils: the perfect renewable resource for polymer science?!. *European Polymer Journal*. **2011**, 4*, 7*5, 837-852.

[32] G. Lligadas, J. C. Ronda, M. Galia, V. Cadiz. Renewable polymeric materials from vegetable oils: a perspective. *Materials Today*. **2013**, 16, 9, 337-343.

[33] S. Miao, P. Wang, Z. Su, S. Zhang. Vegetable-oil-based polymers as future polymeric biomaterials. *Acta Biomaterialia*. **2014**, 10, 4, 1692-1704.

[34] J. C. Ronda, G. Lligadas, M. Galià, V. Cádiz. Vegetable oils as platform chemicals for polymer synthesis. *European Journal of Lipid Science and Technology*. **2010**, 113, 1, 46-58.

[35] M. Galià, L. Montero de Espinosa, J. C. Ronda, G. Lligadas, V. Cádiz. Vegetable oil-based thermosetting polymers. *European Journal of Lipid Science and Technology*. **2010**, 112, 1, 87-96.

[36] A. Adhvaryu, S. Z. Erhan, Z. S. Liu, J. M. Perez. Oxidation kinetic studies of oils derived from unmodified and genetically modified vegetables using pressurized differential scanning calorimetry and nuclear magnetic resonance spectroscopy. *Thermochimica Acta*. **2000,** 364, 1, 87-97.

[37] F. Li, J. Hasjim, R. L. Larock. Synthesis, structure, and thermophysical and mechanical properties of new polymers prepared by the cationic copolymerization of corn oil, styrene, and divinylbenzene. *Journal of Applied Polymer Science*. **2003**, 90, 7, 1830-1838.

[38] K. A. Tallman, B. Roschek, N. A. Porter. Factors influencing the autoxidation of fatty acids: effect of olefin geometry of the nonconjugated diene. *Journal of the American Chemical Society*. **2004**, *126*, 30, 9240-9247.

[39] B. Çakmakli, B. Hazer, I. O. Tekin, F. B. Cömert. Synthesis and characterization of polymeric soybean oil-g-methyl methacrylate (and n-butyl methacrylate) graft

copolymers: biocompatibility and bacterial adhesion. *Biomacromolecules*. **2005**, *6*, 3, 1750-1758.

[40] F. Li, M. L. Hanson, R. C. Larock. Soybean oil–divinylbenzene thermosetting polymers: synthesis, structure, properties and their relationships. *Polymer*. **2001,** 42, 4, 1567-1579.

[41] F. Li, R. C. Larock. New soybean oil–styrene–divinylbenzene thermosetting copolymers. I. Synthesis and characterization. *Journal of Applied Polymer Science.* **2001,** 80, 4, 658-670.

[42] A. M. Motawie, E. A. Hassan, A. A. Manieh, M. E. Aboul-Fetouh, A. F. El-Din. Some epoxidized polyurethane and polyester resins based on linseed oil. *Journal of Applied Polymer Science*. **1995**, 55, 13, 1725-1732.

[43] T. Eren, S. H. Kusefoglu. Synthesis and polymerization of the acrylamide derivatives of fatty compounds. *Journal of Applied Polymer Science*. **2005**, 97, 6, 2264-2272.

[44] Z. S. Petrović. Polyurethanes from vegetable oils. *Polymer Reviews*. **2008**, 48, 1, 109-155.

[45] X. Pan, D. C. Webster. New biobased high functionality polyols and their use in polyurethane coatings. *ChemSusChem*. **2012**, 5, 2, 419-429.

[46] S. Sinadinović-Fišer, M. Janković, Z. S. Petrović. Kinetics of in situ epoxidation of soybean oil in bulk catalyzed by ion exchange resin. *Journal of the American Oil Chemists' Society*. **2001**, 78, 7, 725-731.

[47] X. Kong, J. Liu, J. M. Curtis. Novel polyurethane produced from canola oil based poly (ether ester) polyols: Synthesis, characterization and properties. *European Polymer Journal*. **2012**, 48, 12, 2097-2106.

[48] Z. S. Petrović, A. Zlatanić, C. C. Lava, S. Sinadinović-Fišer. Epoxidation of soybean oil in toluene with peroxoacetic and peroxoformic acids—kinetics and side reactions. *European Journal of Lipid Science and Technology*. **2002**, 104, 5, 293-299.

[49] C. Cai, H. Dai, R. Chen, C. Su, X. Xu, S. Zhang, L. Yang. Studies on the kinetics of in situ epoxidation of vegetable oils. *European Journal of Lipid Science and Technology*. **2008**, 110, 4, 341-346.

[50] T. Vlček, Z. S. Petrović. Optimization of the chemoenzymatic epoxidation of soybean oil. *Journal of the American Oil Chemists' Society*. **2006**, 83, 3, 247-252.

[51] S. Miao, S. Zhang, Z. Su, P. Wang. A novel vegetable oil–lactate hybrid monomer for synthesis of high-Tg polyurethanes. *Journal of Polymer Science Part A: Polymer Chemistry*. **2010**, 48, 1, 243-250.

[52] K. Saremi, T. Tabarsa, A. Shakeri, A. Babanalbandi. Epoxidation of soybean oil. *Annals of Biological Research*. **2012**, 3, 4254-4258.

[53] T. Vlček, Z. S. Petrović. Optimization of the chemoenzymatic epoxidation of soybean oil. *Journal of the American Oil Chemists' Society*. **2006**, 83, 3, 247-252.

[54] H. Dai, L. Yang, B. Lin, C. Wang, G. Shi. Synthesis and characterization of the different soy-based polyols by ring opening of epoxidized soybean oil with methanol, 1, 2-ethanediol and 1, 2-propanediol. *Journal of the American Oil Chemists' Society*. **2009**, 86, 3, 261-267.

[55] S. Caillol, M. Desroches, G. Boutevin, C. Loubat, R. Auvergne, B. Boutevin. Synthesis of new polyester polyols from epoxidized vegetable oils and biobased acids. *European Journal of Lipid Science and Technology*. **2012**, 114, 12, 1447-1459.

[56] A. Zlatanić, C. Lava, W. Zhang, Z. S. Petrović. Effect of structure on properties of polyols and polyurethanes based on different vegetable oils. *Journal of Polymer Science Part B: Polymer Physics*. **2004**, 42, 5, 809-819.

[57] B. K. Sharma, A. Adhvaryu, Z. Liu, S. Z. Erhan. Chemical modification of vegetable oils for lubricant applications. *Journal of the American Oil Chemists' Society*. **2006**, 83, 2, 129-136.

[58] E. Sharmin, S. M. Ashraf, S. Ahmad. Epoxidation, hydroxylation, acrylation and urethanation of Linum usitatissimum seed oil and its derivatives. *European Journal of Lipid Science and Technology*. **2007**, 109, 2, 134-146.

[59] E. Sharmin, S. M. Ashraf, S. Ahmad. Synthesis, characterization, antibacterial and corrosion protective properties of epoxies, epoxy-polyols and epoxy-polyurethane coatings from linseed and Pongamia glabra seed oils. *International journal of biological macromolecules*. **2007**, 40, 5, 407-422.

[60] H. P. Zhao, J. F. Zhang, X. Susan Sun, D. H. Hua. Syntheses and properties of cross-linked polymers from functionalized triglycerides. *Journal of Applied Polymer Science*. **2008**, 110, 2, 647-656.

[61] A. Guo, Y. Cho, Z. S. Petrović. Structure and properties of halogenated and nonhalogenated soy-based polyols. *Journal of Polymer Science Part A: Polymer Chemistry*. **2000**, 38, 21, 3900-3910.

[62] M. Ionescu, Z. S. Petrović, X. Wan. Ethoxylated soybean polyols for polyurethanes. *Journal of Polymers and the Environmental*. **2007**, 15, 237-243.

[63] C. S. Wang, L. T. Yang, B. L. Ni, G. Shi. Polyurethane networks from different soy-based polyols by the ring opening of epoxidized soybean oil with methanol, glycol, and 1, 2-propanediol. *Journal of Applied Polymer Science*. **2009**, 114, 1, 125-131.

[64] L. L. Monteavaro, E. O. da Silva, A. P. O. Costa, D. Samios, A. E. Gerbase, C. L. Petzhold. Polyurethane networks from formiated soy polyols: synthesis and mechanical characterization. *Journal of the American Oil Chemists' Society*. **2005**, 82, 5, 365-371.

[65] J. Lu, S. Khot, R.P. Wool. New sheet molding compound resins from soybean oil. I. Synthesis and characterization. *Polymer*. **2005**, 46, 1, 71-80.

[66] Y. Guo, J. H. Hardesty, V. M. Mannari, J. L. Massingill. Hydrolysis of epoxidized soybean oil in the presence of phosphoric acid. *Journal of the American Oil Chemists' Society*. **2007**, 84, 10, 929-935.

[67] X. Kong, G. Liu, J. M. Curtis. Novel polyurethane produced from canola oil based poly (ether ester) polyols: Synthesis, characterization and properties. *European Polymer Journal*. **2012**, 48, 12, 2097-2106.

[68] S. Miao, S. Zhang, Z. Su, P. Wang. Synthesis of bio-based polyurethanes from epoxidized soybean oil and isopropanolamine. *Journal of Applied Polymer Science*. **2013**, 127, 3, 1929-1936.

[69] G. Lligadas, J.C. Ronda, M. Galià, V. Cádiz. Oleic and undecylenic acids as renewable feedstocks in the synthesis of polyols and polyurethanes. *Polymers*. **2010**, 2, 4, 440-453.

[70] C. Lluch, J. C. Ronda, M. Galià, G. Lligadas, V. Cádiz. Rapid Approach to Biobased Telechelics through Two One-Pot Thiol−Ene Click Reactions. *Biomacromolecules*. **2010,** 11, 6, 1646-1653.

[71] H. Mutlu, L. Monetro de Espinosa, O. Türünç, M. A. Meier. About the activity and selectivity of less well-known metathesis catalysts during ADMET polymerizations. *Beilstein Journal of Organic Chemistry*. **2010**, 6,1, 1149-1158.

[72] Y. Xia, R. C. Larock. Castor oil-based thermosets with varied crosslink densities prepared by ring-opening metathesis polymerization (ROMP). *Polymer*. **2010**, 51, 12, 2508-2514.

[73] H. W. Engels, H. G. Pirkl, R. Albers, R. W. Albach, J. Krause, A. Hoffmann, J. Dormish. Polyurethanes: versatile materials and sustainable problem solvers for today's challenges. *Angewandte Chemie International Edition*. **2013**, 52, 36, 9422-9441.

[74] M. R. Chashmejahanbin, H. Daemi, M. Barikani, A. Salimi. Noteworthy impacts of polyurethane-urea ionomers as the efficient polar coatings on adhesion strength of plasma treated polypropylene. *Applied Surface Science*. **2014**, 317, 688-695.

[75] M. J. N. Pereira, B. Ouyang, C. A. Sundback, N. Lang, I. Friehs, S. Mureli, P. del Nido. A highly tunable biocompatible and multifunctional biodegradable elastomer. *Advanced Materials*. **2013**, 25, 8, 1209-1215.

[76] F. Zia, K. Zia, M. Zuber, S. Kamal, N. Aslam. Starch based polyurethanes: a critical review updating recent literature. *Carbohydrate Polymers*. **2015**, 134, 784-798.

[77] Q. W. Lu, R. R. Hoye, C. W. Macosko. Reactivity of common functional groups with urethanes: models for reactive compatibilization of thermoplastic polyurethane blends. *Journal of Polymer Science Part A: Polymer Chemistry*. **2002,** 40, 14, 2310-2328.

[78] C. Wang, L. Yang, B. Ni, L. Wang. Thermal and mechanical properties of cast polyurethane resin based on soybean oil. *Journal of Applied Polymer Science*. **2009**, 112, 3, 1122-1127.

[79] Z. S. Petrović, A. Guo, W. Zhang. Structure and properties of polyurethanes based on halogenated and nonhalogenated soy–polyols. *Journal of Polymer Science Part A: Polymer Chemistry*. **2000**, 38, 22, 4062-4069.

[80] A. Guo, I. Javni, Z. S. Petrovic. Rigid polyurethane foams based on soybean oil. *Journal of Applied Polymer Science*. **2000**, 77, 2, 467-473.

[81] Y. H. Hu, Y. Gao, D. N. Wang, C. P. Hu, S. Zu, L. Vanoverloop, D. Randall. Rigid polyurethane foam prepared from a rape seed oil based polyol. *Journal of Applied Polymer Science*. **2002**, 84, 3, 591-597.

[82] S. Tan, T. Abraham, D. Ference, C. W. Macosko. Rigid polyurethane foams from a soybean oil-based polyol. *Polymer*. **2011**, 52, 13, 2840-2846.

[83] Y. C. Tu, P. Kiatsimkul, G. Suppes, F. H. Hsieh. Physical properties of water-blown rigid polyurethane foams from vegetable oil-based polyols. *Journal of Applied Polymer Science*. **2007**, 105, 2, 453-459.

[84] H. Pawlik, A. Prociak. Influence of palm oil-based polyol on the properties of flexible polyurethane foams. *Journal of Polymers and the Environment*. **2012**, *20,* 2, 438-445.

[85] P. Rojek, A. Prociak. Effect of different rapeseed-oil-based polyols on mechanical properties of flexible polyurethane foams. *Journal of Applied Polymer Science*. **2012**, 125, 4, 2936-2945.

[86] A. Prociak, P. Rojek, H. Pawlik. Flexible polyurethane foams modified with natural oil based polyols. *Journal of Cellular Plastics*. **2012**, 48, 6, 489-499.

[87] Y. Lu, R. C. Larock. Soybean-oil-based waterborne polyurethane dispersions: effects of polyol functionality and hard segment content on properties. *Biomacromolecules*. **2008**, 9, 11, 3332-3340.

[88] Y. Lu, R. C. Larock. New hybrid latexes from a soybean oil-based waterborne polyurethane and acrylics via emulsion polymerization. *Biomacromolecules*. **2007**, 8, 10, 3108-3114.

[89] Y. Lu, R. C. Larock. Aqueous cationic polyurethane dispersions from vegetable oils. *ChemSusChem*. **2010**, 3, 3, 329-333.

[90] Y. Lu, R. C. Larock. Soybean oil-based, aqueous cationic polyurethane dispersions: Synthesis and properties. *Progress in Organic Coatings*. **2010**, 69, 1, 31-37.

[91] Y. Lu, R. C. Larock. Synthesis and properties of grafted latices from a soybean oil-based waterborne polyurethane and acrylics. *Journal of Applied Polymer Science*. **2011**, 119, 6, 3305-3314.

[92] Y. Lu, Y. Xia, R. C. Larock. Surfactant-free core–shell hybrid latexes from soybean oil-based waterborne polyurethanes and poly (styrene-butyl acrylate). *Progress in Organic Coatings*. **2011**, 71, 4, 336-342.

[93] S. Chuayjuljit, A. Maungchareon, O. Saravari. Preparation and properties of palm oil-based rigid polyurethane nanocomposite foams. *Journal of Reinforced Plastics and Composites*. **2008**.

[94] U. Stirna, U. Cabulis, I. Beverte. Water-blown polyisocyanurate foams from vegetable oil polyols. *Journal of Cellular Plastics*. **2008**, 44, 2, 139-160.

[95] A. Campanella, L. M. Bonnaillie, R. P. Wool. Polyurethane foams from soyoil-based polyols. *Journal of Applied Polymer Science*. **2009**, 112, 4, 2567-2578.

[96] Z. S. Petrović, I. Cvetković, D. Hong, X. Wan, W. Zhang, T. Abraham, I. Malsam. Polyester polyols and polyurethanes from ricinoleic acid. *Journal of Applied Polymer Science*. **2008**, 108, 2, 1184-1190.

[97] A. Palanisamy, M. S. L. Karuna, T. Satyavani, D. R. Kumar. Development and characterization of water-blown polyurethane foams from diethanolamides of karanja oil. *Journal of the American Oil Chemists' Society*. **2011**, 88, 4, 541-549.

[98] A. Palanisamy, B. S. Rao, S. Mehazabeen. Diethanolamides of castor oil as polyols for the development of water-blown polyurethane foam. *Journal of Polymers and the Environment*. **2011**, 19, 3, 698-705.

[99] S. Yadav, F. Zafar, A. Hasnat, S. Ahmad. Poly (urethane fatty amide) resin from linseed oil—A renewable resource. *Progress in Organic Coatings.* **2009**, 64, 1, 27-32.

[100] P. D. Meshram, R. G. Puri, A. L. Patil, V. V. Gite. High performance moisture cured poly (ether–urethane) amide coatings based on renewable resource (cottonseed oil). *Journal of Coatings Technology and Research*. **2013**, 10, 3, 331-338.

[101] T. Vanbésien, A. Sayede, E. Monflier, F. Hapiot. A self-emulsifying catalytic system for the aqueous biphasic hydroformylation of triglycerides. *Catalysis Science & Technology*. **2016**, 6, 9, 3064-3073.

[102] T. Vanbésien, E. Monflier, F. Hapiot. Hydroformylation of vegetable oils: More than 50 years of technical innovation, successful research, and development. *European Journal of Lipid Science and Technology*. **2016**, 118, 1, 26-35.

[103] H. P. Benecke, B. R. Vijayendran, D. B. Garbark, K. P. Mitchell. Low Cost and Highly Reactive Biobased Polyols: A Co-Product of the Emerging Biorefinery Economy. *CLEAN–Soil, Air, Water*. **2008**, 36, 8, 694-699.

[104] M. Desroches, M. Escouvois, R. Auvergne, S. Caillol, B. Boutevin. From vegetable oils to polyurethanes: synthetic routes to polyols and main industrial products. *Polymer Reviews*. **2012**, 52, 1, 38-79.

[105] S. Caillol, M. Desroches, S. Carlotti, R. Auvergne, B. Boutevin. Synthesis of new polyurethanes from vegetable oil by thiol-ene coupling. *Green Materials*. **2013**, 1, 1, 16-26.

[106] M. Desroches, S. Caillol, V. Lapinte, R. Auvergne, B. Boutevin. Synthesis of biobased polyols by thiol− ene coupling from vegetable oils. *Macromolecules*. **2011**, 44, 8, 2489-2500.

[107] O. Türünç, M. A. Meier. The thiol-ene (click) reaction for the synthesis of plant oil derived polymers. *European Journal of Lipid Science and Technology*. **2013**, 115, 1, 41-54.

[108] R. J. González-Paz, C. Lluch, G. Lligadas, J. C. Ronda, M. Galià, V. Cádiz. A green approach toward oleic-and undecylenic acid-derived polyurethanes. *Journal of Polymer Science Part A: Polymer Chemistry*. **2011**, 49, 11, 2407-2416.

[109] D. V. Palaskar, A. Boyer, E. Cloutet, J. F. Le Meins, B. Gadenne, C. Alfos, H. Cramail. Original diols from sunflower and ricin oils: Synthesis, characterization, and use as polyurethane building blocks. *Journal of Polymer Science Part A: Polymer Chemistry*. **2012**, 50, 9, 1766-1782.

[110] O. Kreye, T. Tóth, M. A. Meier. Copolymers derived from rapeseed derivatives via ADMET and thiol-ene addition. *European Polymer Journal*. **2011**, 47, 9, 1804-1816.

[111] O. Vogl, G. D. Jaycox, K. Hatada. Macromolecular design and architecture. *Journal of Macromolecular Science-Chemistry*. **1990**, 27, 13-14, 1781-1854.

[112] M. A. Gauthier, M. I. Gibson, H. A. Klok. Synthesis of Functional Polymers by Post-Polymerization Modification. *Angewandte Chemie International Edition*. **2009**, 48, 1, 48-58.

[113] D. K. Chattopadhyay, D. C. Webster. Thermal stability and flame retardancy of polyurethanes. *Progress in Polymer Science*. **2009**, 34, 10, 1068-1133.

[114] P. Krol. Synthesis methods, chemical structures and phase structures of linear polyurethanes. Properties and applications of linear polyurethanes in polyurethane elastomers, copolymers and ionomers. *Progress in Materials Science*. **2007**, 52, 6, 915-1015.

[115] P. Espeel, F. Goethals, F. Driessen, L. T. T. Nguyen, F. E. Du Prez. One-pot, additive-free preparation of functionalized polyurethanes via amine–thiol–ene conjugation. *Polymer Chemistry*. **2013**, 4, 8, 2449-2456.

[116] P. Espeel, F. Goethals, F. E. Du Prez. One-pot multistep reactions based on thiolactones: extending the realm of thiol− ene chemistry in polymer synthesis. *Journal of the American Chemical Society*. **2011**, 133, 6, 1678-1681.

[117] R. Marín, M. de Paz, N. Ittobane, J. A. Galbis, S. Muñoz-Guerra. Hydroxylated linear polyurethanes derived from sugar alditols. *Macromolecular Chemistry and Physics*. **2009**, 210, 6, 486-494.

[118] B. Begines, F. Zamora, I. Roffé, M. Mancera, J. A. Galbis. Sugar-based hydrophilic polyurethanes and polyureas. *Journal of Polymer Science Part A: Polymer Chemistry*. **2011**, 49, 9, 1953-1961.

[119] Z. Xie, C. Lu, X. Chen, L. Chen, X. Hu, Q. Shi, X. Jing. A facile approach to biodegradable poly (ε-caprolactone)-poly (ethylene glycol)-based polyurethanes containing pendant amino groups. *European Polymer Journal*. **2007**, 43, 5, 2080-2087.

[120] L. Billiet, O. Gok, A. P. Dove, A. Sanyal, A. L. T. T. Nguyen, F. E. Du Prez. Metal-free functionalization of linear polyurethanes by thiol-maleimide coupling reactions. *Macromolecules.* **2011**, 44, 20, 7874-7878.

[121] D. Fournier, B. G. De Geest, F. E. Du Prez. On-demand click functionalization of polyurethane films and foams. *Polymer*. **2009**, 50, 23, 5362-5367.

[122] M. Basko, M. Bednarek, L. Billiet, P. Kubisa, E. Goethals, F. Du Prez. Combining cationic ring-opening polymerization and click chemistry for the design of functionalized polyurethanes. *Journal of Polymer Science Part A: Polymer Chemistry*. **2011**, 49, 7, 1597-1604.

[123] C. Ott, C. D. Easton, T. R. Gengenbach, S. L. McArthur, P. A. & Gunatillake. Applying "click" chemistry to polyurethanes: a straightforward approach for glycopolymer synthesis. *Polymer Chemistry*. **2011**, 2, 12, 2782-2784.

[124] J. Huang, W. Xu. Efficient synthesis of zwitterionic sulfobetaine group functional polyurethanes via "click" reaction. *Journal of Applied Polymer Science*. **2011**, 122, 2, 1251-1257.

[125] D. Fournier, F. Du Prez. "Click" chemistry as a promising tool for side-chain functionalization of polyurethanes. *Macromolecules*. **2008**, 41, 13, 4622-4630.

[126] L. Billiet, D. Fournier, F. Du Prez. Step-growth polymerization and 'click'chemistry: The oldest polymers rejuvenated. *Polymer*. **2009**, 50, 16, 3877-3886.

[127] C. Ferris, M. V. de Paz, J. A. Galbis. L-arabinitol-based functional polyurethanes. *Journal of Polymer Science Part A: Polymer Chemistry*. **2011**, 49, 5, 1147-1154.

[128] C. Ferris, M. V. de Paz, J. A. Galbis. Synthesis of Functional Sugar-Based Polyurethanes. *Macromolecular Chemistry and Physics*. **2012**, 213, 5, 480-488.

[129] R. J. González-Paz, G. Lligadas, J. C. Ronda, M. Galià, V. Cádiz. Thiol-yne Reaction of Alkyne-derivatized Fatty Acids. *Journal of Renewable Materials*. **2013**, 1, 3, 187-194.

[130] R. J. González-Paz, G. Lligadas, J. C. Ronda, M. Galia, V. Cádiz. Thiol–yne reaction of alkyne-derivatized fatty acids: biobased polyols and cytocompatibility of derived polyurethanes. *Polymer Chemistry*. **2012**, 3, 9, 2471-2478.

[131] H. Sardon, J. M. Chan, R. J. Ono, D. Mecerreyes, J. L. Hedrick. Highly tunable polyurethanes: organocatalyzed polyaddition and subsequent post-polymerization modification of pentafluorophenyl ester sidechains. *Polymer Chemistry*. **2014**, 5, 11, 3547-3550.

[132] L. Maisonneuve, O. Lamarzelle, E. Rix, E. Grau, H. Cramail. Isocyanate-free routes to polyurethanes and poly (hydroxy urethane) s. *Chemical reviews*. **2015**, 115, 22, 12407-12439.

[133] J. E. Moses, A. D. Moorhouse. The growing applications of click chemistry. *Chemical Society Reviews*. **2007**, 36, 8, 1249-1262.

[134] C. R. Becer, R. Hoogenboom, U. S. Schubert. Click Chemistry beyond Metal-Catalyzed Cycloaddition. *Angewandte Chemie International Edition*. **2009**, 48, 27, 4900-4908.

[135] B. S. Sumerlin, A. P. Vogt. Macromolecular engineering through click chemistry and other efficient transformations. *Macromolecules*. **2009**, 43, 1, 1-13.

[136] A. Dondoni. The emergence of thiol–ene coupling as a click process for materials and bioorganic chemistry. *Angewandte Chemie International Edition*. **2008**, 47, 47, 8995-8997.

[137] S. M. Trey, C. Nilsson, E. Malmström, M. Johansson. Thiol–ene networks and reactive surfaces via photoinduced polymerization of allyl ether functional hyperbranched polymers. *Progress in organic coatings*. **2010**, 68, 1, 151-158.

[138] M. Bardts, H. Ritter. Microwave Assisted Synthesis of Thiol Modified Polymethacrylic acid and Its Cross-Linking with Allyl Modified Polymethacrylic acid via Thiol-ene "Click" Reaction. *Macromolecular Chemistry and Physics*. **2010**, 211, 7, 778-781.

[139] P. Lundberg, A. Bruin, J. W. Klijnstra, A. M. Nyström, M. Johansson, M. Malkoch, A. Hult. Poly (ethylene glycol)-Based Thiol-ene Hydrogel Coatings– Curing Chemistry, Aqueous Stability, and Potential Marine Antifouling Applications. *ACS applied materials & interfaces*. **2010**, 2, 3, 903-912.

Chapter 3

Synthesis of Castor-Oil Based Polyurethanes Bearing Alkene/yne Groups and Subsequent Thiol-ene/yne Post-Polymerization Modification

This chapter is focused on studying the potential of photoinitiated thiol-ene/yne coupling reaction in the post-polymerization modification process. The introduction of thioglycerol can tune the thermo, mechanical and superficial properties.

UNIVERSITAT ROVIRA I VIRGILI
AVANCES EN SISTEMAS INTERACTIVOS PARA PERSONAS CON PARÁLISIS CEREBRAL
Marc Comí Bonachí

3.1. Introduction

As has been commented at the end of general introduction, highly efficient "click" chemistry methodologies have been increasingly used for post-polymerization functionalization of polymers, during the last decades.[1-3] One of the more relevant methodologies is the introduction of unsaturations in side-chain positions of polymers. In polyesters, polyamides, polyureas and polyurethanes, the polymerization functional monomers strategy permits the facile introduction of alkene/alkyne groups.[4-6] The classical diol monomers used to synthesize functionalized polymers with akene or alkyne pendant groups are represented in Figure 3.1. Usually, these are used in segmented polymer or with chain extenders to create crosslinking points and tuning the final properties.[7]

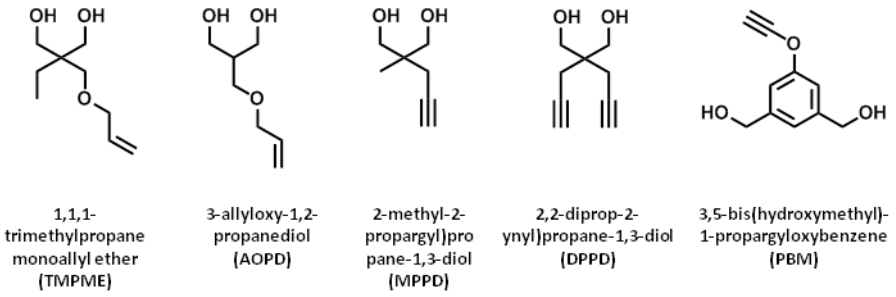

Figure 3.1. Classical diols with alkene/yne pendant groups

One of the most used click reaction applied in a wide range of research fields is the Huisgen 1,3-dipolar addition of azides and alkynes.[8-11] Regarding to post-polymerization modification process applied to polyurethanes (PUs), some strategies have been reported.[12-15] For example, Fournier and Du Prez have shown that Huisgen 1,3-dipolar addition is a promising tool for side-chain functionalization of PUs. They are designed linear PUs having alkyne groups located along the backbone by reacting two different alkyne-functionalized diols (DPPD and PBM shown in Figure 1) with a diisocyanate compound. In the second part of the work, the cooper catalyzed Huisgen 1,3-dipolar cycloaddition was undertaken between the alkyne-functionalized PUs and a variety of azide compounds such as benzyl azide and different fluorinated azide compounds, resulting in side-chain functionalized PUs with varying degree of functionalization.[12] Moreover, Huang and his co-workers have developed the synthesis

and functionalization of PUs containing zwitterionic sulfobetaine groups by the cooper-catalyzed 1,3-dipolar cycloaddition to DPPD (Figura 3.1) main-chain PU units.[13] Recently, Ott et al. was reported a synthetic route to prepare PUs with pendant sugar-moieties in the side-chain of the PU through incorporation of diverse chain extenders (AOPD and DPPD shown in Figure 3.1) capable of undergoing either copper catalyzed Huisgen 1,3-dipolar cycloaddition or thiol-ene click reactions.[14]

This kind of "click" reaction presents a limitation for a several applications due to the presence of copper catalyst. Therefore, it exist efficient reactive systems that do not contain any metal catalyst, such as light-mediated thiol-ene[16,17] and thiol-yne[18-20] radical reactions have become widely used as they effectively combine some benefits of coupling reactions with the advantages of a photoinitiated process resulting in a powerful method for chemical synthesis and tailorable material fabrication. The introduction of new functional groups is carried out attacking the polymer double and triple bonds with a thiol-containing group, such as mercaptoethanol[21] or 3-mercaptopropionic acid in the case that is wanted introduced hydroxyl or carboxylic acid groups into polymer.

The most relevant thiol coupling processes are: thiol-ene (TEC) and thiol-yne (TYC) coupling reaction. The photochemicallly/thermally-induced version of TEC is known to proceded by a radical mechanism to give an anti-Markovnikov-type thioether as shown in Scheme 3.1. This selectivity has been explained by the enhanced stability of the intermediate carbon radical upon addition to the less substituted alkene carbon.[16,17,22] TEC reactions are incorporated inside the click concept because of can be controlled with light, there is no need for an external catalyst, addition is regioselective, reaction conditions are compatible with water and oxygen, they are very atom efficient, they typically give quantitative yields and they are tolerant of a wide variety of functional groups.[23]

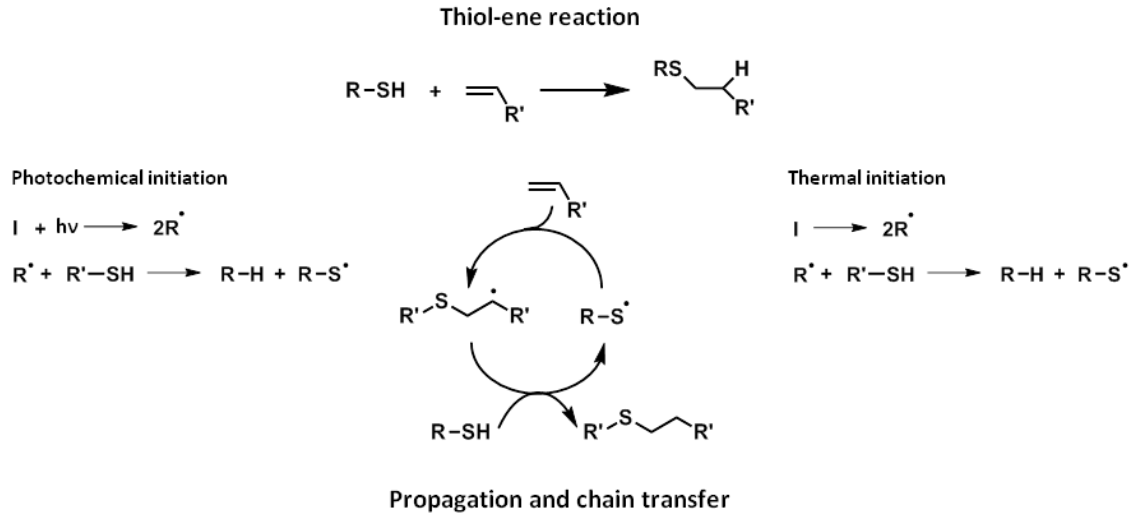

Scheme 3.1. The radical-mediated TEC reaction mechanism

In addition, the TYC reaction is regarded as a sister reaction of radical-mediated TEC reaction. From the viewpoint of mechanism, TYC reaction has three types: free-radical, amine-mediated, and transition-metal catalyzed processes. Moreover, depending on the initiator, the free radical process could be further divided into photo- and thermo-initiated reactions. Scheme 3.2 shows the radical mediated two cycle mechanism of the prevalent TYC click reaction.[24,25]

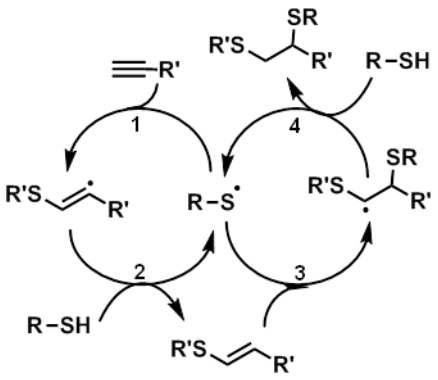

Scheme 3.2. The radical-mediated TYC reaction mechanism

Firstly, the thiyl radicals will be generated from thiol groups by photo- or thermo-initiation process. The step 1, the thiyl radical adds across the ethynyl group to form a vinyl sulfide radical, which could attract a hydrogen atom from a thiol group in the step 2, producing the vinyl sulfide and generating another thiyl radical at the same time. In the step 3 a thiyl radical adds across the double bond of the vinyl sulfide, generating a

dithioether radical, which attracts a hydrogen atom from a thiol groups in the step 4 and forms the disubstituted product and a new thiyl radical.

Whilst in general post-polymerization modification of side-chain functionalized PUs have been widely studied during the past decade through the development of click reactions leading to a variety of usages in polymer chemistry, the photoinitiation TEC and TYC reactions has received limited attention in post-polymerization modification of PU systems. In the few examples described, the pendant reactive groups are introduced into final PU via polymerization of functional monomers. As an example, Basko et al. designs a method for the synthesis of PUs bearing pendant functionalities at the hard–soft segment. Reactive alkyne groups were introduced by cationic ring-opening polymerization of glycidyl propargyl ether using different oligodiols as macroinitiators. The resulting oligodiols, with alkyne side groups located at both chain ends, were subsequently reacted with 1,4-butanediol and hexamethylene diisocyanate (HDI) for the synthesis of PUs. The functionalized PUs have been further modified via photoinitiated thiol–yne coupling reactions with benzyl mercaptan and thioglycerol.[26]

The post-polymerization modification of PUs with reactive side-chain functional groups can develop new properties, such as thermal, mechanical or surface properties. Existing PUs are highly hydrophobic, thus practically leading to limitation in their biomedical applications due to the lack of desirable hydrophilicity. Hydrophilic properties of polyurethanes are usually adjusted by using hydrophilic polyols (such as ethylene oxide based ones) or specific isocyanates.[27] Therefore, new functional bio-based PUs bearing hydrophilic reactive pendant groups such as hydroxyl, carboxyl, amino, and so forth become attractive. The presence of hydroxyls pendant groups permit to PUs absorb water much more than classical PUs and may have applications where water absorption and retention are desirable.[28] Although, it has been reported a enhanced hydrophilicity in PUs by the introduction of hydroxyl groups ring opening of cyclic carbonates with diisocyanate group, this methodology is limited as only two groups per repeating unit are incorporated.[29]

In this chapter, is presented a new facile and versatile strategy based on the incorporation of allyl- and propargyl-groups to diols, step-growth polymerization and the thiol-ene/thiol-yne coupling[12,17] to prepare aliphatic bio-based PUs bearing reactive hydroxyl pendant groups under mild conditions. This was achieved by ring-opening of 10,11-epoxyundecan-1-ol by unsaturated secondary amines to obtain diols that were polymerized with isophorone diisocyanate (IPDI) to produce PUs with pendant alkene and alkyne groups. Finally, these unsaturated side groups have been used as modification sites for further functionalization with thioglycerol as hydrophilic compound.

3.2. Results and discussion

3.2.1. Synthesis of diols

The straightforward and upscalable synthesis of functionalized PUs presented in this chapter is based on obtaining functional diols from 10-undecen-1-ol. This compound can be obtained from castor oil chemical treatment. Castor oil is extracted from the seeds of the castor bean plant (*Ricinus communis*), which is a member of the large spurge family (Euphorblaceae), located in tropical Asia and Africa. Castor oil contains up to 90% of ricinoleic acid, a monounsaturated 18-carbon fatty acid with a hydroxyl function at position 12, which tends to cleavage upon heating. Thus, 10-undecenoic acid can be obtained from the pyrolysis of castor oil at high temperature (>400°C) under vacuum that cleaves the ricinoleate molecule yielding this compound and heptaldehyde. Several mechanisms, including a McLafferty-type rearrangement[30] (Scheme 3.3) and a free-radical mechanism[31] have been proposed for the transformation of ricinoleic acid into 10-undecenoic acid and heptaldehyde. The obtention was carried out by catalytic reduction of the 10-undecenoic acid.

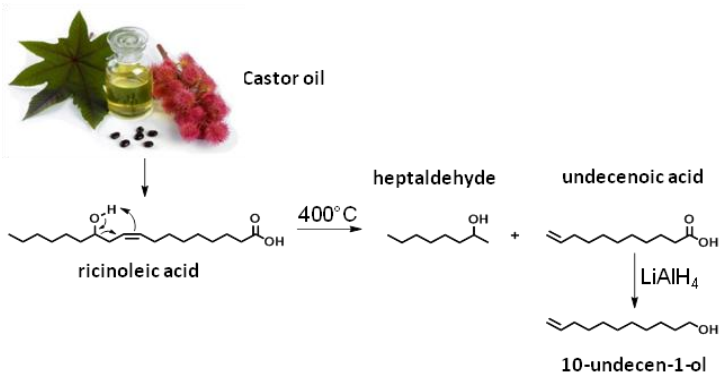

Scheme 3.3. Synthetic route to obtain 10-undecen-1-ol from castor oil

10-undecen-1-ol containing a terminal double bond can be functionalized by different synthetic routes to obtain another a diol. In the case of fatty acids, epoxidation of carbon-carbon double bonds in backbone chain of fatty acid followed by nucleophilic oxirane ring opening is one of the most important and widely studied reactions to produce diols with different functionalities. Carboxylic acid group of fatty acid permits the use of methodologies more eco-friendly without subproducts and with high yields. On the contrary, the epoxidation of 10-undecen-1-ol present some drawbacks related with the formation of ring-opening subproducts due to the large reaction times when it is applied methodologies with green peracids or enzymes. Thus, 10,11-epoxyundecan-1-ol was prepared in 90% yield by reaction of 10-undecen-1-ol with a slight molar excess of 3-chloroperoxybenzoic acid (MCPBA) in 1,2-dichloroethane at 80 °C. The ^{1}H NMR spectrum of the epoxy compound is shown in Figure 3.2, and displays multiplets at about 3.0, 2.8 and 2.5 ppm, corresponding to resonances of the three protons bonded directly to the oxirane ring, along with the complete absence of the vinylic proton signals near 5.8 and 5.0 ppm in the spectrum of starting compound.

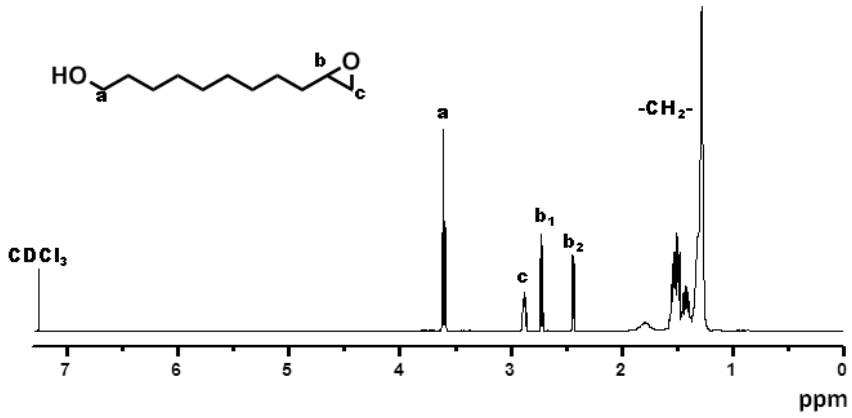

Figure 3.2. ^{1}H NMR spectra of 10,11-epoxy-undecan-1-ol

Afterwards, the ring-opening process of epoxides, catalyzed with boron trifluoride ethylamine complex, resulted highly regioselective and in good yields (87-91%) The scheme of reaction is shown in Figure 3.3. Allyl and propargyl amines were used in the reaction with 10,11-epoxyundecan-1-ol for preparing functional aminodiols with different fatty pendant groups. The amines to synthetize D1 and D2 are N-allylmethylamine and N-methylpropargylamine both commercial, but N-allylpropargylamine was nesecessary to produce by reaction of allylamine with propargyl chloride.[32]

The structural characterization of aminodiols are shown in Figure 3 where it represent their ^{1}H NMR spectra and the corresponding peak assignments, with resonances (ppm) for D_1: one CH_3 peak at 2.24 ppm and the CH_2=CH unsaturation at 5.14 ppm and 5.82 ppm. For D_2: one CH_3 peak at 2.34 ppm and the C≡CH triple bond unsaturation at 2.24 ppm and for D_3 both CH_2=CH unsaturations at 5.19 ppm and 5.78 ppm and the C≡CH triple bond unsaturation at 2.18 ppm. As can be seen, only the ring-opening of the oxirane by the amine nucleophilic attack on the less substituted carbon of the oxirane ring is observed, and in all cases one CH attached to the OH group at 3.62 ppm appears. It is worth noting that show diasterotopic protons (c) are observed in the spectra of D1 and D3, and diasterotopic proton (e) are observed in the spectra of D2 and D3.

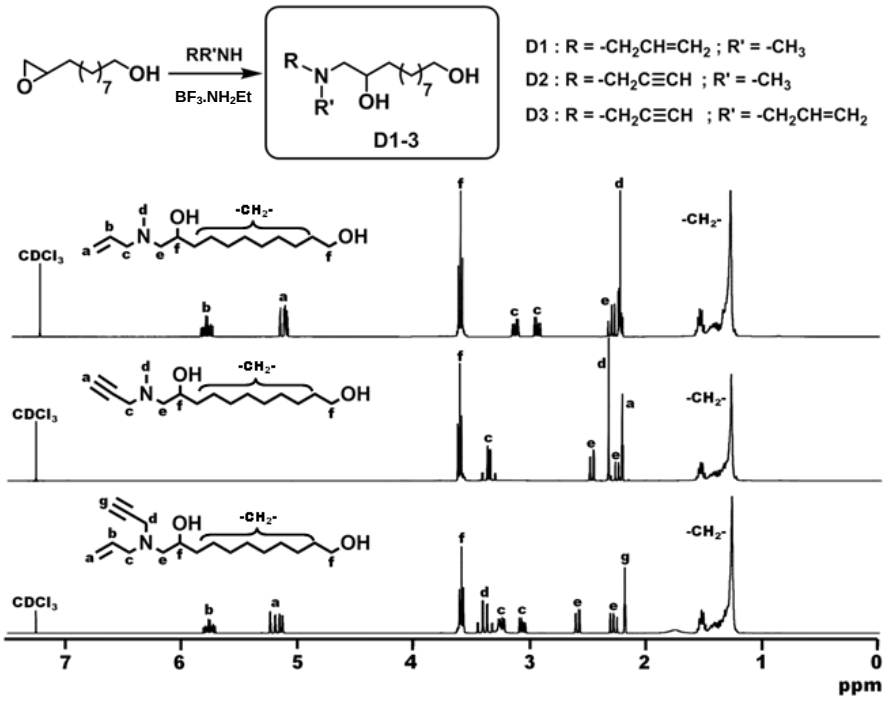

Figure 3.3. ^{1}H NMR spectra of diols D1-3

3.2.2. Polyurethane synthesis

A series of polyurethanes (PUD1-3) were prepared from equimolar amounts of the synthesized aminodiols (D1-3) and commercially available IPDI in DMF solution at 60 °C for 24 h using tin(II) 2-ethylhexanoate as catalyst. IPDI was used owing to its lower toxicity compared to the other commercially available diisocyanates. Moreover, due to its cyclic and asymmetric structure, IPDI is known to enhance the solubility of the PUs, which has been explained as resulting from increasing the free volume between polymer chains.[33] The possibility to form side products depends on the reaction conditions and the diisocyanate used to prepare the polyurethane. Generally, urea, allophanate, biuret, and isocyanurate are the side products that may form during the reaction, but in this case they are not detected under these conditions. The presence of orgatin as catalyst and tertiary amine pendant group in the structure of diols clearly promotes the formation of urethane bond.

PUs were obtained in high yields (86-95%) and showed good solubility in commonly used organic solvents. The molecular weights of PUs were evaluated by SEC and resulted similar in the three cases: M_w PUD1 about 45000 Da, M_w PUD2 48000 Da, M_w PUD3 46000 Da and dispersity (*D* = 1.4). SEC data indicate the formation of reasonably high molar mass polymers. However, the molar mass values provided by SEC should not be taken as absolute values as the SEC calibration was carried out using polystyrene standards.

The structural characterization of PUs was carried out by NMR and FTIR spectroscopy. IPDI is an asymmetric cycloaliphatic diisocyanate and contains Z and E isomers in a 3:1 ratio. The two-isocyanate groups are chemically different; one is bonded directly to cycloaliphatic ring (NCO_{sec}) and the other is bonded through a primary carbon (NCO_{prim}). The molecule consists of a mixture of two isomers, *cis* (Z) and *trans* (E), corresponding to the R and S configuration at C-5, respectively. For each of these isomers, the reactivity of the two NCO groups is different. Thus, different types of NCO groups and urethane moieties are formed during the reaction of the IPDI-diols prepolymers, and are present in the reaction mixture at same time. Now, by ^{1}H NMR spectroscopy we are able to distinguish and quantify the Z and E isomers that are present in the PU.[34]

In Figure 3.4(a) the ^{1}H NMR spectrum of polyurethane from D1 and IPDI is shown as a mixture of both isomers. Signals corresponding to both isomers have unequivocally been identified by means of 2-D NMR gCOSY as is observed in Figure 3.4(b) and HSQCAD spectra. Protons corresponding to the cyclic IPDI were identified: at 3.79 ppm signal (h) corresponding to methine ring undistinguishable for both isomers, and at 3.24 and 2.91 ppm signals (s and i) corresponding to methylene linked to urethane of E and Z isomers. Moreover, while the urethane proton signals from the isocyanate bonded directly to cycloaliphatic ring (j) are undistinguishable for both isomers, the urethane proton signals from the isocyanate bonded through a primary carbon are distinguished, and appears at 4.82 and 4.70 ppm (k and o) for E and Z isomers. The ratio Z/E isomers was 3:1 calculated from signals (s and i) corresponding to methylene linked to urethane.

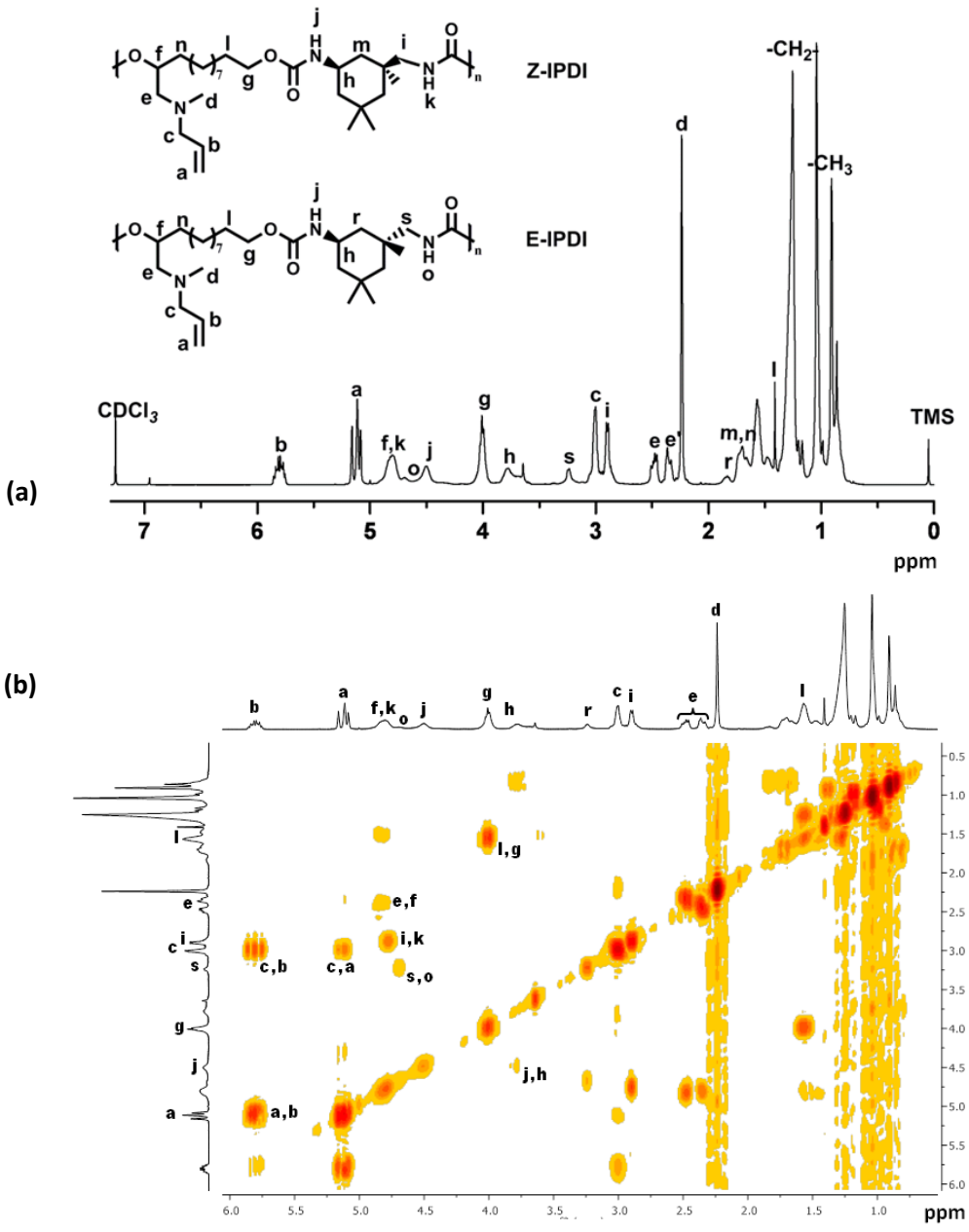

Figure 3.4. (a)^{1}H NMR and (b) 2D NMR gCOSY spectrum of polyurethane from D1 and IPDI.

Moreover, FTIR spectroscopic characterization revealed the expected structural features, including the disappearance of the vibrational band of NCO function, located at 2235 cm^{-1} and the appearance absorption bands of the main chain about 1694, 3320 and 1522 cm^{-1} arising from urethane linkages corresponding to C=O stretching and NH stretching and bending bands respectively.

3.2.3. Polymer modification with thioglycerol

To access the highly functional polyurethanes, thiol-ene (TEC) and thiol-yne (TYC) couplings could be associated. Thiol-ene/yne chemistry was used for grafting functional groups onto polyurethanes bearing double and/or triple bonds that are very reactive.[26,35] Thioglycerol in excess was both added on terminal double bond by TEC and terminal propargylic unsaturation by TYC. The TYC splits in two cycle mechanism taking place the 1,2 double addition to the alkyne. The photoinduced radical addition of thioglycerol into unsaturation carried out at room temperature in presence of DMPA photoinitiator for 2h. Thanks to a simple work-up, the highly functional moieties: 2OH (diol) from PUD1, 4OH (tetraol) from PUD2 and 6OH (hexaol) from PUD3 were successfully synthesized in good yields in all cases (about 80 %). The molecular structure is shown in Figure 3.5.

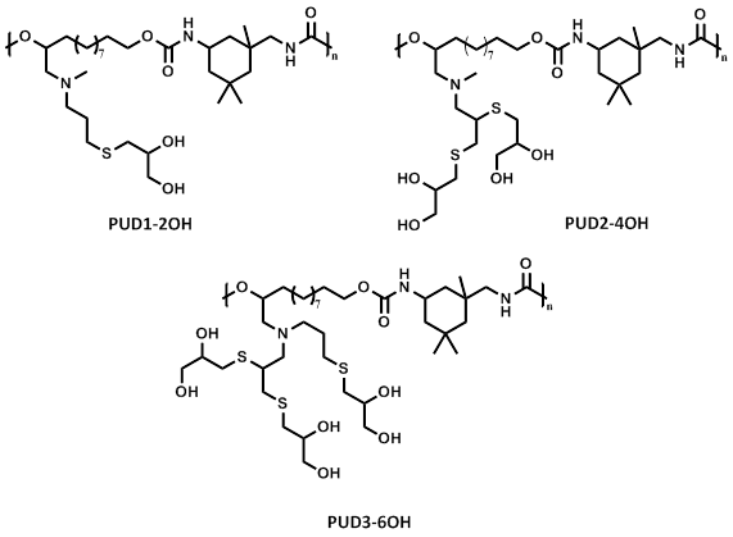

Figure 3.5. Structure of modified PUD1, PUD2 and PUD3 with thioglycerol

SEC analysis of modified PUs: PUD-OHs, gave slightly higher molecular weight values than PUDs. Mw PUD1-2OH about 50000 Da, Mw PUD2-4OH 55000 Da, Mw PUD3-6OH 52000 Da and polydispersity index = 1.5, showing that no degradation occurs along the thiol-ene or thiol-yne coupling. In comparison to PUD1-3, these increases in molecular weight values could be explained by increased branching in the PU chains which makes longer retention times.

The ^{1}H NMR spectra confirmed the chemical structure of modified PUs as illustrated in Figure 3.6 of a representative modified PUD1. The occurrence of thiol-ene reaction was evidenced by the disappearance of characteristic double bond signals at 5.81 and 5.13 ppm and the appearance of new signals corresponding to the coupled thioglycerol, i.e. a complex signal between 2.75 and 2.45 ppm for both methylene directly bonded to sulphur (p and q) and at 3.80 ppm and 3.65 ppm signals of the methane (u) and methylene (t) directly bonded to hydroxyls (assigned by gHSQCAD spectrum).

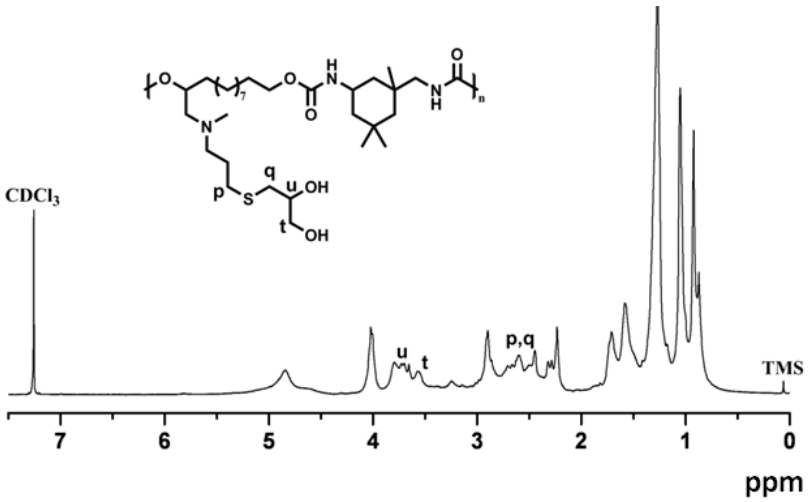

Figure 3.6. ^{1}H NMR spectrum of PUD1 after thiol-ene reaction with thioglycerol

For modified PUD2 and PUD3 although their ^{1}H NMR spectra show broad signals, the disappearance of the ^{1}H NMR signal of the propargyl methylene protons around 3.35-3.40 ppm, along with the appearance of the signals to the coupled thioglycerol are observed. For all reactions performed, the ^{1}H NMR results indicated the occurrence of double addition of thiol molecules to the reacted alkyne groups. The absence of a monothiol adduct and thus the absence of double bonds in the final products after the coupling reaction is in accordance with earlier observations on thiol-yne reactions.[3] It was previously described that the addition of the first thiol to the alkyne is the rate-limiting step, which is followed by the fast second thiol addition to the intermediate thiol-alkene.[36]

To confirm the occurrence of thiol-ene/yne reactions on PUD2 and PUD3, Raman spectra were registered at different times. Figure 3.7 shows spectra as a function of time of reaction of PUD3 with thioglycerol. At first, the characteristic peaks of double and triple bonds of PUD3 at 1644 and 2105 cm^{-1} respectively, clearly appear. After 15 min, only the thiol-ene coupling appears to be started, as signal of triple bond remained unchanged but at 30 min triple bond peak is scarcely observed. The spectrum at 60 min shows the total dissapareance of double and triple bond confirming thiol-ene/yne occurred.

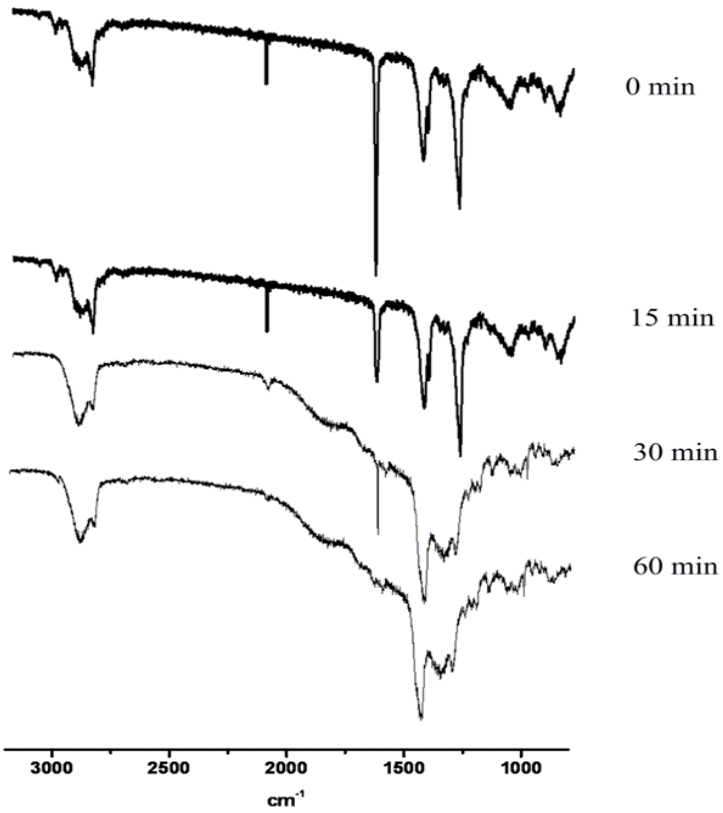

Figure 3.7. Raman spectra of PUD3 and thiol-ene/yne reaction with thioglycerol at different times

3.2.4. Thermal, mechanical and contact angle properties

Thermal characterization of PUDs and modified PUD-OHs was carried out by DSC, DMA and TGA under N_2 atmosphere at a heating rate of 10 °C/min. The DSC traces are shown in Figure 3.8 and the data are summarized in Table 3.1. No melting peaks were observed thus PUs are not semicrystalline. As expected, the presence of cycloaliphatic ring, pendant alkyl chains or asymmetry of the monomer enhances the free volume and hence hinders the packing of the polymer chains. The glass transition temperatures (T_gs) of the three PUDs were near 40 °C and lower T_gs, between 5 ºC and 18 ºC, were found for the modified PUD-OHs. Indeed the presence of high density hydrogen bonding due to the presence of tertiary amine increases the rigidity and thus strongly suppresses the mobility of the polymer chains. Besides the presence of the dangling chains after the modification of PUDs with thioglycerol could act as plasticizers decreasing their T_g values. On the other hand the possibility of hydrogen bonding in PUD3-6OH is higher than in PUD1-2OH increasing its T_g around 13 °C.

.

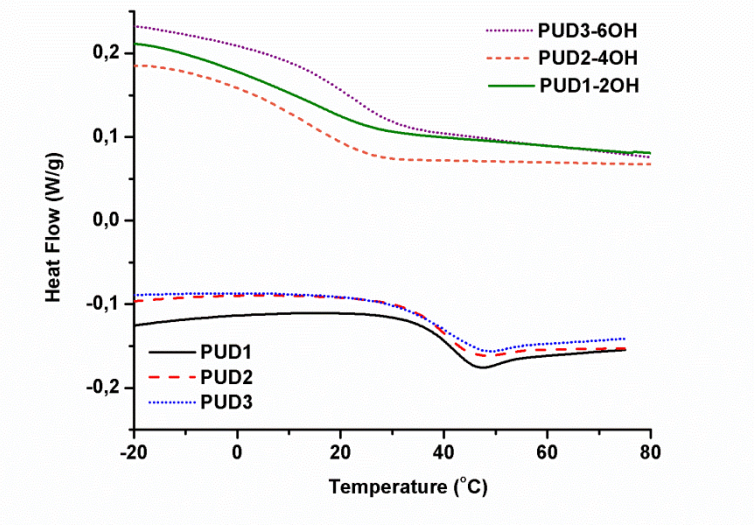

Figure 3.8. DSC traces of amorphous PUD1-3 and PUD-OHs

Table 3.1. Thermal properties for the PUD1-3 and PUD-OHs.

	DSC	DMA	TGA	
Sample	T_g (°C)	T_g(°C)	$T_{5\%}$ (°C)[a]	Td (°C)[b]
PUD1	41	51	281	319/441
PUD2	39	53	282	315/421
PUD3	40	53	290	317/453
PUD1-2OH	5	21	223	312/420
PUD2-4OH	11	26	203	301/423
PUD3-6OH	18	31	186	303/431

[a]Temperature at which 5% weight loss was observed.
[b]Temperature for maximum degradation rate.

The dynamic mechanical behaviour was also investigated as a function of temperature. DMA results are summarized in Table 3.1 and correlated with the data from DSC analysis. The curves of tan δ *versus* temperature, of the three PUDs and the modified PUD-OHs are shown in Figure 3.9. The glass transition temperatures, estimated from DMA as the maximum of tan δ, are in good agreement with the DSC values as ½ ΔCp. The observed differences are explainable by the way of measurement. Indeed, DSC and DMA measure changes of the heat capacity and the mechanical response of the polymer chains during the transition, respectively.

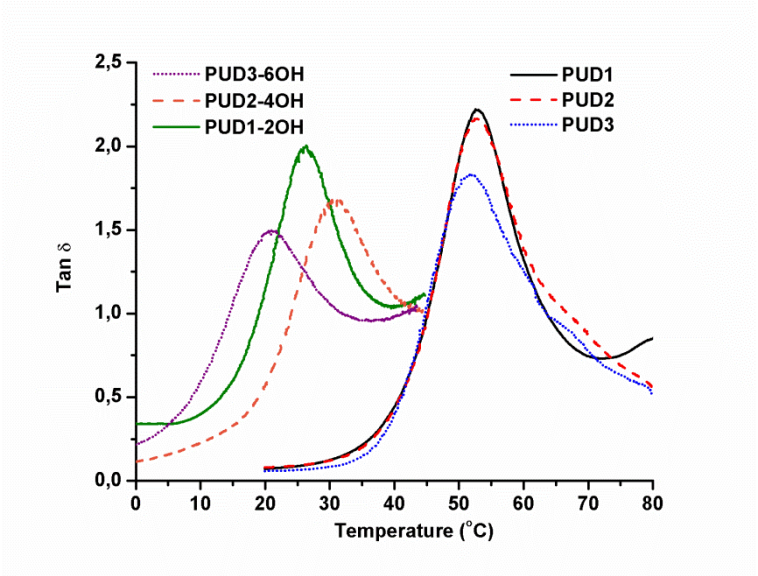

Figure 3. 9. Tan δ as a function of temperature for PUD1-3 and PUD-OHs

Thermal stability of PDU1-3 and modified PUD1-3 with thioglycerol was investigated by TGA in a nitrogen stream and data are summarized in Table 3.1. In general, PUs present low heat resistance due to the presence of thermo-labile urethane linkage. Overall, the PUs were found to have a typical complex decomposition behaviour as clearly displayed by the TGA derivatives of the weight loss as a function of temperature are shown in Figure 3.10. All polymers showed an initial weight loss in the range of 180-280 °C, suggesting that degradation starts at the urethane bond. Studies on the decomposition of the urethane bond indicate that decomposition initial temperature of the urethane bond depends on the structure of both the isocyanate and the diol, and it takes place through dissociation to isocyanate and alcohol, the formation of primary amines and olefins and the formation of secondary amines and carbon dioxide.[37] It can be observed that the initial degradation temperatures are shifted to lower temperature with increasing polyol OH-functionality, i.e for modified PUD-OHs.

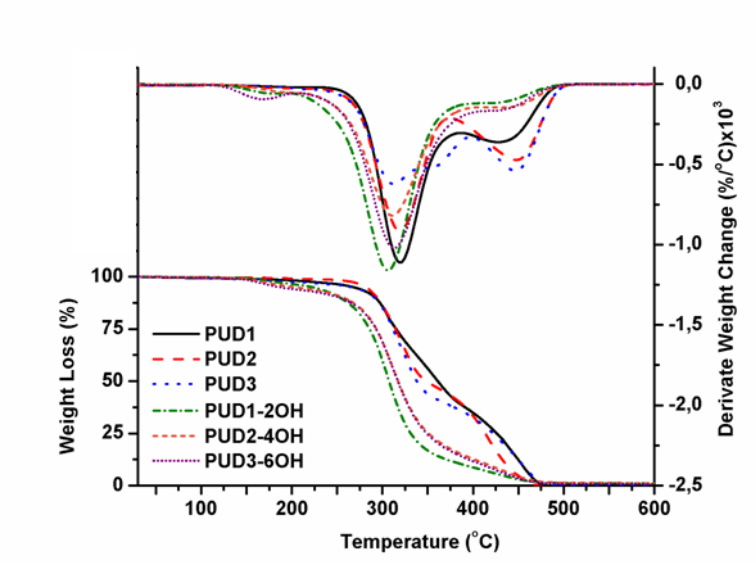

Figure 3.10. TGA and first derivative traces of PUD1-3 and PUD-OHs.

The main degradation step is associated with the aliphatic moieties of the remaining structure and occurs at similar temperatures for all PUs (300-320 °C). This degradation is produced at lower temperature than the one described for conventional oil-derived

aliphatic PUs (i.e castor oil- derived PU)[38] and could be related with the dissociation of the amine and thioether bonds[39] that confer lower stability to the prepared PUs. Finally, the third degradation stage (over 400 °C) is more prominent in the case of the unmodified PUs (a) but occurs at similar temperatures and corresponds to the gasification of any remaining components.[35]

To explain the mechanical behaviour at room temperature, tensile tests were performed on PUDs and PUD-OHs: the Young 's modulus, elongation at break, stress at break and toughness and their standard deviation are given in Table 3.2. The stress-strain curves are depicted in Figure 3.11.

Table 3.2. Mechanical properties of PUD1-3 and PUD-OHs

Sample	Young Modulus (Mpa)	Elongation at break (%)	Stress at break (MPa)	Toughness (MJ/m3)
PUD1	683±9	48.0±0.6	6.72±0.20	456±7
PUD2	726±9	47.0±0.6	5.88±0.18	450±6
PUD3	774±9	45.0±0.6	7.51±0.21	412±6
PUD1-2OH	6.0±0.0	401±6	0.17±0.00	352±4
PUD2-4OH	19.0±0.1	255±3	1.17±0.01	426±5
PUD3-6OH	24.0±0.1	153±2	1.47±0.06	375±4

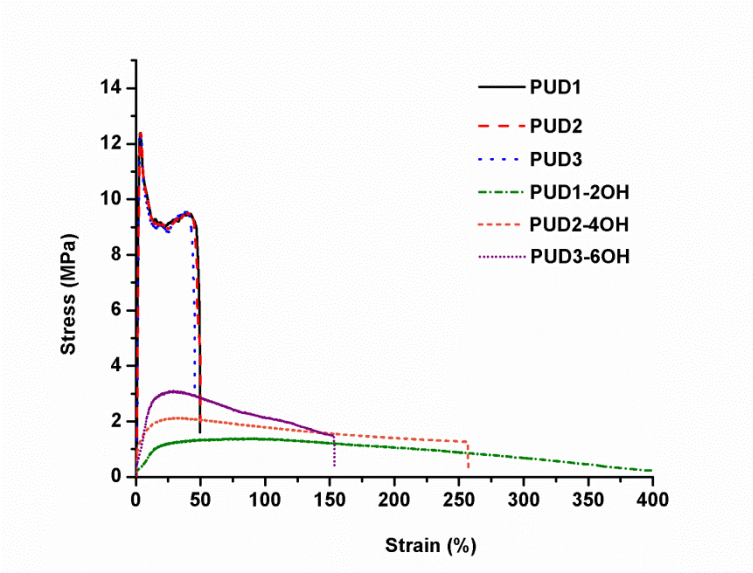

Figure 3.11. Tensile stress versus strain curves of PUD1-3, PUD1-2OH, PUD2-4OH and PUD3-6OH.

Similar high Young's modulus was observed for the three PUDs but significantly lower moduli were obtained for the modified PUD-OHs. The last ones show a behaviour similar to slightly crosslinked amorphous rubbers with low modulus and smooth transition in their stress-strain behaviour. In addition the elongation at break is similar for the three PUDs and higher than that for PUD-OHs. The mechanical properties of these bio-based polymers (E modulus from 683-774 MPa to 6-24 MPa and at break from 45% to 401%) make them suitable materials for a large range of applications.

Hydrophilicity/hydrophobicity balance strongly affects the material applications. PUs prepared from vegetable oils are expected to exhibit a non-wetting surface due to the hydrophobic nature of triglycerides. Contact angle measurements demonstrated the high hydrophobicity of the synthesized PUDs (PUD1: 108 °; PUD2: 110 °; PUD3: 104 °). Modified PUD-OHs were more hydrophilic showing contact angle values of PUD1-2OH: 89 °; PUD2-4OH: 83 °; PUD3-6OH: 77 °). These results agree with the increase of the dangling hydroxyl moieties. Pictures of the contact angle measurements of the PDU3 and PUD3-6OH, after modification with thioglycerol, are shown in Figure 3.12(a), and confirm the change of the surface properties of both films. When hydrophilic treatment was undertaken (pictures on the bottom left), the drop of water spreads over the PU film due to a higher interaction between water and the newly modified PU material.

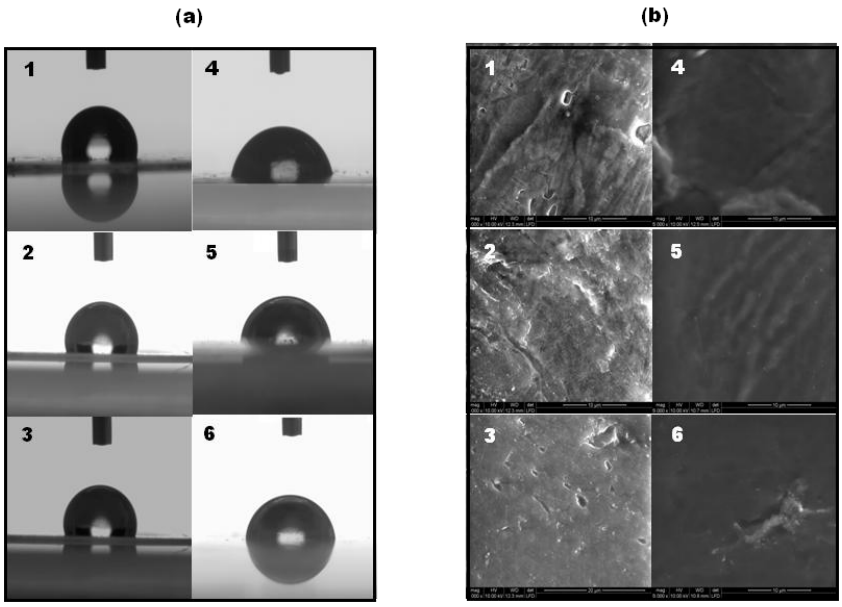

Figure 3.12. Contact angle (a) and ESEM images (b) of PUD1 (1), PUD2 (2), PUD3 (3), PUD1-2OH (4), PUD2-4OH (5), PUD3-6OH (6)

ESEM images of the surface structures show the morphology of surface-modified samples compared to unmodified samples are shown in Figure 3.12(b). The first is accounted for by roughness or heterogeneous composition that is, a surface composition characterized by domains of different surface tensions. The rough hydrophobic surface makes it difficult for water to penetrate the crevices and cracks. After modification, the micrograph of PUD3-6OH shows a more homogeneous distribution on the surface. The results, also interpreted on the basis of SEM micrographs, show that not only hydroxyl terminated bond is the reason of hydrophilic nature of the film, but its homogeneous composition helps a great deal in achieving a greater hydrophilicity of the film.

In brief, an efficient route to obtain allyl- and propargyl-containing diols, that were then polymerized with IPDI to produce alkene- and alkyne-functionalized PUs is described. By thiol-ene/yne coupling of thioglycerol into unsaturation a series of PUs with enhanced hydrophilicity were obtained. Hydroxy-PUs demonstrated variable thermal and mechanical properties depending on the tioglycerol content, which could be explained by the partial breaking of inherent hydrogen bonds in the PU precursor and the new formation of hydrogen bonds between introduced hydroxyl groups and PU chains. The physical interactions are and important approach and permit tuning the PU properties.

3.3. References

[1] H. C. Kolb, M. G. Finn, K. B. Sharpless. Click chemistry: diverse chemical function from a few good reactions. *Angewandte Chemie International Edition*. **2001**. 40, 11, 2004-2021.

[2] M. J. Kade, D. J. Burke, C. J. Hawker. The power of thiol-ene chemistry. *Journal of Polymer Science Part A: Polymer Chemistry*. **2010**, 48, 4, 743-750.

[3] R. Hoogenboom. Thiol–yne chemistry: A powerful tool for creating highly functional materials. *Angewandte Chemie International Edition*. **2010**, 49, 20, 3415-3417.

[4] M. A. Gauthier, M. I. Gibson, H. A. Klok. Synthesis of Functional Polymers by Post-Polymerization Modification. *Angewandte Chemie International Edition*. **2009**, 48, 1, 48-58.

[5] L. Billiet, D. Fournier, F. Du Prez. Combining "click" chemistry and step-growth polymerization for the generation of highly functionalized polyesters. *Journal of Polymer Science Part A: Polymer Chemistry*. **2008**, 46, 19, 6552-6564.

[6] Y. Z. Wang, X. X. Deng, L. Li, Z. L. Li, F. S. Du, Z. C. Li. One-pot synthesis of polyamides with various functional side groups via Passerini reaction. *Polymer Chemistry*. **2013**, 4, 3, 444-448.

[7] K. Hearon, M. A. Wierzbicki, L. D. Nash, T. L. Landsman, C. Laramy, A. T. Lonnecker, K. L. A. Wooley. Processable Shape Memory Polymer System for Biomedical Applications. *Advanced Healthcare Materials*. **2015**. 4, 9, 1386-1398.

[8] D. Fournier, B. G. De Geest, F. E. Du Prez. On-demand click functionalization of polyurethane films and foams. *Polymer*. **2009**. 50, 23, 5362-5367.

[9] L. Billiet, D. Fournier, F. E. Du Prez. Step-growth polymerization and 'click'chemistry: The oldest polymers rejuvenated. *Polymer*. **2009**. 50, 16, 3877-3886.

[10] L. T. T. Nguyen, J. Devroede, K. Plasschaert, L. Jonckheere, N. Haucourt, F. E. Du Prez. Providing polyurethane foams with functionality: a kinetic comparison of different "click" and coupling reaction pathways. *Polymer Chemistry*. **2013**. 4, 5, 1546-1556.

[11] X. Li, J. Hu, D. Sun, Y. Zhang. Nanosilica reinforced waterborne siloxane-polyurethane nanocomposites prepared via "click" coupling. *Journal of Coatings Technology and Research*. **2014**. 11, 4, 517-531.

[12] P. Espeel, F. E. Du Prez. "Click"-inspired chemistry in macromolecular science: matching recent progress and user expectations. *Macromolecules*. **2014**, 48, 1, 2-14.

[13] J. Huang, S. Gu, R. Zhang, Z. Xia, W. Xu. Synthesis, spectroscopic, and thermal properties of polyurethanes containing zwitterionic sulfobetaine groups. *Journal of Thermal Analysis and Calorimetry*. **2013**, 112, 3, 1289-1295.

[14] C. Ott, C. D. Easton, T. R. Gengenbach, S. L. McArthur, P. A. Gunatillake. Applying "click" chemistry to polyurethanes: a straighforward approach for glycopolymer synthesis. *Polymer Chemistry.* **2011**, *2,* 2782-2784.

[15] D. Fournier, B. G. De Geest, F. E. Du Prez. On-demand click functionalization of polyurethane films and foams. *Polymer*. **2009**, 50, 23, 5362-5367.

[16] C. E. Hoyle, C. N. Bowman. Thiol–ene click chemistry. *Angewandte Chemie International Edition*. **2010**. 49, 9, 1540-1573.

[17] A. B. Lowe. Thiol-ene "click" reactions and recent applications in polymer and materials synthesis. *Polymer Chemistry*. **2010**. 1, 1, 17-36.

[18] V. T. Huynh, G. Chen, P. D. Souza, M. H. Stenzel. Thiol–yne and Thiol–ene "Click" chemistry as a tool for a variety of platinum drug delivery carriers, from statistical copolymers to crosslinked micelles. *Biomacromolecules*. **2011**. 12, 5, 1738-1751.

[19] S. B. Rahane, R. M. Hensarling, B. J. Sparks, C. M. Stafford, D. L. Patton. Synthesis of multifunctional polymer brush surfaces via sequential and orthogonal thiol-click reactions. *Journal of Materials Chemistry*. **2012**. 22, 3, 932-943.

[20] M. Bednarek. Coupling reaction with thiols as the efficient method of functionalization of ''clickable" polylactide. *Reactive and Functional Polymers*. **2013**. 73, 8, 1130-1136.

[21] C. Ferris, M. V. de Paz, J. A. Galbis. L-arabinitol-based functional polyurethanes. *Journal of Polymer Science Part A: Polymer Chemistry*. **2011**, 49, 5, 1147-1154.

[22] M. J. Kade, D. J. Burke, C. J. Hawker. The power of thiol-ene chemistry. *Journal of Polymer Science Part A: Polymer Chemistry*. **2010**, 48, 4, 743-750.

[23] K. Griesbaum. Problems and possibilities of the free-radical addition of thiols to unsaturated compounds. *Angewandte Chemie International Edition in English*. **1970**, 9, 4, 273-287.

[24] A. B. Lowe, C. E. Hoyle, C. N. Bowman. Thiol-yne click chemistry: A powerful and versatile methodology for materials synthesis. *Journal of Materials Chemistry*. **2010**, 20, 23, 4745-4750.

[25] A. B. Lowe. Thiol-yne 'click'/coupling chemistry and recent applications in polymer and materials synthesis and modification. *Polymer*. **2014**, 55, 22, 5517-5549.

[26] M. Basko, M. Bednarek, L. T. T. Nguyen, P. Kubisa, F Du Prez. Functionalization of polyurethanes by incorporation of alkyne side-groups to oligodiols and subsequent thiol–yne post-modification. *European Polymer Journal*. **2013**, 49, 11, 3573-3581.

[27] I. Javni, D. P. Hong, Z. S. Petrović. Polyurethanes from soybean oil, aromatic, and cycloaliphatic diamines by nonisocyanate route. *Journal of Applied Polymer Science*. **2013**. 128, 1, 566-571.

[28] H. Bakhshi, H. Yeganeh, S. Mehdipour-Ataei. Synthesis and evaluation of antibacterial polyurethane coatings made from soybean oil functionalized with dimethylphenylammonium iodide and hydroxyl groups. *Journal of Biomedical Materials Research Part A*. **2013**. 101, 6, 1599-1611.

[29] L. Maisonneuve, O. Lamarzelle, E. Rix, E. Grau, H. Cramail. Isocyanate-free routes to polyurethanes and poly (hydroxy urethane) s. *Chemical reviews*. **2015**, 115, 22, 12407-12439.

[30] M. Van der Steen, C. V. Stevens. Undecylenic acid: a valuable and physiologically active renewable building block from castor oil. *ChemSusChem*. **2009**. 2, 8, 692-713.

[31] G. Das, R. K. Trivedi, A. K. Vasishtha. Heptaldehyde and undecylenic acid from castor oil. *Journal of the American Oil Chemists' Society*. **1989**. 66, 7, 938-941.

[32] Y. Li, T. J. Marks. Organolanthanide-Catalyzed Intra- and Intermolecular Tandem C–N and C–C Bond-Forming Processes of Aminodialkenes, Aminodialkynes, Aminoalkeneynes, and Aminoalkynes. New Regiospecific Approaches to Pyrrolizidine, Indolizidine, Pyrrole, and Pyrazine Skeletons. *Journal of the American Chemical Society***. 1998**, 120, 8, 1757-1771.

[33] L. Maisonneuve, T. Lebarbé, T. H. N. Nguyen, E. Cloutet, B. Gadenne, C. Alfos, H. Cramail. Hydroxyl telechelic building blocks from fatty acid methyl esters for the synthesis of poly (ester/amide urethane)s with versatile properties. *Polymer Chemistry*. **2012**. 3, 9, 2583-2595.

[34] A. Prabhakar, D. H. Chattopadadhyay, B. Jagadeesh, K. V. S. N. Raju. Structural investigations of polypropylene glycol (PPG) and isophorone diisocyanate (IPDI)-based polyurethane prepolymer by 1D and 2D NMR spectroscopy. *Journal of Polymer Chemistry Part A Polymer Chem*istry. **2005**, *11*, 1196-1209.

[35] P. D. Pham, V. Lapinte, Y. Raoul, J-J. Robin. Lipidic polyols using thiol-ene/yne strategy for crosslinked polyurethanes. *Journal of Polymer Chemistry Part A Polymer Chem*istry. **2014**, *52*, 1597-1606.

[36] B. D. Fairbanks, E. A. Sims, K. S. Anseth C. N. Bowman. Reaction Rates and mechanisms for radical, photoinitiated addition of thiols to alkynes, and implications for thiol-yne photopolymerizations and click reactions. *Macromolecules*, **2010**, *43*, 4113-4119.

[37] I. Javni, Z. S. Petrović, A. Guo, R. Fuller. Thermal stability of polyurethanes based on vegetable oils. *Journal Applications of Polymer Science.* **2000**, *77*, 1723-1734.

[38] I. Ristic, Z. D. Bjelovic, B. Holló, K. M. Szécsenyi, J. Budinski-Simendic, M. Lazic, M. Kicanovic. Thermal stability of polyurethane materials based on castor oil as polyol component. *Journal of Thermal and Analitical Calorimetry.* **2013**, *111*, 1083-1091.

[39] M. Calle, G. Lligadas, J. C. Ronda, M. Galià, V. Cádiz. Non-isocyanate route to biobased polyurethanes and polyureas via AB-type self-polycondensation. *European Polymer Journal*. **2016**, *84*, 837-848.

Chapter 4

Carboxylic Acid Ionic Modification of Castor-Oil Based Polyurethanes Bearing Amine Groups. Correlation between chemical structure and physical properties.

f

This chapter is devoted to the preparation of supramolecular ionic polyurethanes via acid-base reaction of tertiary amine pendant polyurethane with different carboxylic acids. *The physical properties depend on the chemical structure of the acid incorporated*

UNIVERSITAT ROVIRA I VIRGILI
AVANCES EN SISTEMAS INTERACTIVOS PARA PERSONAS CON PARÁLISIS CEREBRAL
Marc Comí Bonachí

4.1. Introduction

The combination of non-covalent chemistry and polymer science has lead to the emergence of the relatively new field of supramolecular polymer chemistry. The supramolecular concept has attracted increasing attention in macromolecular science in the last three decades, as one can design new supramolecular architectures by the employ of non-covalent synthesis. Non-covalent synthesis is a versatile, diverse and programmable approach to new supramolecular compositions where the properties of the resulting assembles is dependent and derived from specific non-covalent bonding interactions.[1] The non-covalent interactions most employed in supramolecular polymer chemistry are hydrogen bonding, [2-7] metal coordination,[8-10] electoestatic,[11-13] host-guest complexation[14] and π-π stacking.[15,16] Compared to the strong, nonreversible covalent bonds, the weak non-covalent bonds are generally stimuli-responsive, that is, they exhibit reversible association–dissociation behavior on exposure to external stimulus such as light, heat or chemicals. These reversible behaviors endow supramolecular polymers with versatile functions, such as facile processing/recycling,[4,17,] self-healing,[18-21] shape memory[22-25] and high responsivity to stimuli.[26,27]

There are two types of supramolecular polymers which can be categorized into main-[28,29] and side-chain[30,31] supramolecular polymers. Main-chain supramolecular polymers where non-covalent interactions are employed between monomer units to fabricate homopolymers and block copolymers as are shown in Figure 4.1(a). Polymers based on this concept combine many of the attractive features of conventional polymers with properties that result from the reversibility of the bonds between monomeric units. In this case, non-covalent interactions can be adjusted to control specific parameters that determine final polymer properties, such as degree of polymerization, lifetime of the chain and structural conformation.[1]

In contrast, side-chain supramolecular polymers are polymers in which the polymer backbone is based on covalent bonds while the side-chains of the polymer are non-covalently functionalized as is shown in Figure 4.1(b). The main benefit of non-covalent side-chain functionalization is that it combines the robustness of the covalent main-

chain polymer along with the reversibility and flexibility of non-covalent interactions, and hence has been used extensively in synthesizing tailor-made materials with controlled architectures and properties.[2] These materials are composed by fourth relevant parts: the polymer backbone, the side-chain, the non-covalent complex and the functional moiety.

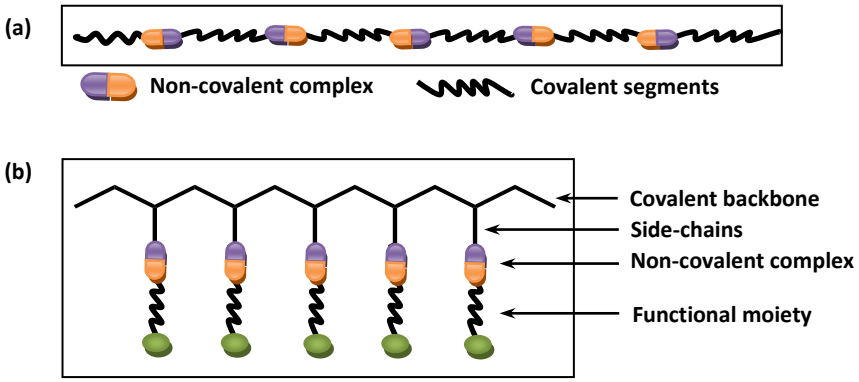

Figure 4.1. Schemmatic representation of (a) main- and (b) side-chain supramolecular polymers.

Generally it exist three strategies to obtain side-chain supramolecular polymers (Scheme 4.1): a) the recognition motifs covalently attached to the polymer backbone are introduced in a post-polymerization step followed by self-assembly, b) the monomers containing terminal recognition units are polymerized and subsequently functionalized and c) the self-assembly step precede the polymerization.[31]

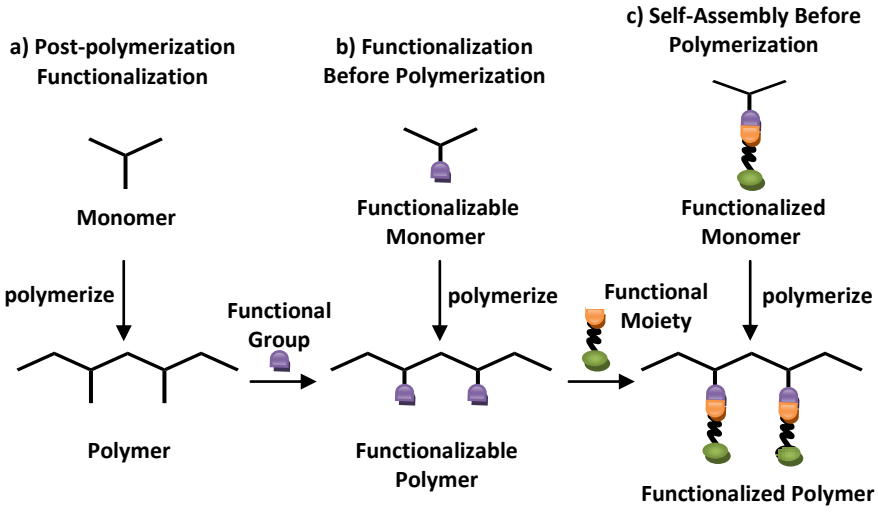

Scheme 4.1. Schematic display of various functionalization strategies.

Over the past few years, several approaches have been used to enhance the properties of polyurethanes (PUs), in this way the synthesis of supramolecular PUs (SPUs) can receive relevant attention. Because non-covalent bonds are reversible, the material properties of SPUs offer an additional level of control through choice of prepolymer constituents and the nature of non-covalent forces that are used.[32] One of the non-covalent interactions more used in the synthesis of SPUs is based on hydrogen bonding. For example, in several reports Chen et al. have reported on pyridine containing SPUs as stimuli responsive materials.[33-36] SPUs based on hydrogen bonds are synthesized from N'N-bis(2-hydroxylethyl) isonicotinamine (BINA), hexamethylene diisocyanate (HDI), and 1,4 butanediol (BDO). Both permanent and reversible net points are reportedly established through hydrogen bonding: the former through the phase separation and H-bonding of BDO-isocyanate segments and the latter through H-bonding interactions between the pyridine ring and urethane N-H group.

In addition, ionic interactions are among the most widely encountered non-covalent interactions in SPUs systems rivaled only by hydrogen bonding interactions in their frequency.[37] The most relevant example of using ionic interactions in materials science is in the field of ionomers which are tailor-made materials. Ionomers are widely used commercially due to their unique physical properties such as enhanced impact strength, thoughness and thermal reversibility.[38] The majority of the ionic functionalized side-chain polymers are based on post-polimerization functionalizations to elude severe interference of the charged ionic centers during the synthesis. The interest in ionomers stems from the large property changes that result from interchain supramolecular bonding of the contact ion pairs. In the last decade, it has increase attention for SPUs ionomers which contains side-chain ionic groups due to for their unique properties with applications in the field of coatings and adhesives. Recently, thermoplastic PU (TPU) sulfonate ionomers with quaternarium ammonium cations were shynthesized for the purpose of internally plasticising TPU.[39]

Moreover, ionic hydrogen bonds are defined as ionic interactions in some reports,[40-43] but in fact as a particular type of hydrogen bond with potential proton transfer between organic cations, such as primary or secondary amine or quaternary ammonium, and anions, such as carboxylates and sulfates groups.[44,45] These bonds are

usually formed by mixing acid and base, the classical acid-base reaction.[46,47] Whilst this type of reversible non-covalent interaction has been used to construct supramolecular systems in recent years,[48-51] in PU systems has not received attention despite is modular character an ease of synthesis.

Hence, in this chapter is described a new attractive and adaptable strategy based on the incorporation of tertiary amine group to diol, step growth polymerization and the side-chain introduction of common carboxylic acids to prepare aliphatic bio-based SPUs under mild conditions. This was achieved by ring-opening of 10,11-epoxyundecen-1-ol by diethylamine to obtain diol that was polymerized with isophorone diisocyanate (IPDI) to produce side-chain functionalized polyurethanes with tertiary amine pendant group. Finally, these tertiary amines side-chain groups have been used as tethered point for further functionalization with different carboxylic acids as supramolecular material.

4.2. Results and discussion

4.2.1. Synthesis of Polyurethanes

In this chapter, the main aim of this work is to develop and efficient and facile methodology to obtain side-chain functionalized monomer from 10-undecen-1-ol. For this reason taking advantage of the previous chapter synthesis was proposed to prepare side-chain tertiary amine group monomer. To simplify the study, it was prepared one monomer only with two functionalities, on the one hand the hydroxyls groups that they were used to polymerize and the tertiary amine pendant group.

As first stage the synthesis of diol was carried out, as described in the previous chapter.[52] The oxirane ring opening of 10,11-epoxyundecan-1-ol with diethylamine, catalysed with boron trifluoride ethylamine complex, was used to prepare the functional aminodiol (D4) with high regioselectivity and in good yield (93%). Its ^{1}H NMR spectrum, recorded in CD_3OD and the corresponding peak assignments are shown in

Figure 4.2. As can be seen, H_b and H_c protons appear as two double quadruplets and two double doblets respectively, due to the non-equivalence of the CH_2 protons when internal hydrogen bonding is present. When the ^1H NMR spectrum was recorded in $CDCl_3$ similar patterns were found but when it was recorded in DMSO-d_6, only a quadruplet was observed for H_b, showing that in this case hydrogen bonding was less significant.

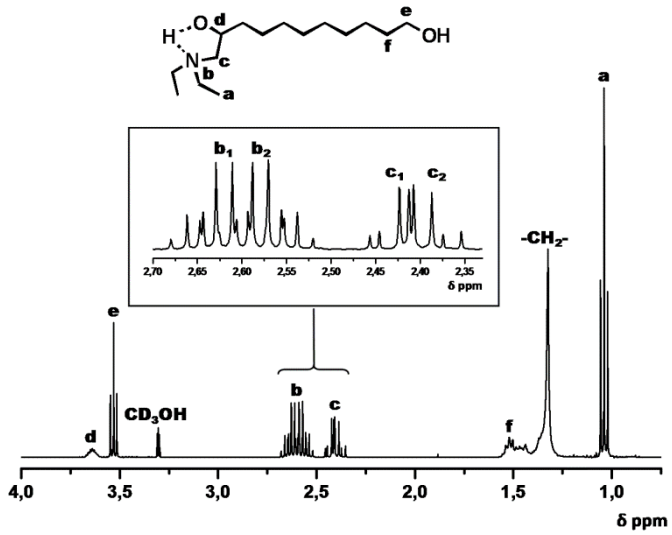

Figure 4.2. ^1H NMR spectra of D4 in CD_3OH

Further, polyurethane was prepared from equimolar amount of the aminodiol and commercially available IPDI in THF solution at 60 °C for 4 h using tin(II) 2-ethylhexanoate as catalyst. The molecular weight of PUD4 was evaluated by SEC, resulting a weight average molecular weight of Mw = 30000 Da and dispersity (D = 1.4).

As can be said in the previous chapter, IPDI is an asymmetric cycloaliphatic diisocyanate and contains Z and E isomers in a 3:1 ratio. Thus, the molecule consists of a mixture of two isomers, *cis* (Z) and *trans* (E), corresponding to the R and S configuretion at C-5, respectively. For each of these isomers, the reactivity of the two NCO groups is different and, consequently, different types of NCO groups and urethane moieties are formed during the reaction of the IPDI-diols prepolymers, and are present in the reaction mixture at same time.

The structural characterization of PU was carried out by NMR and FTIR spectroscopy. In Figure 4.3(a) the ^{1}H NMR spectrum of polyurethane from aminodiol and IPDI is shown as a mixture of both isomers.

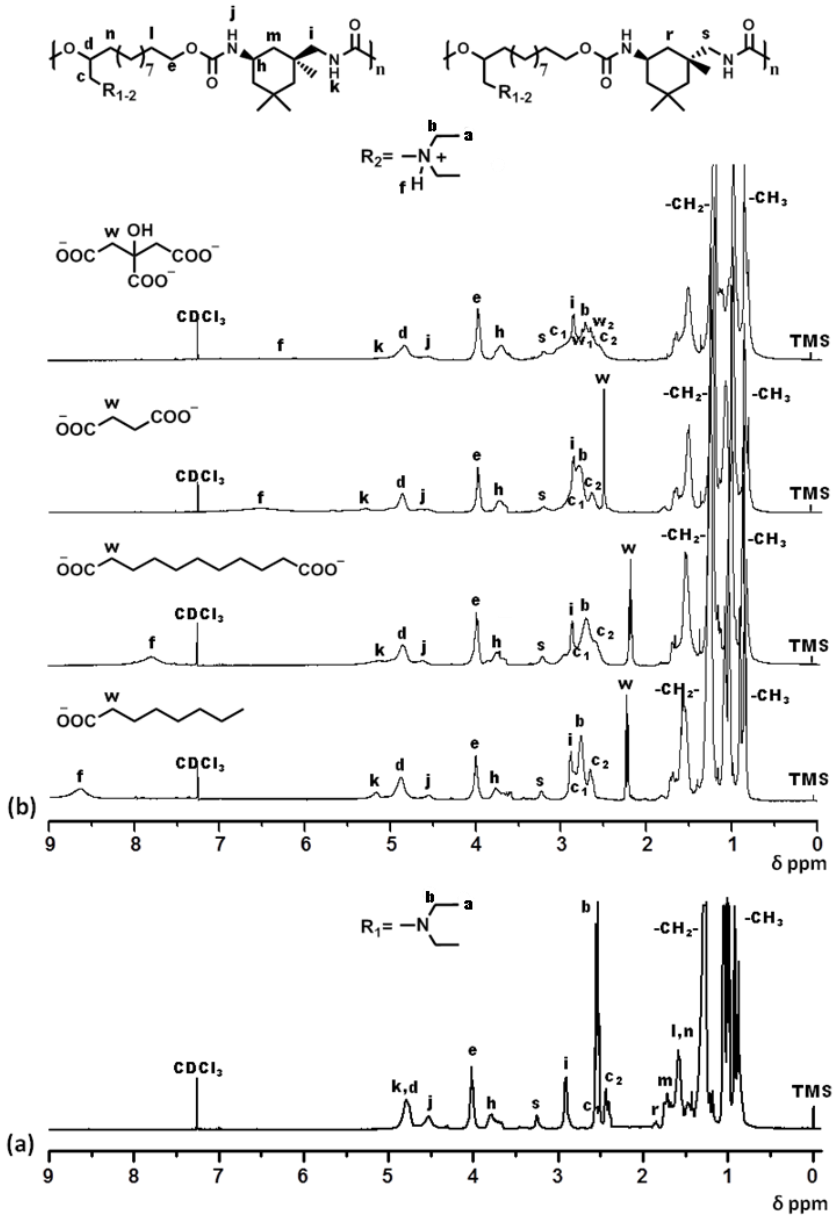

Figure 4.3. ^{1}H NMR spectra of a) PUD4 and IPDI. b) SIPU1-4.

Signals corresponding to both isomers have unequivocally been identified by means of 2-D NMR gCOSY and HSQCAD spectra. Protons corresponding to the cyclic IPDI were identified: at 3.78 ppm signal (h) corresponding to methine ring undistinguishable for both isomers, and at 3.25 and 2.91 ppm signals (s and i) corresponding to methylene linked to urethane of E and Z isomers, respectively. Moreover, the urethane proton signals from the isocyanate bonded directly to cycloaliphatic ring (j) and the urethane

proton signals from the isocyanate bonded through a primary carbon (k) are undistinguishable for both isomers and appear at 4.02 and 4.79 ppm respectively. Both isomers appear in a ratio 1:3 calculated from signals (s and i) corresponding to methylene linked to urethane.

Moreover, FTIR spectroscopic characterization revealed the expected structural features, including the disappearance of the vibrational band of NCO function, located at 2235 cm^{-1} and the appearance of absorption bands (cm^{-1}) of main chain about 1695, 3320 and 1522 cm^{-1} arising from urethane linkages corresponding to C=O stretching and NH stretching and bending bands respectively.

The modification of the amine-containing PU was performed in a THF solution at room temperature and isolated by simple evaporation of solvent under reduced pressure. All supramolecular systems were obtained as light yellow transparent materials, suggesting the homogeneous dispersion of the carboxylic acid component in the PU chains. This observation, together with the fact that thin films became opaque after immersion in aqueous solution due to the precipitation of the carboxylic acid, proved the successful formation of the supramolecular ionic hydrogen bonding systems, since water molecules disrupt such interactions. Four carboxylic acids with different structural characteristics: octanoic acid (1), sebacic acid (2), succinic acid (3) and citric acid (4) were used to prepare supramolecular ionic polyurethanes (SIPU1-4) as can be seen is Scheme 4.2.

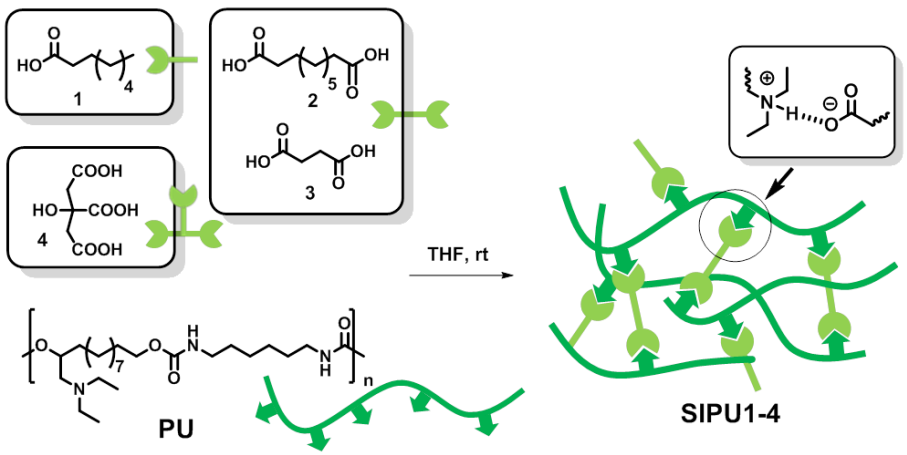

Scheme 4.2. Preparation of SIPU1-4.

To facilitate the structural characterization of these SIPUs, a previous model was prepared with the bis-urethane (BIU) and octanoic acid. The ^{1}H NMR spectra of BIU and the ionic specie resulting from BIU plus octanoic acid, are shown in Figure 4.4. Signals at 2.31 and 0.73 ppm corresponding to methylene bonded to carboxylic group and methyl group of octanoic acid are observed. Moreover, methylene signal (c) and ethyl group signals (a and b) directly bonded to nitrogen suffer a slight deshielding (0.20-0.25 ppm), and a new signal at 8.45 ppm from diethyl ammonium cation appears. Figure 4.3(b) collects the spectra of SIPUs where these changes in chemical shifts are observed when compared with precursor PU (Figure 3a), thus confirming the formation of ionic species.

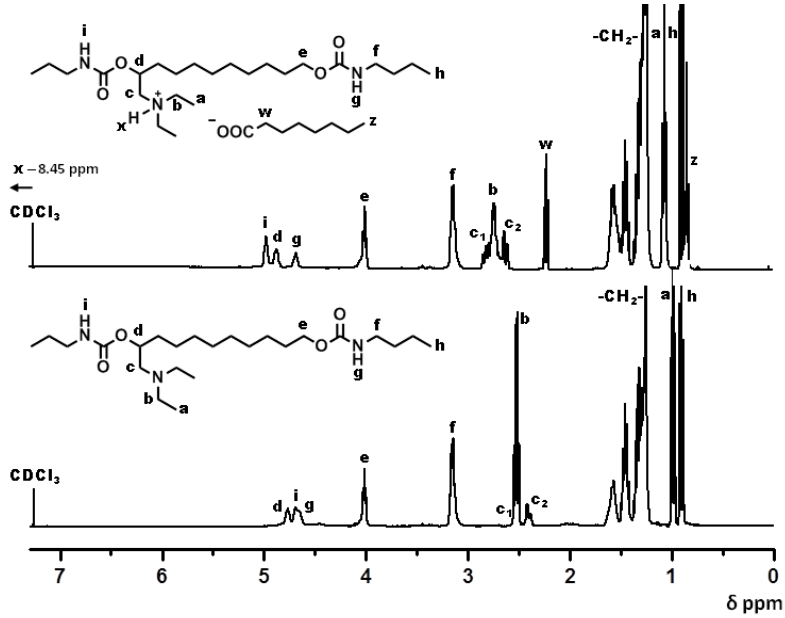

Figure 4.4. ^{1}H NMR spectra of BIU (a) and a mixture of BIU and octanoic acid (b).

To confirm the formation of hydrogen ionic bonds, IR spectra were carried out, but the polymer modification could not be revealed by FTIR, because the signals of urethane and carboxylic/carboxylate groups appear overlapped when BIU or PU were modified with octanoic acid. However, FTIR allowed demonstrate the natural equilibrium between hydrogen bonding and ionic bonding in the modification process when the aminodiol was mixed with octanoic acid. In Figure 4.5, the transformation of carboxylic group of octanoic acid in carboxylate and carboxyl hydrogen bonded amine

group was observed. In contrast, when the monomer was modified with fluoroacetic acid, only the absorption band of carboxylate group appears

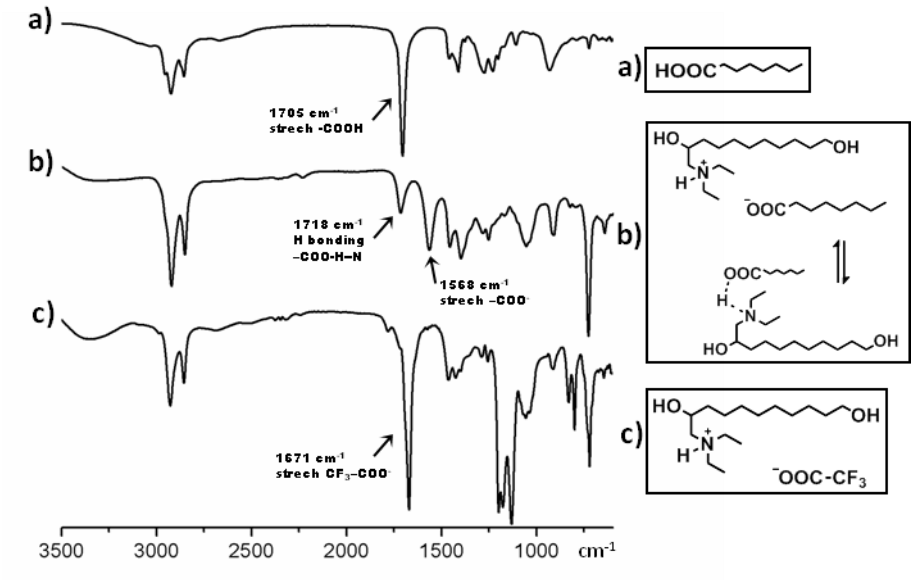

Figure 4.5. FTIR spectra of octanoic acid (a), aminodiol with octanoic acid (b) and aminodiol with trifluoroacetic acid (c).

4.2.2. Thermal, rheological, electrical and mechanical properties

Thermal properties of SIPUs, including thermal phase transition and thermal stability were evaluated by DSC and TGA under N_2 atmosphere at heating rate of 10 °C/min. In Figure 4.6 the DSC traces for each sample related with the second heating of heating-cooling cycle analysis, are shown. The plots indicate that all PUs systems, including the starting PU and SIPUs, form an amorphous phase without showing any trace of crystallization or melting point. The glass transition temperature, T_g, varies between 4 °C for the SIPU1 (modification with octanoic acid), and 58 °C for the SIPU4 (modification with citric acid). Indeed the profusion of inherent hydrogen bonds, due to the presence of tertiary amine, increases the rigidity and thus strongly suppresses the mobility of the polymer chains.

The data are summarized in Table 4.1. SIPU1, obtained from a monofunctional acid with a long alkyl chain, shows the lowest T_g value. The possibility of hydrogen bonding between chains of precursor PU decreases and consequently the physical crosslink

density is reduced. Besides, the presence of a long chain moiety acts as plasticizer. On the other hand, the SIPU4 network formed with citric acid (trifunctional acid with short alkyl chain), shows the highest T_g because the density of physical bonds is considerably increased. For SIPU2 and SIPU3, both from difunctional acids with long and short alkyl chain respectively, intermediate T_g values are found. Thus, modified polyurethanes bring about T_gs that differ in more than 50 °C, making them suitable for a wide range of applications.

Table 4.1. Thermal and rheological properties for PU and SIPUs

	DSC	Rheometer		TGA
Sample	T_g (°C)	T_{nl}(°C)	$T_{5\%}$ (°C)[a]	Td (°C)[b]
PUD4	40	61	269	333/425
SIPU1	4	37	198	206/335/426
SIPU2	25	47	233	329/452
SIPU3	42	61	208	333/438
SIPU4	58	78	195	194/274/336/414

[a]Temperature at which 5% weight loss was observed.
[b]Temperature for maximum degradation rate.

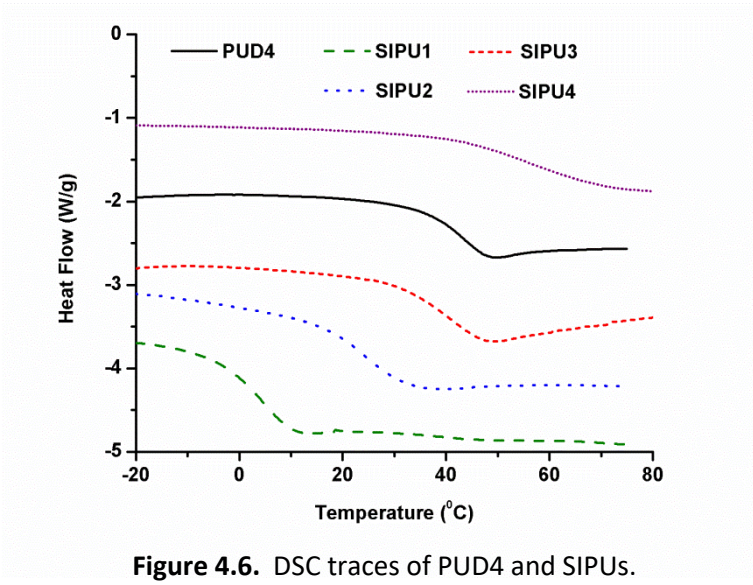

Figure 4.6. DSC traces of PUD4 and SIPUs.

Afterwards, to evaluate the effect of non-covalent interactions in the thermal degradation process of PU system, thermogravimetric measures were carried out. Thermal stability of PU and SIPUs was evaluated by TGA and data are summarized in Table 4.1. Figure 4.7 shows the weight loss upon heating under N_2 atmosphere and corresponding TGA derivatives. Although in general, PUs present low heat resistance due to the presence of thermo-labile urethane linkage, in the thermogram it can be observed that the original PU owns major temperature resistance. This behaviour can be explained recalling that SIPUs contain carboxylate groups vulnerable to earlier degradation by decarboxylation process, suggesting that degradation starts at the modification moiety. As an example, it can be observed in Figure 7(b), as derivative curve citric acid coincides with the first degradation derivate of SIPU4.

Besides this first degradation, the relevant weight loss for all samples occurs in the range of 250-350 °C, corresponding to the typical degradation temperature of the urethane bond. Studies on the decomposition of the urethane bond indicate that decomposition initial temperature depends on the structure of both the isocyanate and the diol. It takes place through dissociation to isocyanate and alcohol, the formation of primary amines and olefins and the formation of secondary amines and carbon dioxide. Finally, the third degradation stage (over 400 °C) corresponds to the gasification of any remaining components.[53]

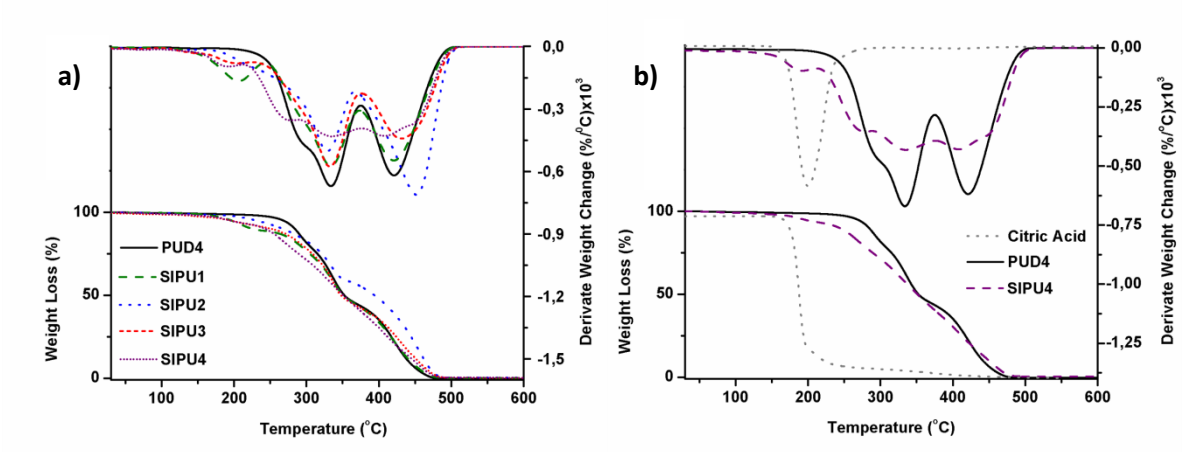

Figure 4.7. TGA and first derivative traces of PUD4 and SIPUs (a), and citric acid PUD4 and SIPUs (b).

Furthermore, an analysis of the rheological behaviour of PU and SIPUs was carried out. The results are shown in Figure 4.8 in which the dynamic storage modulus (G') and loss modulus (G''), taken at frequency of 6.28 rad s^{-1} and deformation 0.5%, are plotted against temperature in a semi-logarithmic format. These plots illustrate the significant changes in viscoelastic properties of SIPUs over the temperature range investigated. For all the samples, at low temperatures the rheological response is elastic, with G' > G'', whereas at high temperatures, the rheological response becomes predominantly viscous, with G''> G'. The constant elastic moduli, G', observed at low temperatures for the studied PU and SIPUs, represent equilibrium values, G_e, that indicate the presence of an elastic network. The experimental evidence of this network is confirmed in Figure 7, which shows the isothermal frequency scans for sample SIPU2, as a representative example of the other samples. At T=20ºC, which corresponds to T<Tnl for SIPU2 (Tnl= 47ºC, Table 1), both, elastic, G' and viscous, G'', moduli are practically independent of frequency and G'>G''; this is the typical conduct of an elastic solid. However, at T=57ºC, above Tnl, the viscous modulus prevails (G''>G') and both moduli depended on frequency, indicating that the network has faded at this temperature.

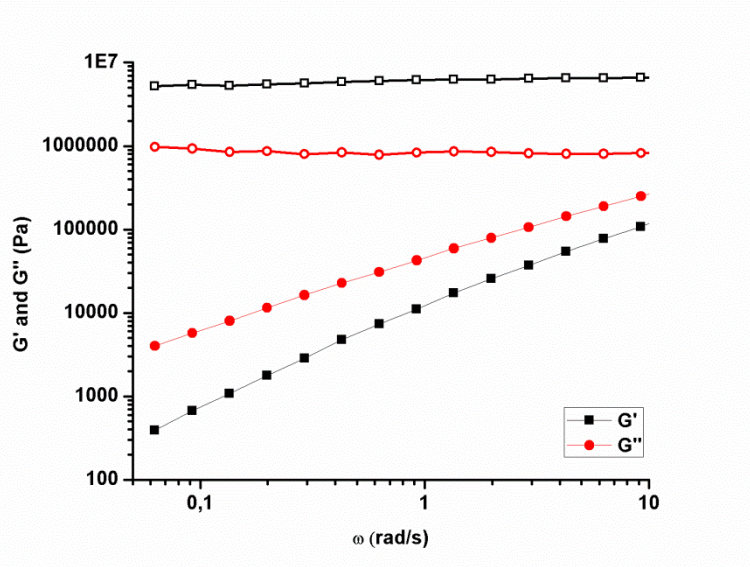

Figure 4.8. Isothermal frequency scans under lineal viscoelastic conditions at temperatures below (20 °C, empty symbol) and above (57 °C, full symbol) Tnl for sample SIPU2. Similar results are obtained for the other samples.

Interestingly enough, the values of G_e are practically the same (G_e= 7x10^6 Pa) for all the samples, notwithstanding precursor PU present only hydrogen bonding and SIPUs present both, hydrogen bonding and ionic interactions. As stated above, hydrogen bonding is due to the presence of tertiary amine in all the samples. This signifies that the contribution of the ionic interaction to the consistence of the network is not determined. However, the effect of the nature and the amount of physical bonds is certainly noticed in the transition from the elastic state (G'>G'') to the viscous state (G''>G'), as can be seen in Figure 4.9. This transition temperature corresponds actually to a transition from a network to a liquid state, T_{nl}, and it is defined as the temperature at which G'=G''. In other words, it represents the temperature where the network lost its properties of elastic solid by rupture of physical interactions, becoming a viscous liquid. It is observed that Tnl is shifted 5 °C with respect to the temperature at which the maximum in G'' is observed. From the point of view of the theory of the linear viscoelasticity,[54] which is out of the scope of this paper, this absence of coincidence signifies that the application of the Maxwell model with a single relaxation time is not possible in this case.

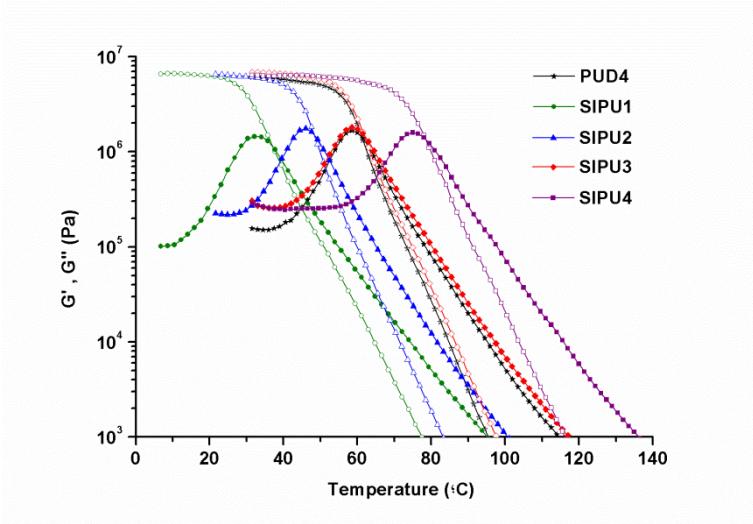

Figure 4.9. Temperature dependence on dynamic storage moduli G' (empty) and loss moduli G" (full) for PU (black) and SIPUs.

The corresponding T_{nl} values of PU and SIPUs network (Table 4.1) are related to their chemical structure. All SIPUs are amine-containing PU modified with carboxylic acids

with different structural characteristics. Therefore, two factors affect T_{nl} transition: The number of acid groups and the alkyl chain length of carboxylic acids. As it can be deduced from Table 4.1, there is a direct correlation between T_{nl} values and T_g values and, consequently, the aforementioned analysis on the effect of the chemical structure on T_g is perfectly applicable to T_{nl}.

Similarly, a correlation between chemical structure and viscoelastic behaviour was found in main chain supramolecular ionic networks based on citric acid and dicationic ionic liquids.[55]

A relevant aspect of the investigated SIPUs is its rapid thermal reversibility. The analysis carried out consisted in temperature ramps on heating and cooling from 30°C to 100°C with a stabilised time for 2 minutes in every step. The thermoreversible character of SIPU4 is shown in Figure 4.10 as an example of the behaviour observed for all the samples. Similar G' and G'' values are obtained on a continuous heating and cooling cycle, without any hysteresis symptom, indicating the rapid thermal reversibility of the SIPUs, due to the noncovalent nature of the involved interactions between chains that can break and re-form rapidly.[51]

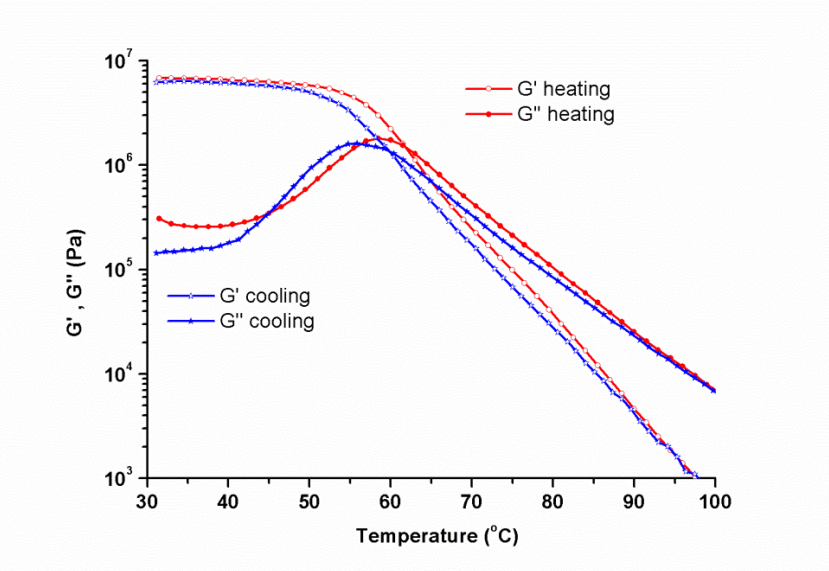

Figure 4.10. Temperature ramps on heating and cooling for SIPU4.

In view of the good reversibility results, a recyclability analysis for SIPUs was performed. After a first heating at 120°C, the samples were cooled and then removed from the rheometer. Then they were triturated to powder and moulded at 50°C under pressure to obtain recycled samples which were analysed again. This process was repeated for three times. The results for SIPU4 are shown in Figure 4.11. As can be inferred, the sample maintains basically its thermo-mechanical properties, since only a slight increase of T_{nl} is observed and exclusively after three cycles.

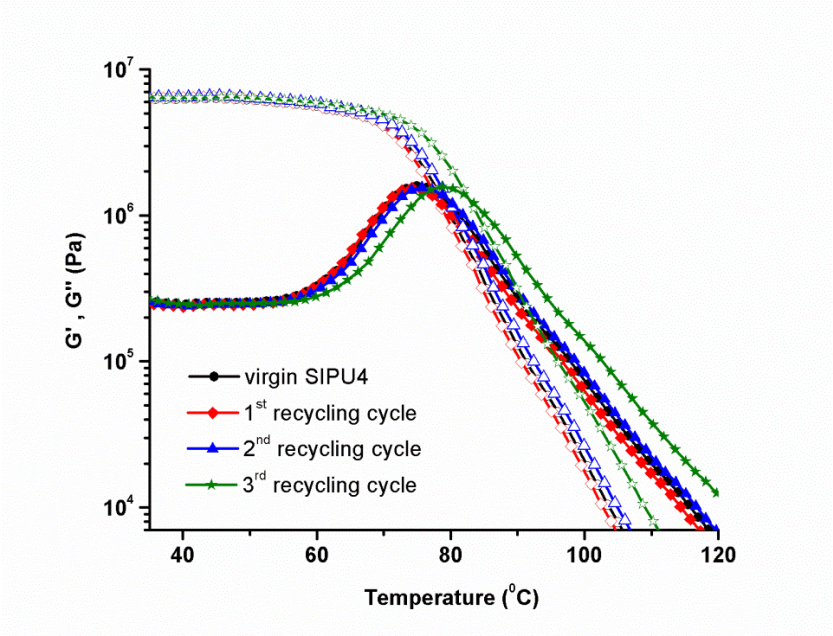

Figure 4.11. Temperature ramps of SIPU4 after recycling cycles.

To have a complementary survey of the break of the elastic network, as well as to assess the ionic character of SIPUs related to precursor PU, ionic conductivity versus temperature was measured. The network disruption caused by temperature, should lead to a rapid increase of the ionic conductivity, because the dramatic viscosity decrease associated to network rupture, leads to an increase of the ionic mobility. Our results, shown in Figure 4.12, confirm this assumption, which has been verified also for other ionomers or ionic supramolecular networks.[50] The measurements were carried out from 30 °C to 80 °C for all samples, except for SIPU4 whose analysis was carried from 30 °C to 130 °C, as conductivity was not observed up to 80 °C. The observed rapid increase of the ionic conductivity as temperature overtakes a certain value constitutes an evidence of the breakup of the elastic network. Although an exact evaluation of the network to liquid, Tnl, transition is not possible from the results of Figure 4.12, it is seen that the order sequence from the lower to the higher temperature for the

disruption is: SIPU1<SIPU2<SIPU3<SIPU4. Hence, comparing the results of Figure 4.12 with those of Tnl shown in Table 1, the effect of the chemical structure on the inception of the breakup of the network is confirmed: The network is more stable the higher the functionality of the acid is and the shorter is the alkyl chain.

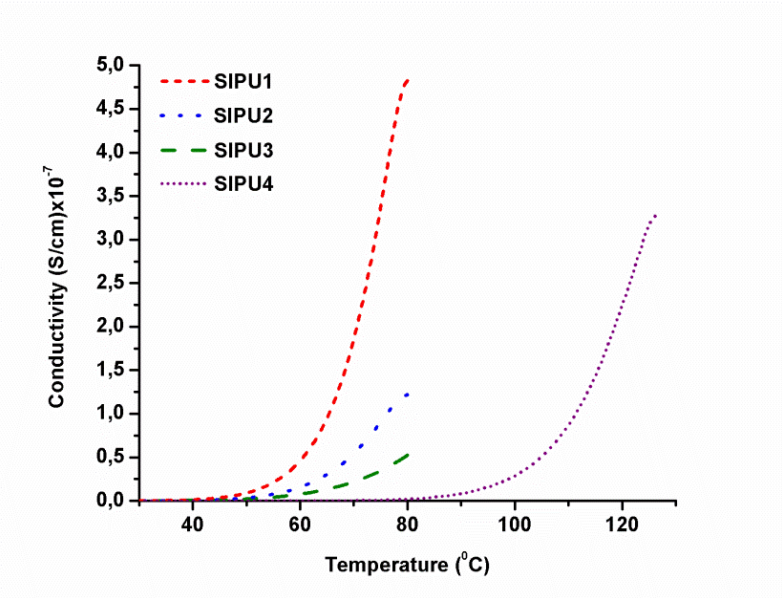

Figure 4.12. Ionic conductivity versus temperature for PUD4 and SIPUs. The conductivity of PUD4 is not observed in the figure because is very low ($1x10^{-11}$ S/cm).

A study of how the established structure-rheology correlation is reflected in ultimate properties, such as tensile mechanical properties, was carried out. Tensile tests were performed on SIPUs networks. For the sake of approaching to the end use properties, measurements were carried out at room temperature (T=23ºC). Consequently, in view of the results of Table I, we have to point out that the tests were performed above or in the vicinity of T_g for SIPU1 and SIPU2, but below T_g for SIPU3 and SIPU 4. Therefore the results should be discussed considering this reality. The stress-strain curves are depicted in Figure 4.13 and the Young's modulus, elongation at break and stress at break are given in Table 4.2.

A similar Young's modulus was observed for networks SIPU1 and SIPU2, a typical derived from large alkyl chain acids: octanoic and sebacic acids respectively. The small elastic region suggests the elastomeric character of these samples at room temperature. In comparison, SIPU1 from monofunctional acid presents a considerable higher elongation at break (approaching 500%) than SIPU2, which present the

restriction of ionic hydrogen bond network. Moduli significantly higher were obtained for SIPU3 and SIPU4, because measurements were performed below Tg. Ionic networks obtained form di- or triacids with short alkyl chain limit the mobility of PU chains increasing the elastic region and obtaining materials rigids at room temperature.

Table 4.2. Mechanical properties of PUD4 and SIPUs.

Sample	Young's Modulus (Mpa)	Elongation at break (%)	Stress at break (MPa)
PUD4	88.4±0.7	20.4±2	2.74±0.17
SIPU1	22.3±0.3	494±9	0.70±0.04
SIPU2	24.0±0.3	77±6	1.55±0.14
SIPU3	89.8±0.7	50±4	4.99±0.23
SIPU4	122±1	45±4	6.53±0.24

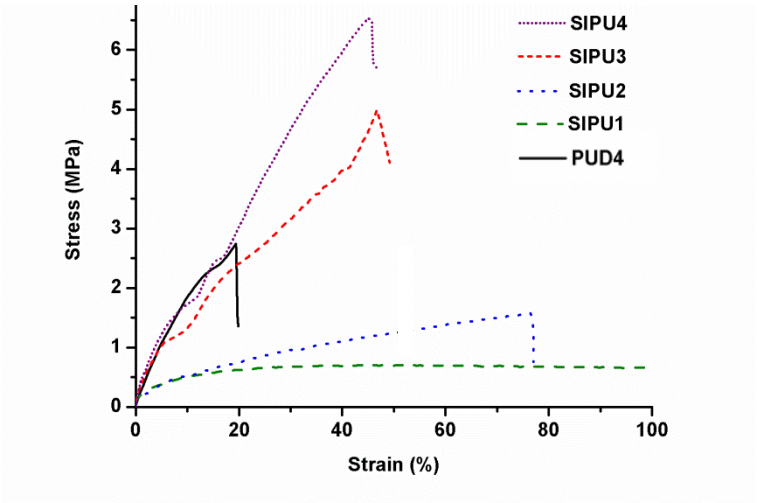

Figure 4.13. Stress versus strain curves of PUD4 and SIPUs

In summary, the post-synthetic non-covalent modification of tertiary amino-side chain functional PUs using carboxylic acids is a straightforward approach for the preparation of supramolecular PUs from renewable sources with easy property tuning. The resultant SIPUs contain diethyl ammonium and carboxylate moieties that are bonded by a combination of ionic hydrogen bonds. The presence of ionic interactions permits these materials a rapid reversibility and recyclability when submitted to temperature

cycles. These results can be used in stimuli-response materials research, such as self-healing or shape memory properties and expanding the range of application of conventional polyurethane.

4.3. References

[1] L. Brunsveld, B. J. B. Folmer, E. W. Meijer, R. P. Sijbesma. Supramolecular polymers. *Chemical Reviews*. **2001**. 101, 12, 4071-4098.

[2] R. F. Lange, M. Van Gurp, E. W. Meijer. Hydrogen-bonded supramolecular polymer networks. *Journal of Polymer Science Part A: Polymer Chemistry*. **1999**, 37, 19, 3657-3670.

[3] C. Lin, T. Xiao, L. Wang. Hydrogen-Bonded Supramolecular Polymers. In *Hydrogen Bonded Supramolecular Structures*. Springer Berlin Heidelberg. **2015**. 321-350.

[4] P. Cordier, F. Tournilhac, C. Soulié-Ziakovic, L. Leibler. Self-healing and thermoreversible rubber from supramolecular assembly. *Nature*. **2008**, 451, 7181, 977-980.

[5] S. Sivakova, D. A. Bohnsack, M. E., Mackay, P. Suwanmala, S. J. Rowan. Utilization of a combination of weak hydrogen-bonding interactions and phase segregation to yield highly thermosensitive supramolecular polymers. *Journal of the American Chemical Society*. **2005**, 127, 51, 18202-18211.

[6] J. Scavuzzo, S. Tomita, S. Cheng, H. Liu, M. Gao, J. P. Kennedy, L. Jia. Supramolecular Elastomers: Self-Assembling Star–Blocks of Soft Polyisobutylene and Hard Oligo (β-alanine) Segments. *Macromolecules*. **2015**, 48, 4, 1077-1086.

[7] D. W. Balkenende, R. A. Olson, S. Balog, C. Weder, L. Montero de Espinosa. Epoxy Resin-Inspired Reconfigurable Supramolecular Networks. *Macromolecules*. **2016**, 49, 20, 7877-7885.

[8] S. Bode, L. Zedler, F. H. Schacher, B. Dietzek, M. Schmitt, J. Popp, U. S. Schubert. Self-Healing Polymer Coatings Based on Crosslinked Metallosupramolecular Copolymers. *Advanced Materials*. **2013**, 25, 11, 1634-1638.

[9] P. Wei, X. Yan, F. Huang. Supramolecular polymers constructed by orthogonal self-assembly based on host–guest and metal–ligand interactions. *Chemical Society Reviews*. **2015**. 44, 3, 815-832.

[10] M. Enke, S. Bode, J. Vitz, F. H. Schacher, M. J. Harrington, M. D. Hager, U. S. Schubert. Self-healing response in supramolecular polymers based on reversible zinc–histidine interactions. *Polymer*. **2015**, *69*, 274-282.

[11] M. Wathier, M. W. Grinstaff. Synthesis and properties of supramolecular ionic networks. *Journal of the American Chemical Society*. **2008**, 130, 30, 9648-9649.

[12] L. Zhang, L. R. Kucera, S. Ummadisetty, J. R. Nykaza, Y. A. Elabd, R. F. Storey, R. A. Weiss. Supramolecular multiblock polystyrene–polyisobutylene copolymers via ionic interactions. *Macromolecules*. **2014**, 47, 13, 4387-4396.

[13] H. Yoon, E. J. Dell, J. L. Freyer, L. M. Campos, W. D. Jang. Polymeric supramolecular assemblies based on multivalent ionic interactions for biomedical applications. *Polymer*. **2014**, 55, 2, 453-464.

[14] T. W. Chuo, T. C. Wei, Y. L. Liu. Electrically driven self-healing polymers based on reversible guest–host complexation of β-cyclodextrin and ferrocene. *Journal of Polymer Science Part A: Polymer Chemistry*. **2013**, 51, 16, 3395-3403.

[15] L. R. Hart, N. A. Nguyen, J. L. Harries, M. E. Mackay, H. M. Colquhoun, W. Hayes. Perylene as an electron-rich moiety in healable, complementary π–π stacked, supramolecular polymer systems. *Polymer*. **2015**. 69, 293-300.

[16] S. Burattini, B. W. Greenland, D. H. Merino, W. Weng, J. Seppala, H. Colquhoun, S. J. Rowan. A healable supramolecular polymer blend based on aromatic π– π stacking and hydrogen-bonding interactions. *Journal of the American Chemical Society*. **2010**, 132, 34, 12051-12058.

[17] C. X. Sun, M. A. J. Van der Mee, J. G. P. Goossens, M. Van Duin. Thermoreversible cross-linking of maleated ethylene/propylene copolymers using hydrogen-bonding and ionic interactions. *Macromolecules*. **2006**, 39, 9, 3441-3449.

[18] M. Burnworth, L. Tang, J. R. Kumpfer, A. J. Duncan, F. L. Beyer, G. L. Fiore, C. Weder. Optically healable supramolecular polymers. *Nature*. **2011**, 472, 7343, 334-337.

[19] F. Herbst, D. Döhler, P. Michael, W. H. Binder. Self-Healing Polymers via Supramolecular Forces. *Macromolecular rapid communications*. **2013**, 34, 3, 203-220.

[20] C. Yu, C. F. Wang, S. Chen. Robust Self-Healing Host–Guest Gels from Magnetocaloric Radical Polymerization. *Advanced Functional Materials*. **2014**, 24, 9, 1235-1242.

[21] X. Xing, L. Li, T. Wang, Y. Ding, G. Liu, G. Zhang. A self-healing polymeric material: from gel to plastic. *Journal of Materials Chemistry A*. **2014**, 2, 29, 11049-11053.

[22] G. Liu, C. Guan, H. Xia, F. Guo, X. Ding, Y. Peng. Novel Shape-Memory Polymer Based on Hydrogen Bonding. *Macromolecular Rapid Communications*. **2006**, 27, 14, 1100-1104.

[23] C. Liu, H. Qin, P. T. Mather. Review of progress in shape-memory polymers. *Journal of Materials Chemistry*. **2007**, 17, 16, 1543-1558.

[24] L. Sun, W. M. Huang, Z. Ding, Y. Zhao, C. C. Wang, H. Purnawali, C. Tang. Stimulus-responsive shape memory materials: a review. *Materials & Design*. **2012**, 33, 577-640.

[25] G. J. Berg, M. K. McBride, C. Wang, C. N. Bowman. New directions in the chemistry of shape memory polymers. *Polymer*. **2014**, 55, 23, 5849-5872.

[26] S. Dong, B. Zheng, Y. Yao, C. Han, J. Yuan, M. Antonietti, F. Huang. LCST-Type Phase Behavior Induced by Pillar [5] arene/Ionic Liquid Host–Guest Complexation. *Advanced Materials*. **2013**, 25, 47, 6864-6867.

[27] M. Guo, L. M. Pitet, H. M. Wyss, M. Vos, P. Y. Dankers, E. W. Meijer. Tough stimuli-responsive supramolecular hydrogels with hydrogen-bonding network junctions. *Journal of the American Chemical Society*. **2014**, 136, 19, 6969-6977.

[28] S. L. Li, T. Xiao, C. Lin, L. Wang. Advanced supramolecular polymers constructed by orthogonal self-assembly. *Chemical Society Reviews*. **2012**. 41, 18, 5950-5968.

[29] E. Elacqua, D. S. Lye, M. Weck. Engineering orthogonality in supramolecular polymers: from simple scaffolds to complex materials. *Accounts of Chemical Research*. **2014**. 47, 8, 2405-2416.

[30] M. Weck. Side-chain functionalized supramolecular polymers. *Polymer International*. **2007**. 56, 4, 453-460.

[31] J. M. Pollino, M. Weck. Non-covalent side-chain polymers: design principles, functionalization strategies, and perspectives. *Chemical Society Reviews*. **2005**. 34,3, 193-207.

[32] A. Gooch, C. Nedolisa, K. A. Houton, C. I. Lindsay, A. Saiani, A. J. Wilson. Tunable self-assembled elastomers using triply hydrogen-bonded arrays. *Macromolecules*. **2012**, 45, 11, 4723-4729.

[33] S. Chen, J. Hu, C. W. Yuen, L. Chan. Supramolecular polyurethane networks containing pyridine moieties for shape memory materials. *Materials Letters*. **2009**, 63, 17, 1462-1464.

[34] S. Chen, J. Hu, C. W. Yuen, L. Chan. Novel moisture-sensitive shape memory polyurethanes containing pyridine moieties. *Polymer*. **2009**, 50,19, 4424-4428.

[35] S. Chen, J. Hu, C. W. Yuen, L. Chan. Fourier transform infrared study of supramolecular polyurethane networks containing pyridine moieties for shape memory materials. *Polymer International*. **2010**, 59, 4, 529-538.

[36] S. J. Chen, J. L. Hu, S. G., Chen, C. L. Zhang. Study on the structure and morphology of supramolecular shape memory polyurethane containing pyridine moieties. *Smart Materials and Structures*. **2011**, 20, 6, 065003.

[37] C. F. Faul, M. Antoniett. Ionic self-assembly: Facile synthesis of supramolecular materials. *Advanced Materials*. **2003**. 15, 9, 673-683.

[38] A. Eisenberg, J. S. Kim. *Introduction to ionomers*. Wiley. **1998**.

[39] Zander, Z. K.; Wang, F.; Becker, M. L.; Weiss R. A. Ionomers for Tunable Softening of Thermoplastic Polyurethane. *Macromolecules*. **2016**. 49, 3, 926-934.

[40] A. Noro, M. Hayashi, Y. Matsushita. Design and properties of supramolecular polymer gels. *Soft Matterials*. **2012**. 8, 24, 6416-6429.

[41] M. A. Aboudzadeh, M. E. Fernandez, E. Munoz, A. Santamaria and D. Mecerreyes, *Macromolecular Rapid Communication.* **2014**. 35, 460–465

[42] M. A. Aboudzadeh, M. E. Muñoz, A. Santamaría, R. Marcilla, D. Mecerreyes. Facile Synthesis of Supramolecular Ionic Polymers That Combine Unique Rheological, Ionic Conductivity, and Self-Healing Properties. *Macromolecular Rapid Communications*. **2012**. 33, 4, 314-318.

[43] M. A. Aboudzadeh, M. E. Munoz, A. Santamaría, M. J. Fernandez-Berridi, L. Irusta, D. Mecerreyes. Synthesis and rheological behavior of supramolecular ionic networks based on citric acid and aliphatic diamines. *Macromolecules*. **2012**. 45, 18, 7599-7606.

[44] M. Meot-Ner. The ionic hydrogen bond. *Chemical reviews*. **2005**. 105, 1, 213-284.

[45] T. Noguchi, K. Kishikawa, S. Kohmoto. Tailoring of ionic supramolecular assemblies based on ammonium carboxylates toward liquid-crystalline micellar cubic mesophases. *Liquid Crystals*. **2008**. 35, 8, 1043-1050.

[46] E. Yashima, T. Matsushima, Y. Okamoto. Chirality assignment of amines and amino alcohols based on circular dichroism induced by helix formation of a stereoregular poly

((4-carboxyphenyl) acetylene) through acid-base complexation. *Journal of the American Chemical Society*. **1997**. 119, 27, 6345-6359.

[47] K. C. F. Leung, P. M. Mendes, S. N. Magonov, B. H. Northrop, S. Kim, K. Patel, J. F. Stoddart. Supramolecular self-assembly of dendronized polymers: Reversible control of the polymer architectures through acid-base reactions. *Journal of the American Chemical Society*. **2006**. 128, 33, 10707-10715.

[48] A. Noro, M. Hayashi, Y. Matsushita. Design and properties of supramolecular polymer gels. *Soft Matterials*. **2012**. 8, 24, 6416-6429.

[49] M. A. Aboudzadeh, M. E. Fernandez, E. Munoz, A. Santamaria and D. Mecerreyes, *Macromolar Rapid Communication.* **2014**. 35, 460–465

[50] M. A. Aboudzadeh, M. E. Muñoz, A. Santamaría, R. Marcilla, D. Mecerreyes. Facile Synthesis of Supramolecular Ionic Polymers That Combine Unique Rheological, Ionic Conductivity, and Self-Healing Properties. *Macromolecular Rapid Communications*. **2012**. 33, 4, 314-318.

[51] M. A. Aboudzadeh, M. E. Munoz, A. Santamaría, M. J. Fernandez-Berridi, L. Irusta, D. Mecerreyes. Synthesis and rheological behavior of supramolecular ionic networks based on citric acid and aliphatic diamines. *Macromolecules*. **2012**. 45, 18, 7599-7606.

[52] M. Comí, G. Lligadas, J. C. Ronda, M. Galià, V. Cádiz. Synthesis of castor-oil based polyurethanes bearing alkene/alkyne groups and subsequent thiol-ene/yne post-modification. *Polymer*. **2016**, *103*, 163-170.

[53] I. Javni, Z. S. Petrović, A. Guo, R. Fuller. Thermal stability of polyurethanes based on vegetable oils. *Journal of Applications in Polymer Science.* **2000**, 77, 1723-1734.

[54] Ferry, J. F. Viscoelastic Properties of Polymers. Wiley-Interscience: New York, **1980**.

[55] M. A. Aboudzadeh, M. E. Muñoz, A. Santamaria, D. Mecerreyes. New supramolecular ionic networks based on citric acid and geminal dicationic ionic liquids. *RSC Advances*. **2013**, 3, 8677-8682.

Chapter 5

Post-Synthetic Non-Covalent Crosslinked Polyurethanes as Self-Healing Elastomers from Renewable Sources

Taking advantage of the previous chapter methodology, this chapter is focused to synthesize supramolecular polyurethane networks with elastomeric properties at room temperature as efficient self-healing materials.

UNIVERSITAT ROVIRA I VIRGILI
AVANCES EN SISTEMAS INTERACTIVOS PARA PERSONAS CON PARÁLISIS CEREBRAL
Marc Comí Bonachí

5.1. Introduction

Living organisms are able to recover from injuries to resume active and reproductive functions. The ability to continue these metabolic processes determines the longevity of their existence. Synthetic materials are designed to be functional, but do not possess metabolic attributes. To prolong their lifespan, the concept of self-repairing has been explored and became the central topic of scientific interests and technological significance.[1-5] Recent advances and numerous successful approaches to repair mechanically damaged materials have been developed in the last decade.[6,7] There are two events during self-repairing that are particularly critical: (1) physical flow of molecular segments at or near a wounded area and (2) re-bonding of cleaved bonds after mechanical damage. These events may occur continuously, depending upon interplay between kinetics and thermodynamics. Ideally, one can envision diffusion of chain ends, followed by their re-bonding.[8,9] Still another property of the respective self-healing process could be used to distinguish material subclasses, leading to the terms 'extrinsic' and 'intrinsic' self-healing. Extrinsic self-healing materials themselves do not owe a hidden intrinsic capability for self-healing; rather, the healing process is based on external healing components, such as micro- or nanocapsules, intentionally embedded into the matrix materials to make them self-healing. The content of these capsules becomes the mobile phase upon damage.[10,11] On the other hand, intrinsic self-healing requires no separate healing agents, which is to be preferred but, depending on the material class and healing mechanism, not always feasible.[12,13]

Intrinsic self-healing systems based on polymers have received special attention in the last decades.[14-17,] A critical factor to achieve desirable mobility of polymer chains is the presence of free volume.[18] The well-known concept of free volume ought to describe an average chain mobility typically reflected in the glass transition temperature (T_g) that impact such properties as permeability, diffusivity, flexibility, and others.[19] Due to limited chain mobility and a lack of bond reformation abilities, common polymers do not show self-repair attributes. There are few classes of reactions to offer self-repairing through the cleavage and reformation of specific bonds. These entities are incorporated into polymer, and are typically categorized into reversible covalent and non-covalent bonds. The presence of these reversible bonds introduces molecular

level heterogeneities along a polymer backbone or as pendant groups; which may further facilitate the formation of new phases with extended length scales. Indeed, materials capable of autonomous healing upon damage have numerous potential applications.[20,21] So far, self-healing has been demonstrated in linear polymers, supramolecular networks,[22-24] dendrimer-clay systems,[25] metal ion-polymer systems,[26,27] and multicomponent systems.[28,29]

As described in the introduction of the previous chapter, integrity of supramolecular polymers is achieved by the formation of non-covalent interactions.[30-32] This is tipically accomplished by the presence of the associative groups non-covalently attached to main chain or side chain of the polymers. In some cases, these assembles bind lineal polymers or prepolymers into networks with plastic or rubber behaviour resulting from the non-covalent cross-linking by non-covalent interactions.[33,34] Thus, heterogeneities are inherent for many supramolecular networks affecting their physical and chemical properties, and facilitating self-repair.

The general process of self-repairing is depicted in Figure 5.1, demonstrating the basic steps of self-healing mechanism in supramolecular polymers.[35] First, the undamaged material, consisting of polymer chains containing supramolecular bonds, forms a network by bonds able to connect and reconnect via reversible “sticker-like” behaviour. Thus, in contrast to conventional polymeric materials, the strength of the material is generated by the “stickiness” of the supramolecular bonds and is not generated by covalent bonds or chain entanglements. Crucial for this network formation is a specific interaction between the two different supramolecular bonds, linking the polymer chains. After damage has occurred via external forces leading to a crack, the generated new interface contains a multitude of unbound supramolecular bonds, which remain “sticky” at the fractured surface for a certain period of time. Thus, recombination of the two fragments leads to reformation of the supramolecular bonds closing the gap and healing the damaged site.[22]

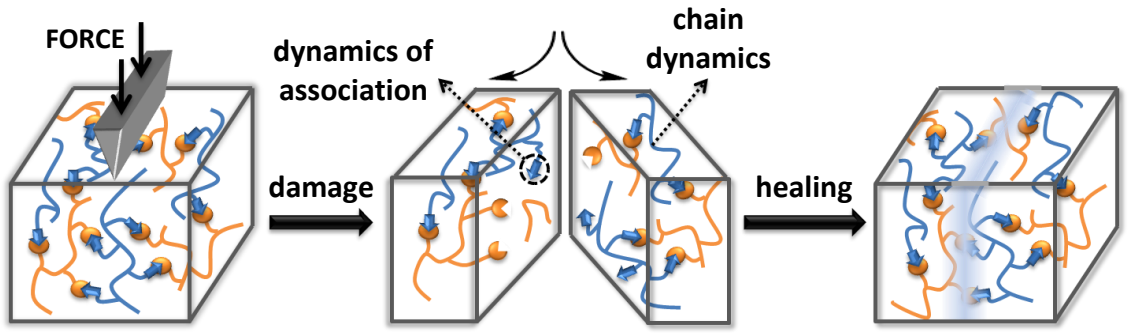

Figure 5.1. Schemmatic representation of self healing process.[22]

Several features make supramolecular chemistry particulary attractive when comes to self-healing: reversibility and speed, directionality, and sensitivity. In contrast to covalent bonding, these networks can be remodelled rapidily and reversibly form from fluid-like to solid-like states.[36] The possibility to repeatedly conduct the healing process even after multiple damages have ocurred is the most important benefit of supramolecular self-healing materials.

On the whole, in PU not many intrinsic self-healing mechanisms have been reported.[37] Much less attention has recieved the field of supramolecular PU as a self-healing materials, where the reversible bonds are responsible for intrinsic self-healing, despite its modular character and ease of synthesis.[38,39] Lin and Li reported the design of PU hydrogels with intermolecular quadruple hydrogen-bonding interactions. These PUs were fabricated by the copolymerization of a PU macromonomer containing two terminal double bonds with a monomer bearing the 2-ureido-4-pyrimidone unit, capable to form reversible interactions. The results indicate that the prepared PU hydrogels can autonomously and rapidly repair occurring incisions or cracks at ambient temperature without the need for any stimulus. These hydrogels possess high deformability under both tensile and compressive stress and strong recoverability upon removal of stress, thus exhibiting outstanding self-healing, elasticity, robustness and toughness.[38]

Alternatively, the design and synthesis of zwitterionic PUs with sulfobetaine groups have also been considered for obtaining self-healing materials. In this case, non-covalent ionic interactions are crucial to achieve PUs with self-healing capabilities. For

example, Chen et al. synthesized zwitterionic PUs that by immersing in moisture-rich conditions and drying at low temperature demonstrated good self-healing properties. The self-healing mechanism is ascribed to the spontaneous attraction of zwitterions, followed by slower re-entanglement.[39]

Considering its high stability and facile accessibility demonstrated in the previous chapter, ionic hydrogen bonding holds promise for the facile fabrication of stimuli-responsive PUs networks is presented and discussed. Therefore, in this chapter the synthesis and studies of novel adaptive elastomers constructed from linear PU featuring tertiary amino groups as side chain functionalities and carboxylic acid as non-covalent crosslinkers. These materials exhibit some promissing material properties such as effective energy dissipation upon deformation through unzipping the ionic hydrogen bonding network, combined with good shape regeneration property and recycling/reshaping capability due to their recoverable nature. More importantly, the resulting elastomers possess the inherent ability of self-healing.

5.2. Results and discussion

5.2.1. Synthesis of supramolecular polyurethane networks (SPUN)s

Elastomeric SPUNs were easily prepared by a proton transfer reaction between a carboxylic acid and linear PU featuring tertiary amino groups as side chain functionalities (PU2), both coming from renewable sources. Taking advantage of the versatility of our approach, five small-molecular biological carboxylic acids with different aliphatic chain lengths and functionality: sebacic acid (1), succinic acid (2), suberic acid (3), citric acid (4) and oxalic acid (5) were selected to broad the properties of the networks by non-covalently bridging all the tertiary amine nitrogen centers through ionic hydrogen bonds (Scheme 5.1).

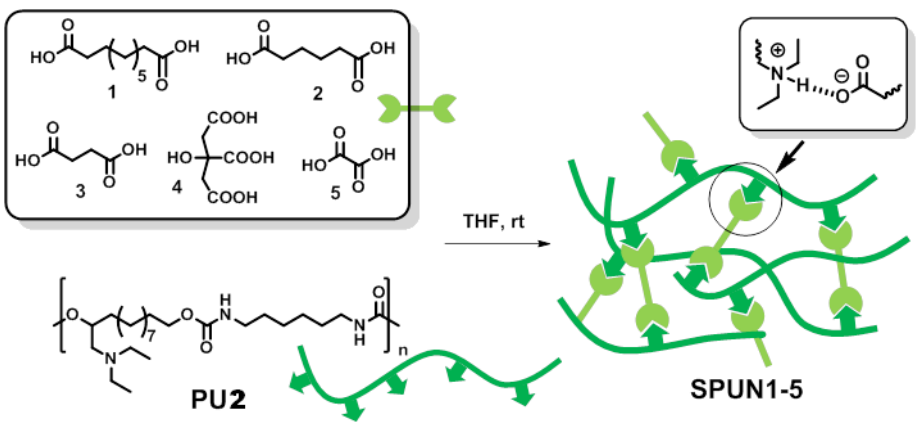

Scheme 5.1. Preparation of SPUNs

The preparation of SPUNs is described in detail in the chapter 7 (Experimental Part). Briefly, D4 was synthesized from 10-undecen-1-ol, as a derivative of non-edible castor oil, following a high yield synthetic route previously described in previous chapters that uses epoxidation and ring-opening with diethylamine as key steps.[40] The corresponding poly(amino urethane) polymer (PU2) was prepared using hexamethylene diisocyanate (HDI) in THF at 60ºC. A high yield (93%) of PU2 was recovered, with the resulting polymer exhibiting a weight-average molecular mass (M_w) of 40600. The analysis of PU2 by FTIR and ^{1}H NMR spectroscopies confirmed that polymerization reaction proceeded successfully. Characteristic IR absorption bands arising from urethane linkages were observed at 1688 cm^{-1} (C=O stretching), 3325 cm^{-1} (NH stretching) and 1530 cm^{-1} (NH bending). As shown in Figure 5.2(a), ^{1}H NMR spectrum is in full concordance with the expected chemical structure of PU2. Next, the post-synthetic cross linking of PU2 was performed using one of the selected carboxylic acids, as small non-covalent cross-linker, to produce SPUNs with ionic hydrogen bonds as cross-linking points (Scheme 5.1). SPUNs were prepared by mixing both components in THF at room temperature and isolated by simple evaporation of the solvent under reduced pressure. All supramolecular assemblies were obtained as light yellow transparent materials, suggesting the homogeneous dispersion of the solid CA component in the network. This observation, together with the fact that thin films these materials became opaque after immersion in an aqueous solution due to the precipitation of the carboxylic acid, proved the successful formation of the

supramolecular ionic hydrogen bonding networks, since water molecules disrupt such interactions.

The structure of the non-covalent assemblies was first investigated by FTIR spectroscopy. It is worth to remark that in the case of previous supramolecular ionic networks, the appearance of a band associated to carboxylate moieties in the range 1550-1620 cm^{-1} was considered as a direct proof of the proton transfer process between carboxylic acid groups and nitrogen from the amine and the generation of ionic species.[41] Unfortunately, in SPUNs overlapping of this signal occurred with N-H bending of urethane linkages. Nevertheless, carboxylic acid and carboxylate bands could be observed at 1718 and 1568 cm^{-1}, respectively, in an equimolar mixture of D4 and octanoic acid used as a model non-covalent assembly. This confirms the coexistence of molecular and proton transfer-generated ionic hydrogen bonded complexes.

Furthermore, SPUNs were characterized by ^{1}H NMR in a solution of $CDCl_3$ showing similar features associated to the proton transfer in previous works.[41] Chemical shift changes were analyzed using as a reference linear PU2 (Figure 2.1(a)). Figure 2.1(b) shows the representative ^{1}H NMR spectrum of the SPUN1, where the resonances at 2.53 ppm and 2.42 ppm attributed to the protons (b) and (c) adjacent to the tertiary amines are deshielded (by 0.13 ppm for b), as a result of the protonation of the adjacent tertiary amine. Furthermore, the characteristic signal at 8-9 ppm corresponding to the protons of the carboxylic acid groups completely disappeared and the signal associated to the protonation of the tertiary amino groups appeared at around 6.5 ppm. Another feature of the ^{1}H NMR spectra is that the signals of the ionic network are broader, which means that the mobility was reduced.

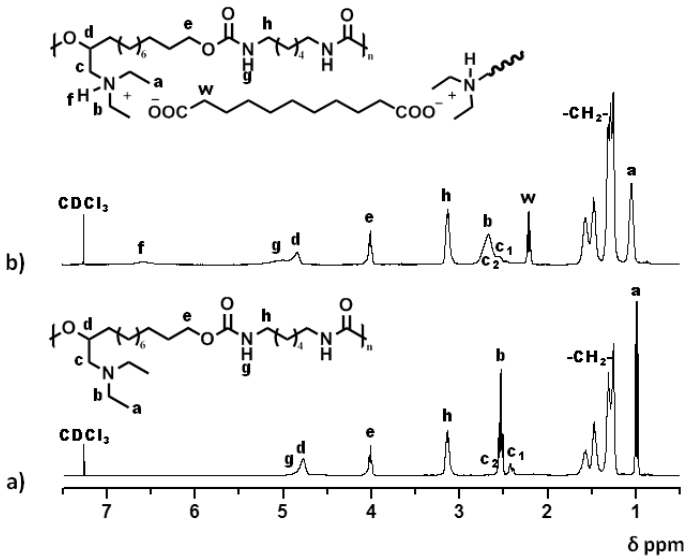

Figure 5.2. ^{1}H NMR spectra of a) PU2 and b) SPUN1.

5.2.2. Thermal properties.

Thermal properties of SPUNs including thermal phase transition and thermal stability were evaluated by DSC and TGA under N_2 atmosphere at heating rate of 10°C/min, using the non-crosslinked poly(amino urethane) PU2 as reference. The key parameters of the thermal analysis are summarised in Table 5.1. Figure 5.3 shows the DSC traces for each sample related with the second heating of heating-cooling cycle analysis. For all SPUNs the introduction of the acid crosslinker into PU2 inhibited the crystallization of carboxylic acid component and led to the formation of an amorphous phase in the solid-state with single T_g, suggesting that complementary interactions between PU2 and carboxylic acid tie together the tertiary amine centers. In addition, the T_gs of the SPUNs increased gradually from 2 to 25 °C with decreasing the chain length or increasing the functionality of the crosslinker. The shortest oxalic acid and the trifunctional citric acid produced SPUN4 and SPUN5 with the highest T_g values due to the restricted mobility of the network. This indicates that the presence of complementary ineractions in the bulk state plays an important role in controling the miscibility-compatibility between both components, which further results in the formation of a homogeneous supramolecular network with easy property tuning by changing the structure/functionality or the amount of crosslinker.

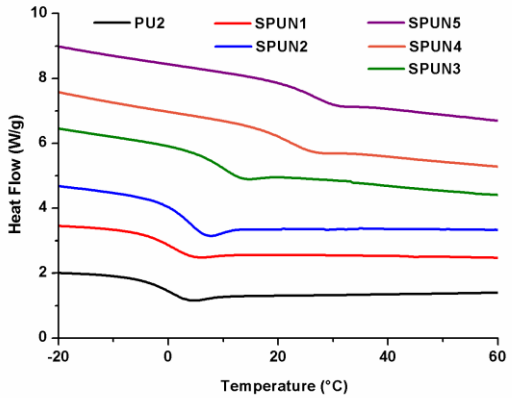

Figure 5.3. DSC traces of PU2 and SPUNs.

Table 5.1. Thermal properties for PU and SPUNs

	DSC	TGA	
Sample	T_g (°C)	$T_{5\%}$ (°C)[a]	T_d (°C)[b]
PU2	0	264	291/333/427
SPUN1	2	228	340/463
SPUN2	4	231	325/460
SPUN3	8	194	190/331/461
SPUN4	20	207	196/347/442
SPUN5	25	189	191/341/463

[a]Temperature at which 5% weight loss was observed.
[b]Temperature for maximum degradation rate.

Thermal stability of PU2 and SPUNs was investigated out by TGA. Figure 5.4(a) shows the weight loss upon heating under N_2 atmosphere. All networks showed lower thermal stability than the control linear PU2 due to decarboxylation/evaporation of carboxylic acid component at high temperature. Figure 5.4(b), thermal degradation and first derivate of PU2, SPUN5 and oxalic acid is shown. The plot displays that the first degradation of SPUN5 coincides with the degradation temperature of oxalic acid. However the main degradation step for all samples occurs in the range of 250-350°C, corresponding to the typical degradation temperature of the urethane bonds. Finally, a third degradation stage occurs over 400 °C and it corresponds to the gasification of any remaining components.

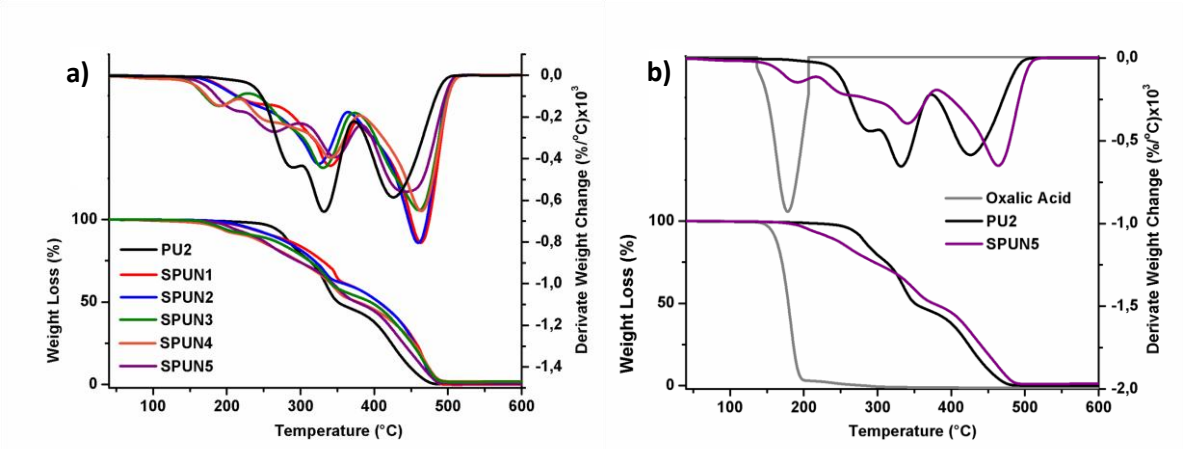

Figure 5.4. TGA and first derivate traces of (a) PU and SPUNs; (b) PU, SPUN5 and oxalic acid .

5.2.3. Mechanical properties.

In order to characterize the synthesized SPUNs with respect to their mechanical properties, uniaxial tensile testing was carried out. The recorded stress-strain curves gave information about the Young's modulus, the elongation and stress at break, as well as the tension energy from the area below the curve (Table 5.2). As control, an additional network, CPU, containing covalent crosslinks was synthesized by thiol-ene photopolymerization (Scheme 5.2) and tested as well beside PU2. As will be shown later, without reversible ionic hydrogen-bonding capability, the control CPU network is drastically different from the SPUNs, lacking extensibility, or any adaptive properties.

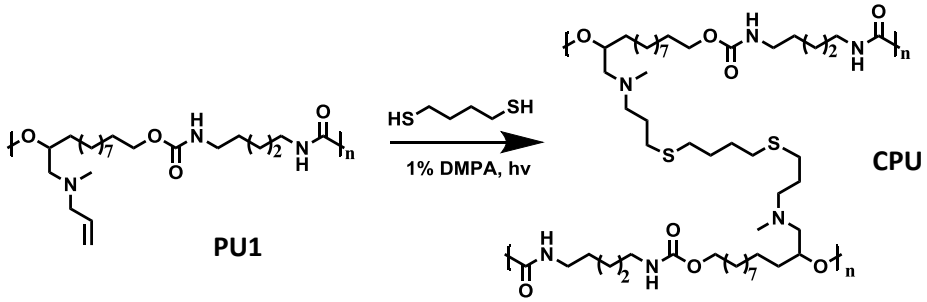

Scheme 5.2. Preparation of CPU.

Table 5.2. Mechanical properties of PU2, SPUNs and CPU.

Sample	Young's Modulus (MPa)	Elongation at break (%)	Stress at break (MPa)	Tensile energy (MJ/m^3)
PU2	0.49±0.03	2987±23	0.0077±0.0002	1.15±0.03
SPUN1	0.21±0.03	536±15	0.53±0.10	2.55±0.04
SPUN2	0.24±0.03	530±11	0.65±0.11	2.75±0.24
SPUN3	0.74±0.03	1943±21	0.0124±0.0002	5.5±0.7
SPUN4	1.9±0.5	512±7	2.59±0.12	8.4±0.4
SPUN5	9.7±0.4	518±10	3.24±0.18	10.6±0.8
CPU	11.24±0.21	123±2	3.89±0.23	4.2±0.5

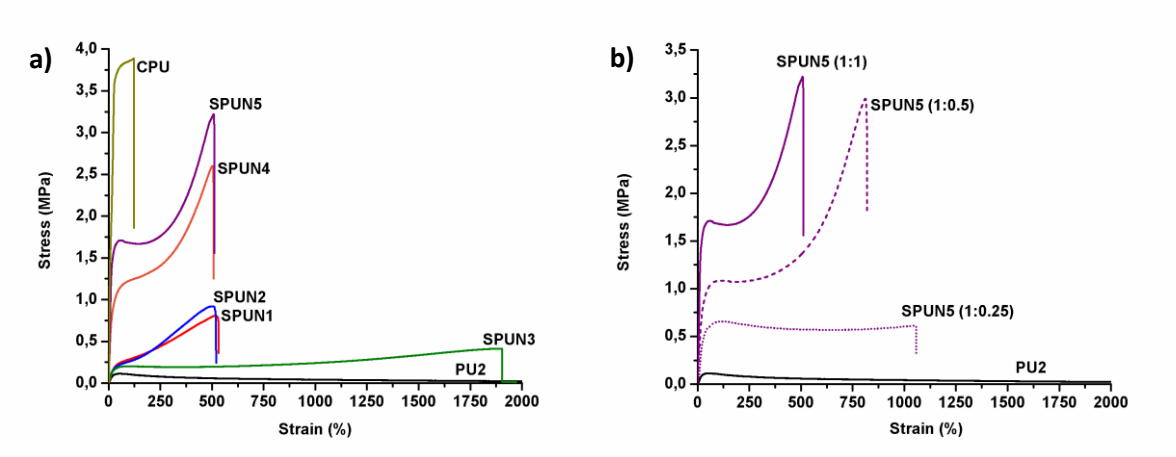

Figure 5.5. Stress-strain curves of (a) PU2, SPUNs and CPU; (b) PU and SPUN5 with different amine:acid ratio.

PU2 shows a stress-strain behavior that is typical for thermoplastics above their T_g. After a small increase of stress in the initial elastic region, the sample shows pronounced yielding and could be drawn up to the limit of the tensile test machine; it is practically flowing lacking internal cohesion. In contrast, SPUNs clearly exhibited a completely different mechanical response behaviour, showing an increasing curve upon elongation until the fracture lenght was reacted at around 500 % elongation. The continuosly rising stress-strain curves of SPUNs may induced by the continuosly ocurring cleavage of ionic hydrogen bonds that have formed in the material as a result of position changes and reorganization processes during stretching, hence leading to form a harder network which requires an increased energy uptake in order to elongate. Interestingly, a sharp bend in the curve for SPUN4 and SPUN5 was clearly observed around 220% strain. This pronunced strain hardening is assumed to be the result of position changes and reorganization processes during stretching, hence leading to a greater proportion of ionic hydrogen bonds that form non-covalent network.

On the contrary, CPU network, where covalent bonds serve as sacrificial bonds, is elastic but brittle, showing very poor elongation at break. In this case, once brittle network is broken the covalent bonds cannot be recovered. Moreover, it should be noted that only SPUNs samples contracted almost to their original dimensions after failure with time or upon heat treatment, showing shape-regeneration properties,

which may originated from the reversible nature of ionic hydrogen bonds, and suggesting interesting self-healing properties for the prepared materials.

It is worth to remark that SPUN3 behaviour is an exception and their properties are more similar to PU2 than others SPUNs. This behaviour can be explained by reduced cross-link density. The presence of intramolecular hydrogen bonds in monoanions of succinic acid via reaction with different amines, has been reported.[42] For this reason, succinic acid was discarted to continue this study. Figure 5.5(b) shows the stress-strain curves of PU2 and SPUN5 with different amine:carboxilic acid ratios. Decreasing the content of carboxilic acid decrease the ionic crosslink and the samples lead to increase the elongation at break and decrease the stress at break and Young's modulus. The presence of non-covalent crosslinks in SPUNs is expected to provide stress-relaxation response to the networks because in the presence of an external loading, these dynamic bonds can break and reform succesibely to dissipate the energy avoiding local stress concentration.

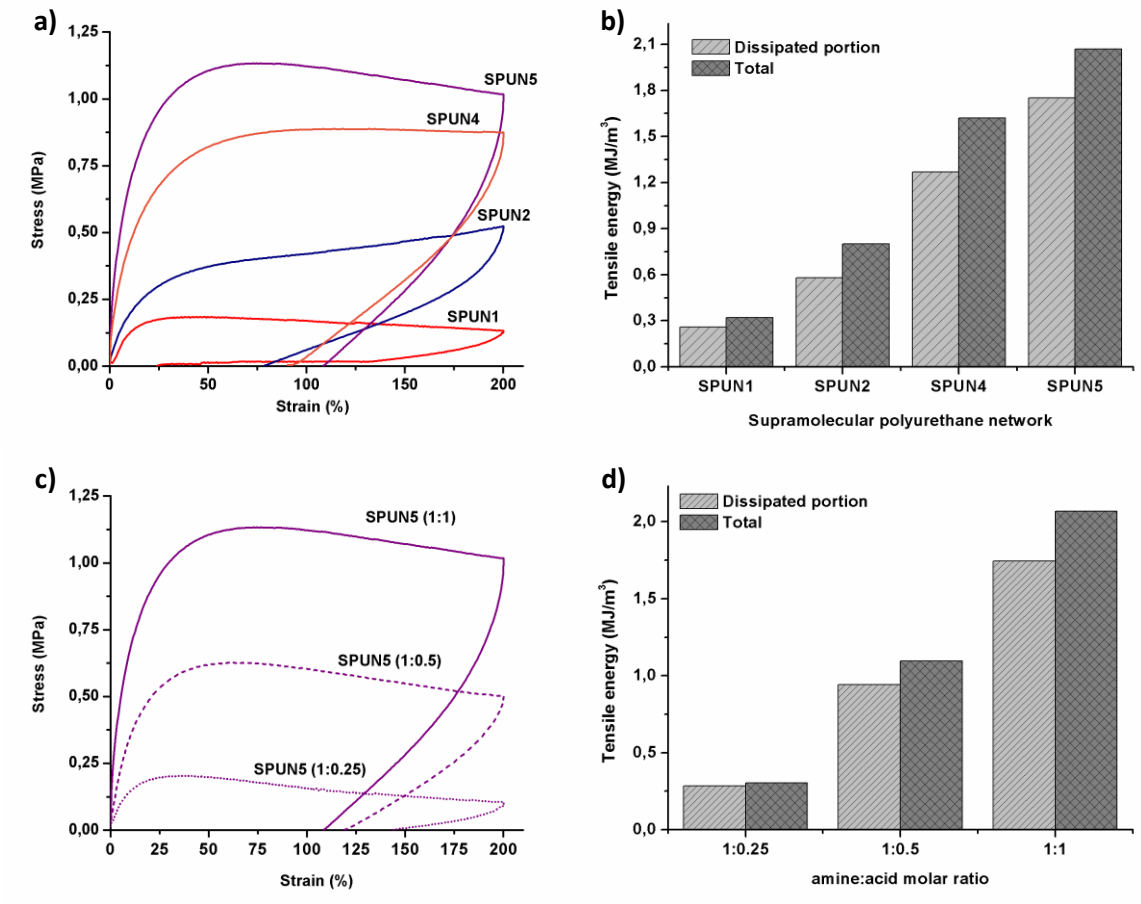

Figure 5.6. Loading-unloding curves (a,c) and total energy and dissipated portion (b,d) of SPUNs; and SPUN5 with different amine:acid ratio.

As noted erlier, the incorporation of ionic hydrogen bonding interactions as crosslinks in SPUNs is and effective means of dissipating any deformation energy that is applied to the system. This energy dissipation can be studied by applying and releasing strain (loading-unloading), either in isolated or repeated cycles. Viscoelastic systems that can be disperse the applied energy will typically exhibit different load and unload stress-strain curves (hysteresis), with the area between the two curves equal to the energy dissipated per unit volume. When the SPUNs were subjected to a loading unloading cycle a pronounced hysteresis was observed in the stress-strain curve (Figure 5.6(a,b)), which indicates the uptake and dissipation of energy in the material, with the magnitude increasing at higher cross-linking densities (Figure 5,6(c,d)).

Moreover, loading-unloading cycles at different strains 5, 10, 25, 50 and 100% for all SPUNs were carried out. As an example, the loading-unloading curves of SPUN5 is shown in Figure 5.7(a). Common behaviour of hysteresis loops can be observed during loading-unloading cycles and the loops become larger when strain is raised, implying that the network of the ionic cross-linking can effectively dissipated the applied energy during the stretching for all samples. Figure 5.7(b) shows the dissipated portion and total toughness for each strain deformation of SPUN5.

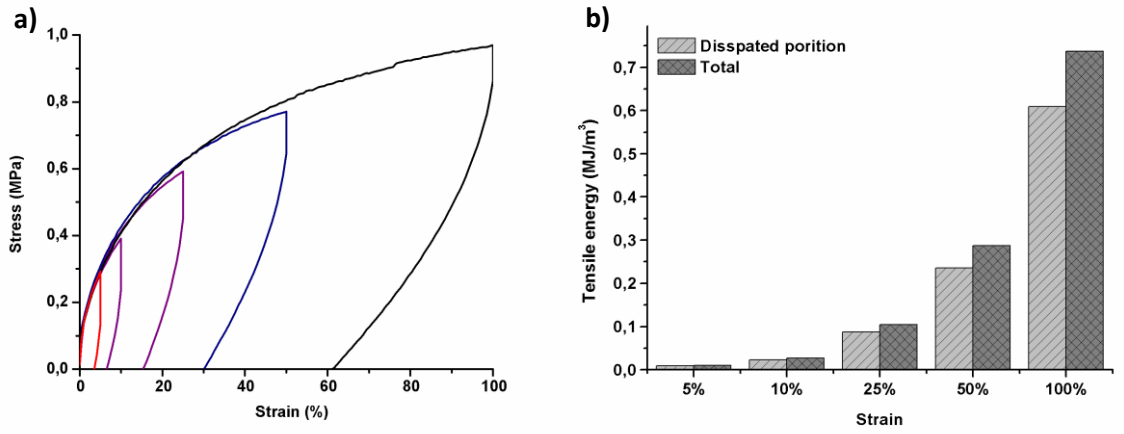

Figure 5.7. Loading-unloding curves of SPUN5 under different strains (a) and total energy and dissipated portion (b).

Then, multiple repetition of the cyclic process provided additional information about the ability of sample to regenerate its shape in time. As an example, SPUN2 was subjected to eight succesive loading unloading cycles with a maximun strain of 100%,

as shown in Figure 5.8(a). Because the material is not able to recover its original shape, the consecutive stress-strain cycles show a decreasing tensile strength maximun and an overall decrease of the energy, being more pronounced from the first to the second cycle since the curves of the subsequent cycles almost orvelapped.

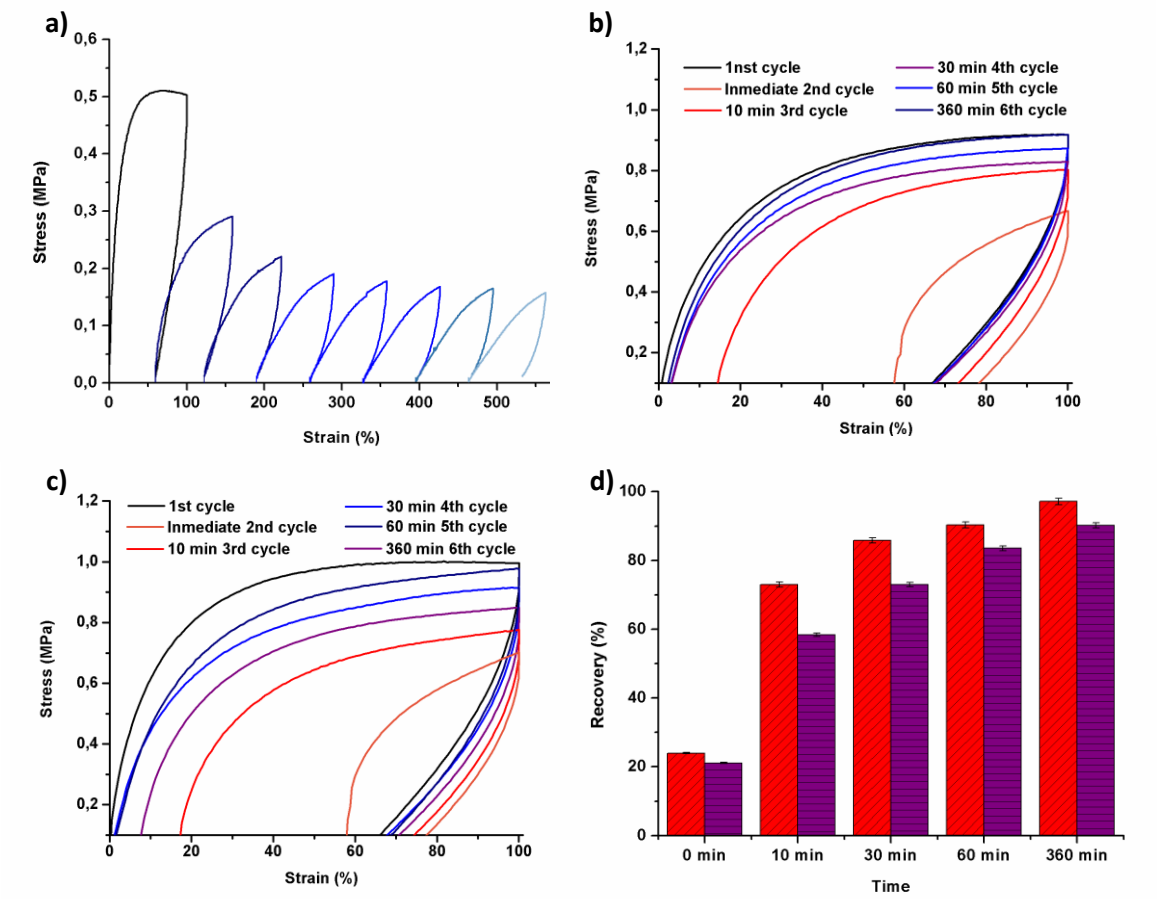

Figure 5.8. (a) Eight succesibe loading-unloading cycles of SPUN2, loading-unloding cyles of (b) SPUN2 and (c) SPUN5 performed after 0, 10, 30, 60 and 360 min, and (d) recovery efficiency of SPUN2 and SPUN5 as a function of recovery time.

To demonstrate that mechanical properties could be recovered, the sample was allowed to rest at room temperture a prescribed time after a first loading-unloading cycle. With the increase in the waiting time, the hysteresis loop recover back to that of the first cycle, suggesting different recovery rates depending on the time of recuperation. Figure 5.8 can be observed the loading-unloading cycles at different recovery time of SPUN2 (b) and SPUN5 (c). Figure 5.8(d) is shown the recovery results of this two networks versus the time waiting between cycles. Neverthless, SPUN2 was able to recover more than 80% of their mechanical properties if the second loading is delayed by 1h. Analysing SPUN2 behaviour, it can be seen how this network recovers

faster the prior mechanical properties than SPUN5 because its lower T_g allows polymer chains to diffuse and rearrange faster at room temperature.

5.2.4. Self-healing, recycling and reshaping properties.

Based on results from recovery experiments, self-healing ability of the prepared SPUNs was studied. Delightfully, these biobased elastomers exhibited promising qualitative self-healing properties. Without adding any solvent, healing agent, or external stimuli, by simply placing two cut pieces together allowing 1h for physical interactions to re-establish the network at the interface, the healed SPUN1 could be stretched to aproximately four times its initial lenght (Figure 5.9).

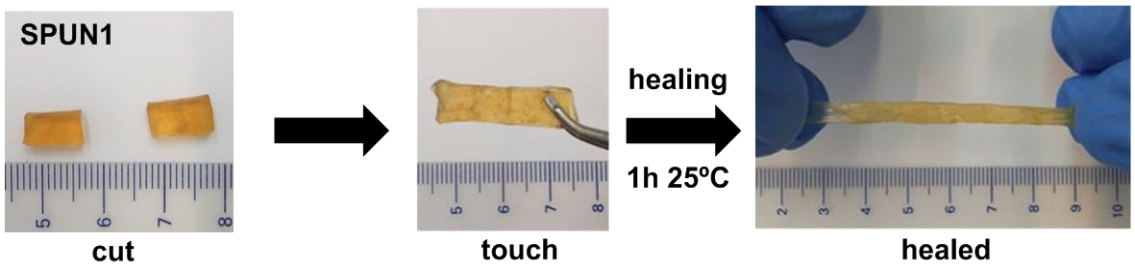

Figure 5.9. Digital images showing the self-healing performance of SPUN1.

To further quantitatively evaluate the self-healing performance of the prepared SPUNs, tensile stress-strain tests were performed on the virgin and self-healed specimens. Three different self-healing times 1h, 12h and 24h were observed after cut, and the sample were tested in tension. Representative tensile curves of rectangular specimens from SPUN5 with different healing times are shown in Figure 5.10(a). The stress-strain curves illustrate that the healing efficiency relies on the healing time and the chain mobility of the system. In the Figure 10(b) can be observed the results of healing efficiency versus time for SPUNs. SPUN1 and SPUN2 with the lower T_g exhibit the fastest healing speed and the self-healing efficiency significantly improved with extending the healing time, reaching an optimal healing of up to 90% recovery of tension energy of virgin sample. Indeed, after healing for 1h, both samples can be healed up to about 60% of its original tension energy, which indicated that more than

half self-healing process ocurred within the first hour after bringing the two cut pieces back in contact.

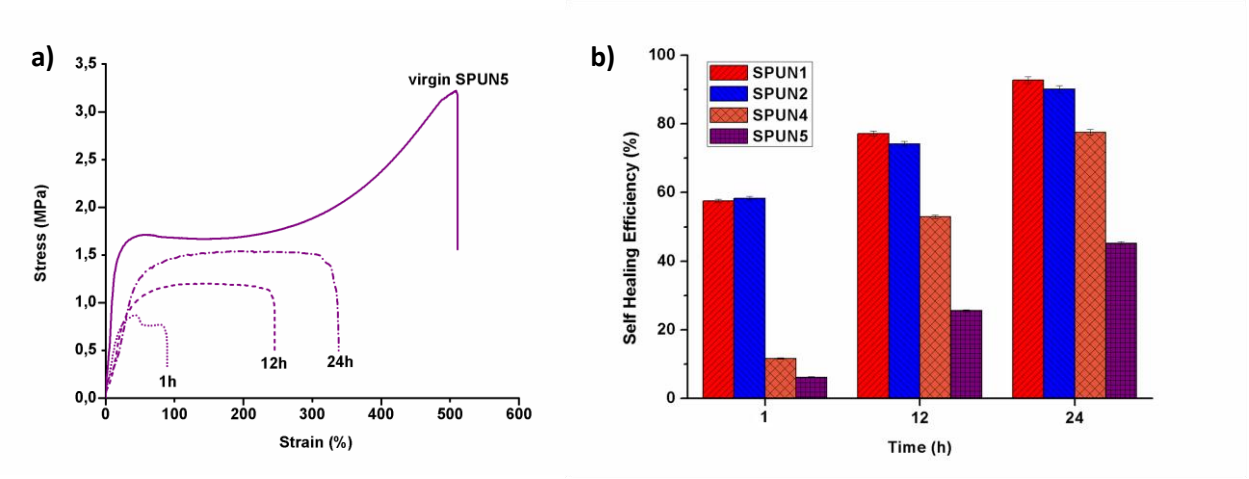

Figure 5.10. Mechanical properties of healed SPUN5(a) and self-healing efficiencies of SPUNs(b) as a function of healing time.

As expected, a decrease in the healing eficiency was observed in systems with lower polymeric chains mobility at room temperature. As an example, SPUN4 recovers half of tension energy at after 12h or SPUN5 recovers only 40% of its original tension energy after 24h.However, accelerate healing speed and increased healing efficiency could be realized at moderate temperature. In Figure 5.11(a) was shown the mechanical properties of healed SPUN5 during 1h at different temperatures, the self-healing efficiency increase from 5 to 82 % for SPUN5. These results suggest that healing time and temperature are important parameters to obtain better healing property. This observation is reasonable because the self-healing properties of SPUNs are attributed to the formation of dynamic hydrogen ionic bonds derived from acid-base reaction, which are similar to those of the reported non-covalent bond based self-healing materials; upon mechanical damage, the non-covalent associations are more likely to break due to their lower strengh compared to covalent bonds, resulting in the presence of a large number of reactive non-associated groups on the surfaces. Once the fracture sufaces being putted back togheter, the non-association grups will react with each other and the broken hydrogen ionic bonds reformed at the interfaces assisted with the difussion and rearrange of polymer chains over time. Thus, long

healing time and moderate temperature is favourable beacuse helps the non-associated groups to pair more efficienly across the interface.

Additionally, the impact of the waiting time of the cut specimens before being brought into contact was investigated. Figure 5.11(b) shows the mechanical properties of three samples of APE1 were cut and kept apart for different durations, and the self-healing efficiencies were subsequently tested after being healed 1h at room temperature. The self-healing efficiency dropped dramatically to 39% and 12% after two fractured surfaced were left apart for 6h and 12%, respectively. The self-healing efficiency results can be observed in Figure 5.11(c).

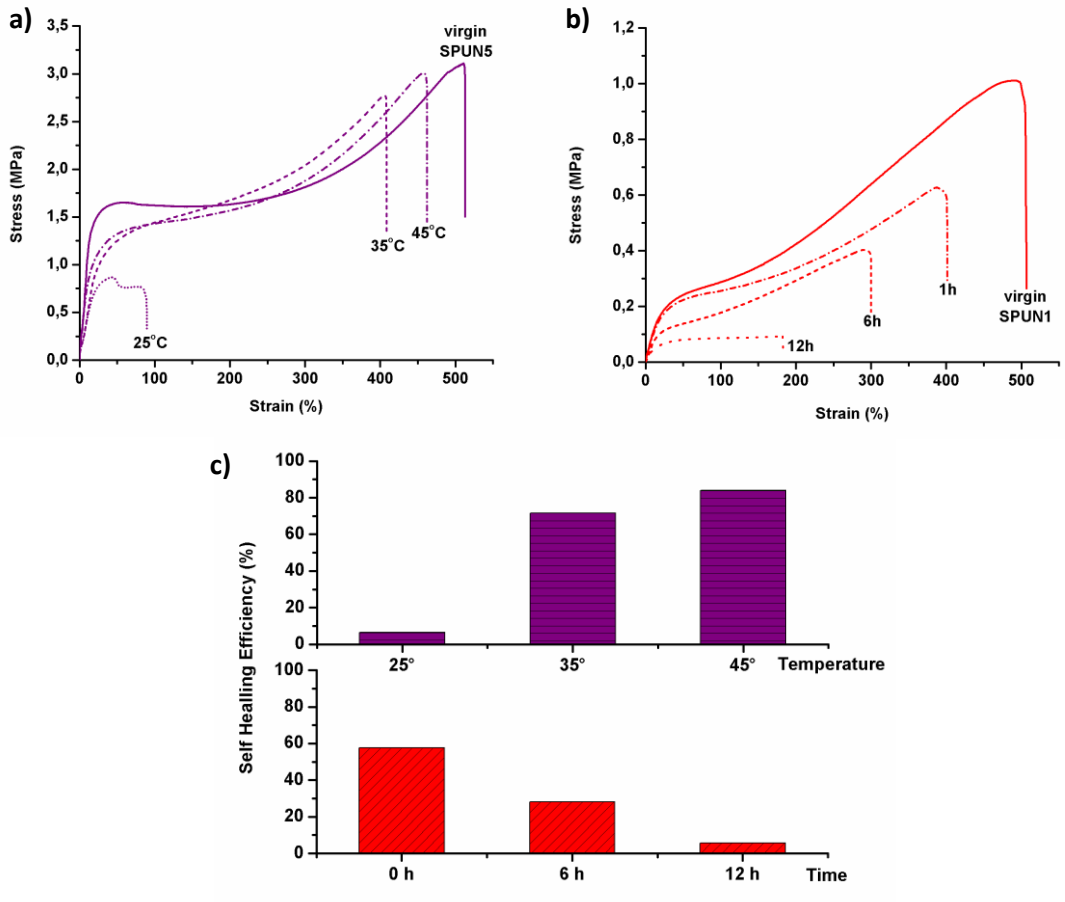

Figure 5.11. Mechanical properties of healed (a) SPUN5 during 1h at different temperatures, (b) SPUN2 as a fuction of cut-union time and (c) self-healing efficiencies of SPUN5 and SPUN2.

Considering the thermal reversibility ionic hydrogen bonds, the recycling and reshaping properties of SPUNs were investigated. The recycling of SPUN4 was achieved by applying heat and pressure to small pieces of polymer in a Teflon mould. As can be seen in Figure 5.12, SPUN4 could be reprocessed two times obtainig a new sample with defect-free appearance by the effective healing via the dynamic ionic hydrogen bonding cross-linkig and rearragement of polymer chains. The tensile analysis shows that after the first cycle the sample could regain 93% of the original fracture energy and after the second cycle the sample could regain 95% of the first recycling cycle fracture energy. Although recycled SPUN4 samples could be elongated to a greater extend until failure, and obvious decrease in ultimate strength was observed.

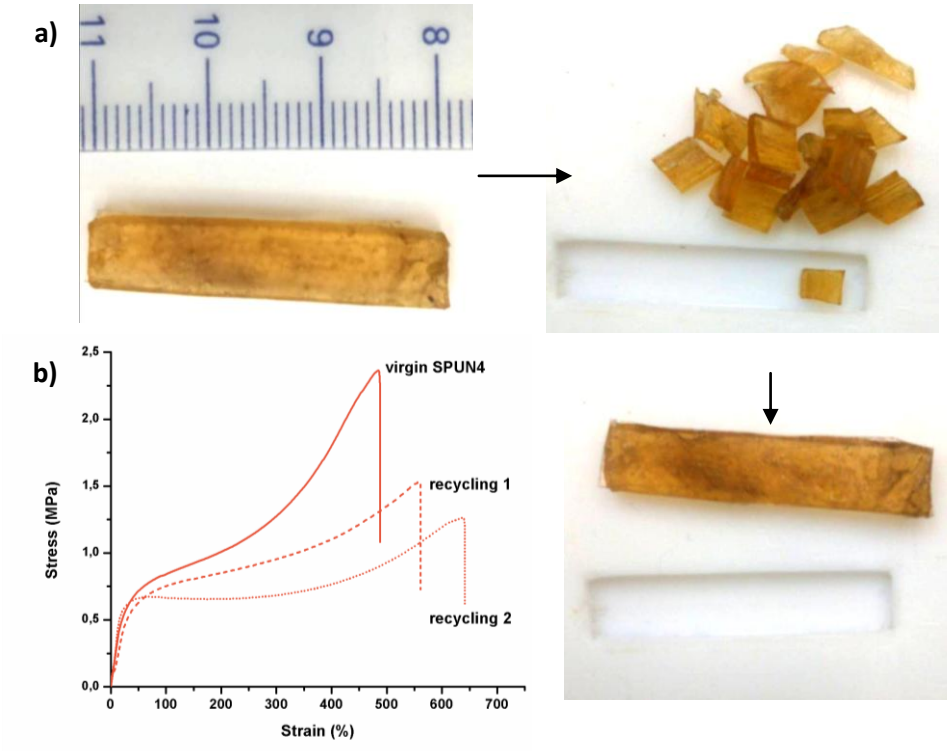

Figure 5.12. Recycling process (a) and tensile stress-strain curves of virgin and recycled SPUN4 (b).

For the covalently cross-linked network CPU, the pieces could not be reporcessed under the same conditions. As expected, synthesized SPUNs could also be reshaped several times after synthesis by heating, moulding and cooling as can be seen in Figure 5.13.

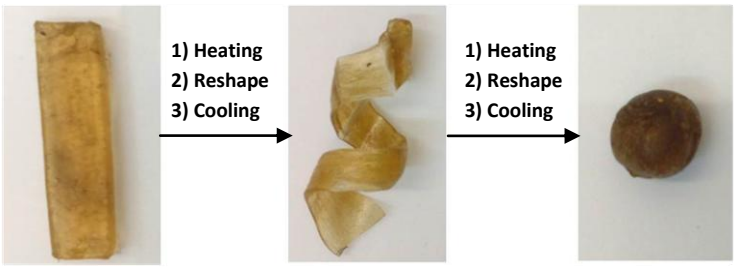

Figure 5.13. Reshaping test for SPUN5; a) original shape, b) helical specimen, which is obtained by moulding the specimen a) at 60 °C during 1 h and cooling, and c) spherical shape, which is obbtained by moulding the specimen b) at 60 °C during 1 h and cooling.

In conclusion, the prepared materials exhibit some promising adaptive material properties such as effective energy dissipation upon deformation through unzipping the ionic hydrogen bonding network, combined with good shape-regeneration property and recycling/reshaping capability arising from their recoverable nature. More importantly, the resulting biobased elastomers possess the inherent self-healing ability, which can be seen as an upgrade of their sustainability. These results envision that the proposed strategy can be extended to combination of non-covalent and covalent interactions to access a new range of responsive materials.

5.3. References

[1] R. P. Wool. Self-healing materials: a review. *Soft Matter*. **2008**, 4, 3, 400-418.

[2] Y. C. Yuan, T. Yin, M. Z. Rong, M. Q. Zhang. Self healing in polymers and polymer composites. Concepts, realization and outlook: a review. *Polymer Letters*. **2008**, 2, 4, 238-250.

[3] B. J. Blaiszik, S. L. B. Kramer, S. C. Olugebefola, J. S. Moore, N. R. Sottos, S. R. White. Self-healing polymers and composites. *Annual Review of Materials Research*. **2010**, 40, 179-211.

[4] D. G. Bekas, K. Tsirka, D. Baltzis, A. S. Paipetis. Self-healing materials: a review of advances in materials, evaluation, characterization and monitoring techniques. *Composites Part B: Engineering*. **2016**, 87, 92-119.

[5] V. K. Thakur, M. R. Kessler. Self-healing polymer nanocomposite materials: A review. *Polymer*. **2015**, 69, 369-383.

[6] D. Y. Wu, S. Meure, D. Solomon. Self-healing polymeric materials: a review of recent developments. *Progress in Polymer Science*. **2008**, 33, 5, 479-522.

[7] Y. Yang, Y, M. W. Urban. Self-healing polymeric materials. *Chemical Society Reviews*. **2013**, 42,17, 7446-7467.

[8] E. B. Murphy, F. Wudl. The world of smart healable materials. *Progress in Polymer Science*. **2010**, 35, 1, 223-251.

[9] N. Roy, B. Bruchmann, J. M. Lehn. DYNAMERS: dynamic polymers as self-healing materials. *Chemical Society Reviews*. **2015**, 44, 11, 3786-3807.

[10] H. Ullah, K. A. Azizli, Z. B. Man, M. B. C. Ismail, M. I. Khan. The potential of microencapsulated self-healing materials for microcracks recovery in self-healing composite systems: A review. *Polymer Reviews*. **2016**, 56, 3, 429-485.

[11] D. Y. Zhu, M. Z. Rong, M. Q. Zhang. Self-healing polymeric materials based on microencapsulated healing agents: From design to preparation. *Progress in Polymer Science*. **2015**, 49, 175-220.

[12] P. Cordier, F. Tournilhac, C. Soulie-Ziakovic, L. Leibler. Self-healing and thermoreversible rubber from supramolecular assembly. *Nature*. **2008**, 451, 977–980.

[13] V. Kostopoulos, A. Kotrotsos, A. Baltopoulos, S. Tsantzalis, P. Tsokanas, T. Loutas, A. W. Bosman. Mode II fracture toughening and healing of composites using supramolecular polymer interlayers. *Express Polymer Letters*. **2016**, 10, 11, 914-926.

[14] N. Zhong, W. Post. Self-repair of structural and functional composites with intrinsically self-healing polymer matrices: A review. *Composites Part A: Applied Science and Manufacturing*. **2015**, 69, 226-239.

[15] J. J. Cash, T. Kubo, A. P. Bapat, B. S. Sumerlin. Room-temperature self-healing polymers based on dynamic-covalent boronic esters. *Macromolecules*. **2015**, 48, 7, 2098-2106.

[16] A. Das, A. Sallat, F. Böhme, M. Suckow, D. Basu, S. Wießner, G. Heinrich. Ionic modification turns commercial rubber into a self-healing material. *ACS applied materials & interfaces*. **2015**, 7, 37, 20623-20630.

[17] M. Q. Zhang, M. Z. Rong. Intrinsic self-healing of covalent polymers through bond reconnection towards strength restoration. *Polymer Chemistry*. **2013**, 4, 18, 4878-4884.

[18] Y. Yang, X. Ding, M. W. Urban. Chemical and physical aspects of self-healing materials. *Progress in Polymer Science*. **2015**, 49, 34-59.

[19] F. Liu, W. L. Jarrett, M. W. Urban. Glass (Tg) and stimuli-responsive (TSR) transitions in random copolymers. *Macromolecules*. **2010**, 43, 12, 5330-5337.

[20] R. J. Wojtecki, M. A. Meador, S. J. Rowan. Using the dynamic bond to access macroscopically responsive structurally dynamic polymers. *Natural Materials*. **2011**, 10, 14–27

[21] M. D. Hager, P. Greil, C. Leyens, S. van der Zwaag, U. S. Schubert. Self-healing materials. *Advanced Materials*. **2010**, 22, 5424–5430.

[22] A. W. Bosman, R. P. Sijbesma, E. W. Meijer. Supramolecular polymers at work. *Materials Today*. **2004**, 7, 4, 34-39.

[23] F. Herbst, D. Döhler, P. Michael, W. H. Binder. Self-healing polymers via supramolecular forces. *Macromolecular rapid communications*. **2013**, 34, 3, 203-220.

[24] M. Burnworth M. Optically healable supramolecular polymers. *Nature*. **2011**, 472, 334–337.

[25] Q. Wang, J. L. Mynar, M. Yoshida, E. Lee, M. Lee, K. Okuro, T. Aida, T. High-water-content mouldable hydrogels by mixing clay and a dendritic molecular binder. *Nature*. **2010**, 463, 7279, 339-343.

[26] B. P. Lee, P. B. Messersmith, J. N. Israelachvili, J. H. Waite. Mussel-inspired adhesives and coatings. *Annual review of materials research*. **2011**, 41, 99.

[27] N. Holten-Andersen, M. J. Harrington, H. Birkedal, B. P. Lee, P. B. Messersmith, K. Y. C. Lee, J. H. Waite. pH-induced metal-ligand cross-links inspired by mussel yield self-healing polymer networks with near-covalent elastic moduli. *Proceedings of the National Academy of Sciences*. **2011**, 108, 7, 2651-2655.

[28] S. H. Cho, S. R. White, P. V. Braun. Self-healing polymer coatings. *Advanced Materials*. **2009**, 21, 6, 645-649.

[29] G. V. Kolmakov, R. Revanur, R. Tangirala, T. Emrick, T. P. Russell, A. J. Crosby, A. C. Balazs. Using nanoparticle-filled microcapsules for site-specific healing of damaged substrates: creating a “repair-and-go” system. *ACS nano*. **2010**, 4, 2, 1115-1123.

[30] A. W. Bosman, R. P. Sijbesma, E. W. Meijer. Supramolecular polymers at work. *Materials Today*. **2004**. 7, 4, 34-39.

[31] M. A. Aboudzadeh, M. E. Fernandez, E. Muñoz, A. Santamaria and D. Mecerreyes. *Macromolecular Rapid Communication.* **2014**. 35, 460–465

[32] M. A. Aboudzadeh, M. E. Muñoz, A. Santamaría, R. Marcilla, D. Mecerreyes. Facile synthesis of supramolecular ionic polymers that combine unique rheological, ionic conductivity, and self-healing properties. *Macromolecular Rapid Communications*. **2012**. 33, 4, 314-318.

[33] L. Yang, X Tan, Z Wang, X. Zhang. Supramolecular polymers: historical development, preparation, characterization, and functions. *Chemical reviews*. **2015**. 115, 15, 7196-7239.

[34] T. Aida, E. W. Meije, S. I. Stupp. Functional supramolecular polymers. *Science*. **2012**. 335, 6070, 813-817.

[35] T. Yan, K. Schröter, F. Herbst, W. H. Binder, T. Thurn-Albrecht. Unveiling the molecular mechanism of self-healing in a telechelic, supramolecular polymer network. *Scientific Reports*. **2016**, 6.

[36] G. M. van Gemert, J. W. Peeters, S. H. Söntjens, H. M. Janssen, A. W. Bosman. Self-healing supramolecular polymers in action. *Macromolecular Chemistry and Physics*. **2012**. 213, 2, 234-242.

[37] Y. Heo, H. A. Sodano. Self-Healing Polyurethanes with Shape Recovery. *Advanced Functional Materials*. **2014**, 24, 33, 5261-5268.

[38] Y. Lin, G. Li. An intermolecular quadruple hydrogen-bonding strategy to fabricate self-healing and highly deformable polyurethane hydrogels. *Journal of Materials Chemistry B*. **2014**, 2, 39, 6878-6885.

[39] S. Chen, F. Mo, Y. Yang, F. J. Stadler, S. Chen, H. Yang, Z. Ge. Development of zwitterionic polyurethanes with multi-shape memory effects and self-healing properties. *Journal of Materials Chemistry A*. **2015**, 3, 6, 2924-2933.

[40] M. Comí, G. Lligadas, J. C. Ronda, M. Galià, V. Cádiz. Synthesis of castor-oil based polyurethanes bearing alkene/alkyne groups and subsequent thiol-ene/yne post-modification. *Polymer*. **2016**. 103, 163-170.

[41] L. González, A. Ladegaard Skov, S. Hvilsted. Ionic networks derived from the protonation of dendritic amines with carboxylic acid end-functionalized PEGs. *Journal of Polymer Science Part A: Polymer Chemistry*. **2013**, 51, 6, 1359-1371.

[42] J. Guo, P. M. Tolstoy, B. Koeppe, G. S. Denisov, H. H. Limbach. NMR study of conformational exchange and double-well proton potential in intramolecular hydrogen bonds in monoanions of succinic acid and derivatives. *The Journal of Physical Chemistry A*. **2011**. 115, 35, 9828-9836.

Chapter 6

Biobased Polyurethanes with Shape-Memory Properties through Covalent and Non-Covalent Approaches

In this chapter the orthogonal post-polymerization modification permits to combine covalent and non-covalent cross-links. The study is devoted to investigate the changes in thermal and mechanical properties depending on the covalent crosslink content. Shape-memory properties were also evaluated.

UNIVERSITAT ROVIRA I VIRGILI
AVANCES EN SISTEMAS INTERACTIVOS PARA PERSONAS CON PARÁLISIS CEREBRAL
Marc Comí Bonachí

6.1. Introduction

The synthesis of new polymers, inspired in the principles that nature has developed over millions of years, has been an important aim for scientists in the last decades. Natural materials are able to adapt to the conditions of their surrounding environment. In this context, one of the most inspiring features is their ability to change a specific property upon an external trigger.[1,2] Shape memory polymers (SMPs) are defined as responsive materials capable of changing their shape in response to an external stimulus.[3] Thus, these polymers are able to memorize a permanent shape and that can be manipulated in a way that certain temporary shape will be fixed under appropriate conditions.[4-6] According to the stimulus,[7] shape memory effects (SMEs) are divided into thermal-induced SMEs,[8] light-induced SMEs,[9] and electro-active SMEs.[10] Recently, SMPs have become increasingly important due to the growing number of applications, such as actuators,[11] biomedical devices,[12-15] smart clothing,[16] flexible electronics, aircraft devices,[17,18] information carriers,[19] and assembly/disassembly.[20,21] Thermally-responsive SMPs can be used in most of these applications since their shape recovery is generally triggered be heating the specimen above a transition temperature.

Generally, thermally-responsive SMPs possess at least two different phases, as can be seen in Figure 6.1: a stable network and a second phase, which can be influenced by the external trigger. The former phase stabilizes the whole SMP and is responsible to retain the original shape, i.e. the deformation of this phase is the driving force for the shape recovery. This stable phase can be achieved by the introduction of chemical cross-linking, crystalline phases or interpenetrating networks.[22-24] The second reversible phase is able to immobilize or fix a temporary shape and prevent elastic recovery until the appropriated stimulus is applied. This occurs by crystallization (i.e. a melting transition will lead to the shape recovery), a glass transition, a transition between different liquid crystalline phases or reversible covalent cross-linking.[25,26]

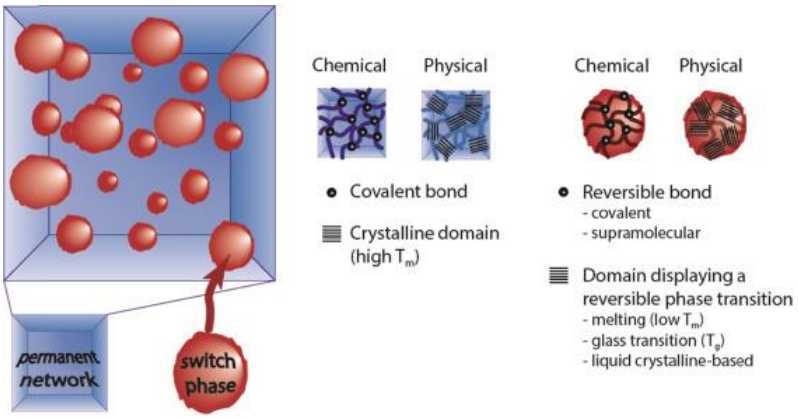

Figure 6.1. General structure of SMPs consisting of a stable network, which determines the shape and a reversible phase, which can be triggered by external stimuli.

Recent research on SMPs tends to develop a multi-shape memory effect, which can fix two or more temporary shapes and recover from the first temporary shape to the other temporary shapes one by one, until ultimately finally obtaining a permanent shape.[27-30] SMPs with multi-SME, are believed to have significant and broad technology impacts. It is important to note that currently known triple-SMP systems possess two well separated phase transitions and that the two temporary shapes are introduced above and between both transitions temperatures.[31-34] For instance, triple-memory properties could be achieved by designing two thermal transitions in multi-block segmented polyurethanes,[35-37] grafting polymers,[38,39] semi-interpenetrating polymer networks,[40] polymer blends,[41,42] or polymer composites.[43] Another strategy relies on a single broad thermal transition since the broad thermal transition could be thought to multiple distinct transitions.[44,45] The broad glass transition temperature can be modulated with easy changes in the material composition.[46,47] Xie and Li had achieved step-wise multi-shape memory and recovery by using the broad transition in perfluorosulphonic acid ionomers (PFSA). [48,49] Although many kinds of multi-SMPs have been reported previously, PFSA is still very important thermoplastic multi-SMPs which can be processed into thin films for building bulk smart devices.[¡Error! Marcador no definido.]

In the case of PUs, shape memory polyurethane (SMPU) composed of hard segment and soft segment has been extensively researched.[50-52] It is generally accepted that hard segments can bind themselves via hydrogen bonding or crystallization making the SMPU very solid below melting temperature (Tm). Reversible phase transformation of

soft segment either amorphous phase or semi-crystalline phase is reported to be responsible for the thermal-induced SMEs of SMPU. Thus, the SMEs of traditional SMPUs can be controlled through the molecular weight of soft segment, mole ratio between hard and soft segment, and polymerization process.[53]

In addition to Tg-type-SMPs with amorphous switching segment and Tm-type-SMPs with crystalline switching segment,[50,51] supramolecular SMPs based on thermal-reversible non-covalent bonding recently have been another new kind of SMPs.[54] In these systems, the reversible non-covalent interactions are used to stabilize mechanically strain stated in polymer elastomers; and shape recovery is achieved upon heating due to the dissociation of non-covalent bonds. The design of SMPUs based on hydrogen bonds relies mostly on pyridine side-chain groups.[55-57] Chen et al. synthesized supramolecular polyurethane networks that contain pyridyl units and found that the nitrogen atoms on pyridine form hydrogen bonds with urethane linkages. Due to the temperature effects, these hydrogen bonds can lead to polyurethane that achieves 91.7 % shape memory recovery. Alternatively, the design and synthesis of novel zwitterionic PUs with sulfobetaine groups have also been considered for obtaining biocompatible SMPUs.[58-60] In this case, non-covalent ionic interactions are crucial to achieve the SMPs. For example, Chen et al. synthesized novel zwitterionic multi-shape-memory polyurethanes (ZSMPUs) capable of remembering four different shapes. Moreover it was demonstrated that increasing the sulfobetaine content promotes the phase mixing and zwitterions serve as organic fillers in the zwitterionic polyurethane. Combining the pyridine side-chain group with post-polymerization modification by ring-opening of 1,3-propansultone, Chen et al. reported pyridine type ZSMPUs composed of a hard phase and an amorphous soft phase with a broad glass transition. These materials have more than 86% shape recovery and more than 95% shape fixity when a heat stimulus is applied.[61]

As was been demonstrated along the previous chapters, the properties of the PUs synthesized in this Thesis can be tuned through covalent and non-covalent approaches. Pursuing the preparation of novel SMPs, this chapter is focused on combining the previously described covalent and non-covalent approaches to fabricate dually cross-linked networks. It is expected that covalent cross-links will form a

permanent network which can enhance the mechanical strength and maintain the permanent shape of the polymers, while non-covalent bonds will constitute reversible network. This physical network will be used to fix the temporary shape after load and cooling and prevent elastic recovery until heat is applied. As can be seen in Scheme 6.1 and reported for other functional materials fabrication.[62-65]

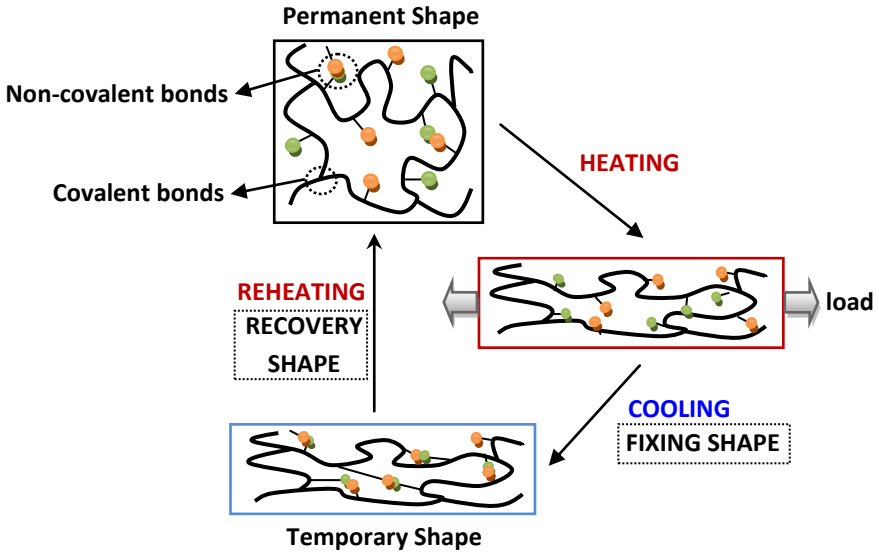

Scheme 6.1. Schemmatic representation of thermal dual-SME in networks based on covalent and non-covalent cross-links.

6.2. Results and discussion

6.2.1. Synthesis of ionic-covalent polyurethane networks (ICPUNs).

The linear PU selected for this study must contain two different functionalities; a functional group that can be modified with covalent bond, while also other that can be modified by ionic hydrogen bonds. Following the methodology of the chapter 3, 11-allylmethylaminoundecan-1,10-diol (D1), that contains terminal alkene and tertiary amine group, was used to prepare a linear PU.[66]

As described in the previous chapters, the thermal and mechanical properties of PUs depend on the chemical structure of the selected isocyanate. It was previously demonstrated that while IPDI (a cyclic diisocyanate) produces rigid PUs when combined with castor-oil-derived diols, hexamethylene diisocyanate (HDI) produces soft materials with Tg below room temperature. In this study, HDI was used, due to

obtain flexible polymer films at room temperature, that can conserve a shape and at the same time can be easily deformed without failure. The molecular weight of PU was evaluated by SEC and resulted about M_w 39000 Da and dispersity of 1.4.

The structural characterization of PU1 was carried out by NMR and FTIR spectroscopy. Figure 6.2(a) shows the ^{1}H NMR spectrum of polyurethane from aminodiol (D1) and HDI. Protons corresponding to the linear diisocyanate were identified at 3.15 ppm signal (i) from methylenes linked to urethane group. Moreover, the signals of methine (f) and methylene (g) directly bonded to urethane group were appeared at 4.85 and 4.01 ppm.

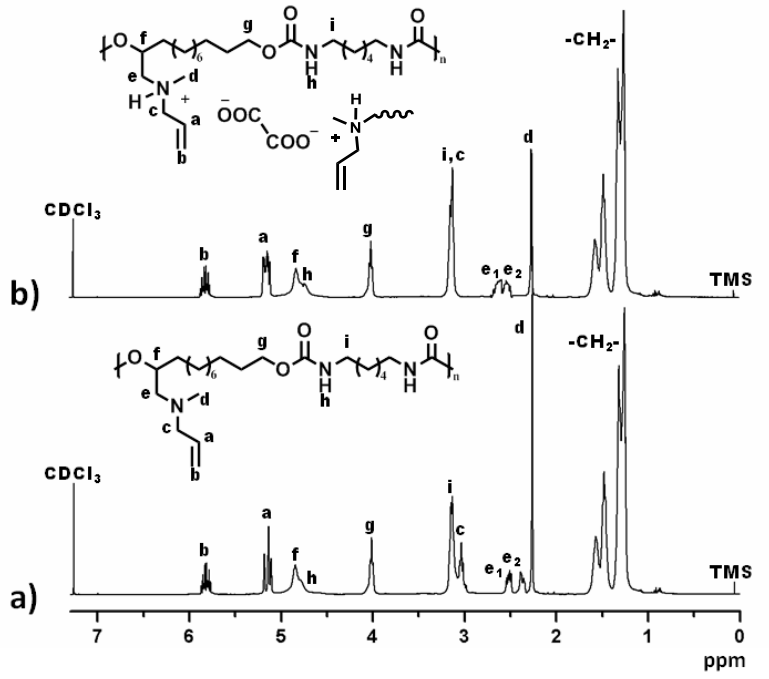

Figure 6.2. ^{1}H NMR spectra of PU1(a) and SPU1N (b).

Moreover, FTIR spectroscopic characterization revealed the expected structural features. Including the disappearance of the vibrational band of NCO function, located at 2235 cm^{-1} and the appearance absorption bands of the main chain about 1693, 3319 and 1530 cm^{-1} arising from urethane linkages corresponding to C=O stretching and NH stretching and bending bands respectively.

The preparation of ICPUNs from PU1 in THF solution at room temperature was carried out in two steps (Scheme 6.2), taking advantage of different reactivity of side-chain functional groups. In the first step a reversible network interpenetrating the PU chains was prepared. As can be seen in the chapter 4 and 5, the incorporation of physical linkages was carried out by acid-base reaction between tertiary amine and carboxylic acid group. Among these acids, oxalic acid is the shortest alkyl chain diacid and forms the most restrictive reversible network at room temperature, improving the thermal and mechanical properties in comparison with PU precursor. The methodology of previous chapter is repeated and supramolecular PU1 network (SPU1N) was obtained as light yellow transparent materials, suggesting the homogeneous dispersion of the solid diacid in the PU chains. The reversible network was presented as ionic hydrogen bonds between allylmethyl amminium cation in PU side-chain linked to oxalate dianion. Figure 6.3(b) shows ^{1}H NMR spectra of SPU1N, where methylene signals (e and c) directly bonded to nitrogen suffering a slight deshielding (0.15-0.25 ppm).

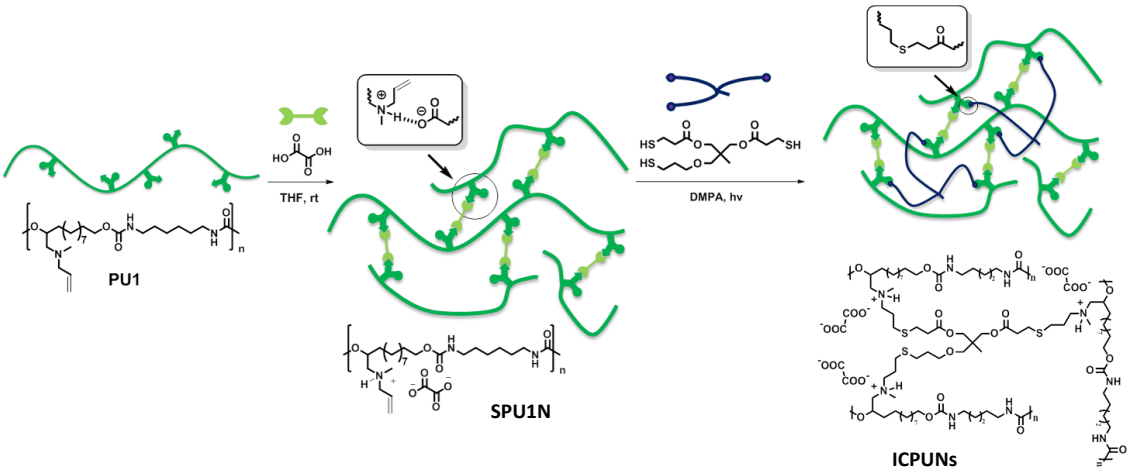

Scheme 6.2. Post-polymerization modification process.

In the second step, the covalent network was obtained by post-polymerization modification via photoinitiated thiol-ene coupling reaction, using different amounts of trimethylpopane tris(3-mercaptopropionate) (TMMP) in the presence of DMPA. Four samples with 7% (ICPUN7%), 15% (ICPUN15%), 30% (ICPUN30%) and 60% (ICPUN60%) of alkenes groups in PU side-chain modified by alkyl sulphide bonds were obtained after reaction and solution casting process. FTIR spectra was used to monitor the

formation of the covalent networks by the disappearance of the vibrational band of S-H bond located at 2568 cm^{-1}.

6.2.2. Thermal and mechanical properties

The thermal properties of different ICPUNs were evaluated DSC and TGA under N_2 atmosphere at heating rate of 10°C/min. Figure 6.3 shows the DSC traces corresponding to the second heating scan of a heating-cooling cycle analysis. It can be seen that all ICPUNs are polymers without showing any trace of exothermic or endothermic peak directly related with melting or crystallization phase transitions. As was seen in the chapter 5, of oxalic acid irruption between PU chains, reduces the mobility of the PU chains due to the incorporation of physical cross-links. As can be seen in Table 6.1 that glass transition temperature (T_g) increases gradually with the increase of TMMP content. This behaviour demonstrates that T_g increases due to the restriction of chain mobility by the formation of covalent networks.[65] The T_g values are raised from 24 to 36°C, making these networks suitable for biomedical devices thanks to their similarity to body or biomedical application temperature.

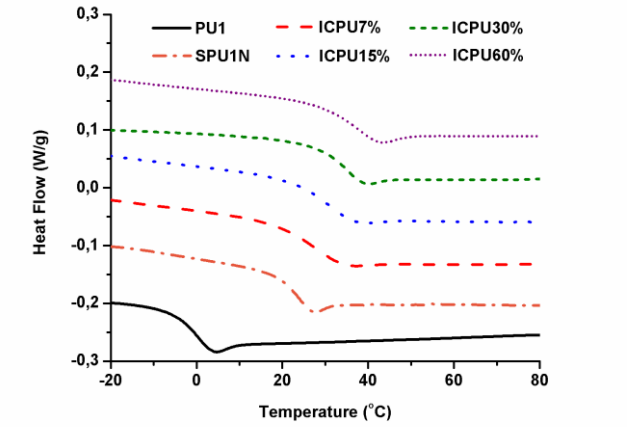

Figure 6.3. The second DSC heating scans traces of PU1, SPU1N and ICPUNs

Figure 6.4(a) shows the thermogravimetric analysis the first derivate for all the synthezised ICPUNs. The degradation of ICPUNs take place in three main steps. The first degradation peak appears around 200 °C, is produced for the descarboxylation/evaporation process of the physical cross-linking, in this case, oxalate moiety, this was confirmed overlapping the TGA curves of oxalic acid and ICPUN60%. (Figure 6.4(b)). The main degradation step (300-400 °C) in Figure 6.4(a) is associated with the urethane dissociation, mainly depending on the isocyanate and alcohol structures used.[67] Finally, the third degradation stage, over 400 °C, corresponds to the gasification of any remaining backbone components.[68]

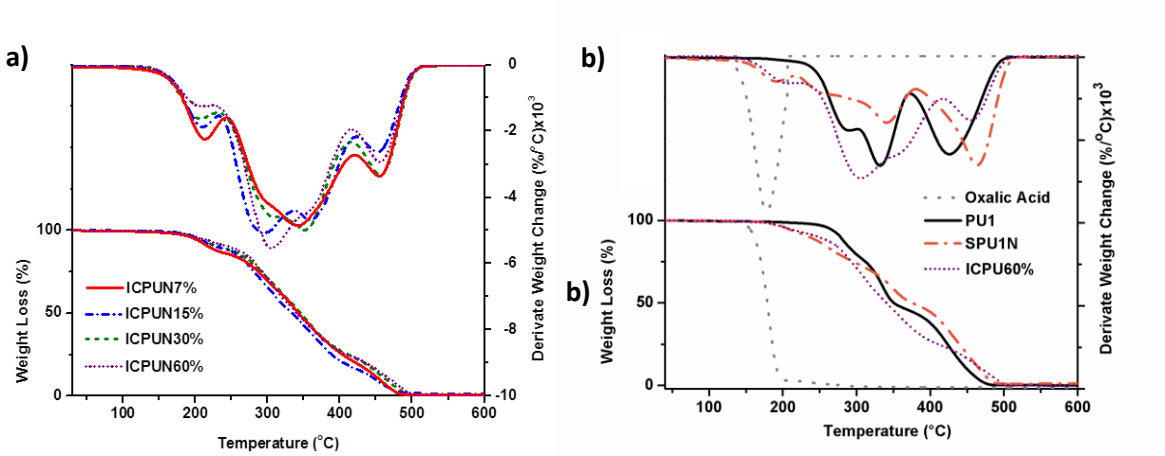

Figure 6.4. TGA and first derivative curve of oxalic acid, PU1, SPU1N and ICPU60% (a), and ICPUNs (b).

Table 6.1. Thermal properties for PU1, SPU1N and ICPUNs.

	DSC	DMA	TGA	
Sample	T_g (°C)	T_g(°C)	$T_{5\%}$ (°C)[a]	Td (°C)[b]
PU1	-1	-	262	289/337/424
SPU1N	22	30	186	191/343/465
ICPUN7%	25	40	199	213/341/454
ICPUN15%	27	41	202	210/354/452
ICPUN30%	31	48	205	206/350/456
ICPUN60%	36	49	208	210/364/484

[a]Temperature at which 5% weight loss was observed.
[b]Temperature for maximum degradation rate.

The dynamomechanical behaviour of ICPUNs was investigated by DMTA. Figure 6.5 shows the elastic modulus and the dissipation factor as a function of the temperature. At low temperatures there is a solid state with *E*' at a high modulus plateau and at higher temperatures there is a rubbery state with a lower *E*'. The storage moduli at the solid plateau increase remarkably in comparison to SPU1N, indicating that the incorporation of covalent cross-links can be of benefit for improving mechanical performance. From the DMTA curves, the plateau of the E' in the rubbery state can be used to make qualitative comparisons of of the level of covalent cross-linking among the various polymers. In this case, the storage moduli at the rubbery plateau increase when the TMMP content increase and it is maintained up to 120 °C for all networks, whereas in SPU1N, without covalent crosslink, E' tends to decrease at 60 °C and eventually flows.

DMTA also allows determining the T_g of cross-linked materials. It can be detected as the maximum of the Tan δ. The glass transition temperature determined from the peak of Tan δ is higher than the one determined by DSC (Table 6.1), which can be related to the heat transporting hysteresis for large scale samples in DMTA. Consistent with DSC results, this peak shows a shift of maxima when increasing. The height of the Tan δ peak increases as the content of TMMP decreases, according to the lower cross-linking density that causes lower limitations on freedom of chain mobility. For all ICPUNs was observed a broad curve of Tan δ. This broad T_g was also reported in the perfluorosulfonate ionomer and the polyethylene-based carboxylated ionomer. [48,69] These results demonstrate that the ionic interactions among the side chains greatly influence the mobility of the backbone. The broad glass transition can be viewed as the collective contribution of an infinite number of transitions, each corresponding to infinitely sharp transition temperatures continuously distributed across the broad transition.[48] The slow dissociation of ionic hydrogen bonds or the creep relaxation of side chains upon heating, makes the polymer show a broad glass transition.

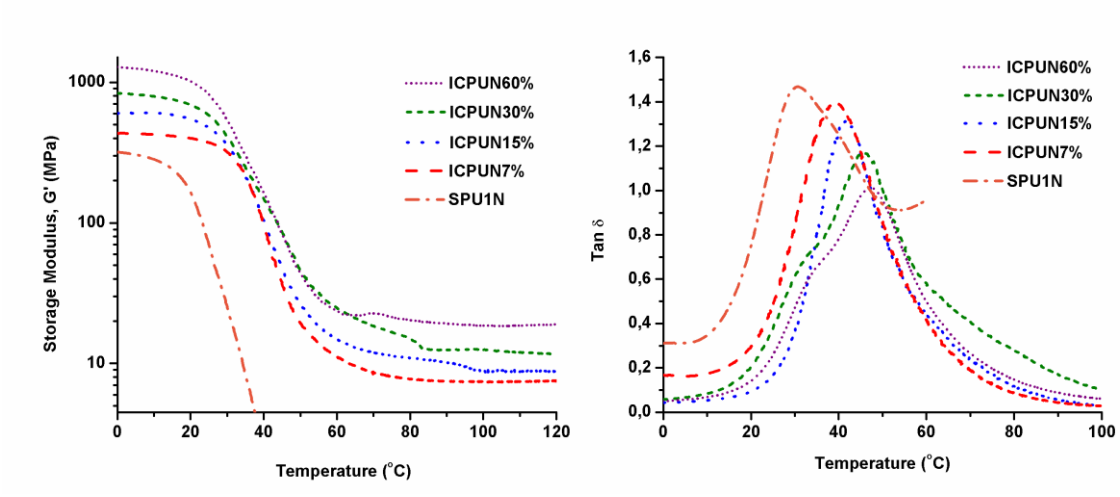

Figure 6.5. E' (a) and Tan δ (b) as a function of temperature for SPU1N and ICPUNs.

The thermo-mechanical results suggested that temporary shape of these networks can be fixed at room temperature, for this reason, mechanical properties were investigated by uniaxial tensile testing was carried out. The recorded stress-strain curves are shown in Figure 6.6 and the results of Young's modulus, elongation at break, stress at break and their standard deviation are given in Table 6.2. Confirming the results of the chapter 5, PU1 without cross-linking shows a stress-strain behaviour that is typical for thermoplastics above their T_g, it is practically flowing lacking internal cohesion. In contrast, SPU1N clearly exhibited completely different mechanical response behaviour, showing an increasing curve upon elongation until the fracture length due to form harder network which requires an increased energy uptake in order to elongate. In addition, the incorporation of chemical cross-links leads to a remarkable improvement in the mechanical strength but decrease in the elongation at break. This indicates that the mechanical properties of the PU network can be systematically tuned by varying the covalent cross-linking content. It can be observed that the tensile stress at break increases by ICPUNs from 3.9 to 13.9 MPa when the content of the TMMP cross-linker changed from 7 to 60%, while the elongation at break decreases from 507 to 188%. This is because the ionic hydrogen bonds formed by the acid-base reaction between oxalic acid and side-chain tertiary amine group can reversibly break and re-form to rearrange the PU chains along the stretching direction, leading to the good extensively. On the contrary, covalent cross-links form an

irreversible elastic network, which restricts the mobility of polymer chains, resulting in an enhanced mechanical strength but poor extensibility.

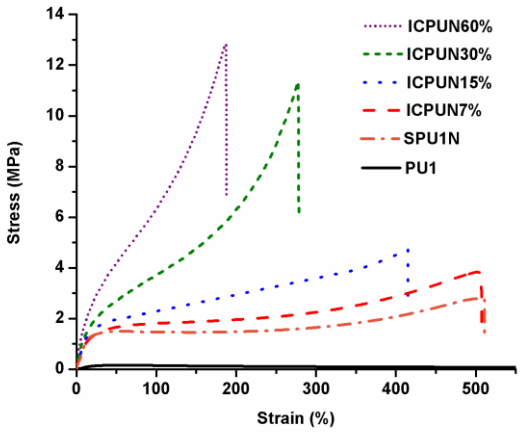

Figure 6.6. Stress-strain curves of PU1, SPU1N and ICPUNs

Table 6.2. Mechanical properties of PU1, SPU1N and ICPUNs.

Sample	Young Modulus (Mpa)	Elongation at break (%)	Stress at break (MPa)
PU1	0.39±0.03	2987±23	0.0077±0.0002
SPU1N	9.2±0.4	516±10	2.51±0.16
ICPUN7%	2.4±0.1	507±8	3.9±0.2
ICPUN15%	4.8±0.1	415±8	5.8±0.4
ICPUN30%	9.3±0.1	278±6	11.4±0.9
ICPUN60%	17.1±0.2	188±2	13.9±0.9

The superior mechanical properties of ICPUNs compared to SPU1N can be explained by the combination of covalent and non-covalent network structure. To deeply investigate the mechanical properties of ICPUNs at room temperature, cyclic tensile loading-unloading tests were conducted. Figure 6.7(a) shows loading-unloading curves of the ICPUNs with different cross-linking densities during at the same strain of 50%. With the increase of the covalent cross-linking content, the hysteresis loops become smaller in agreement with the elastic mechanism of the permanent covalent network. The plot in Figure 6.7(b) shows the calculated total tensile energy, the dissipated portion and recovered energy for each sample. In this case, the percentage of energy dissipated versus the total energy for each sample is 68% for ICPUN7%, 56% for

ICPUN15%, 19% for ICPUN30% and 16% for ICPUN60%. The lower dissipated portion observed in ICPUN30% and ICPUN60% suggest that major presence of covalent cross-linking restrict the movement of the PU chains, thus the stress is likely to be concentred and high percentage of this tensile energy is elastically recovered.

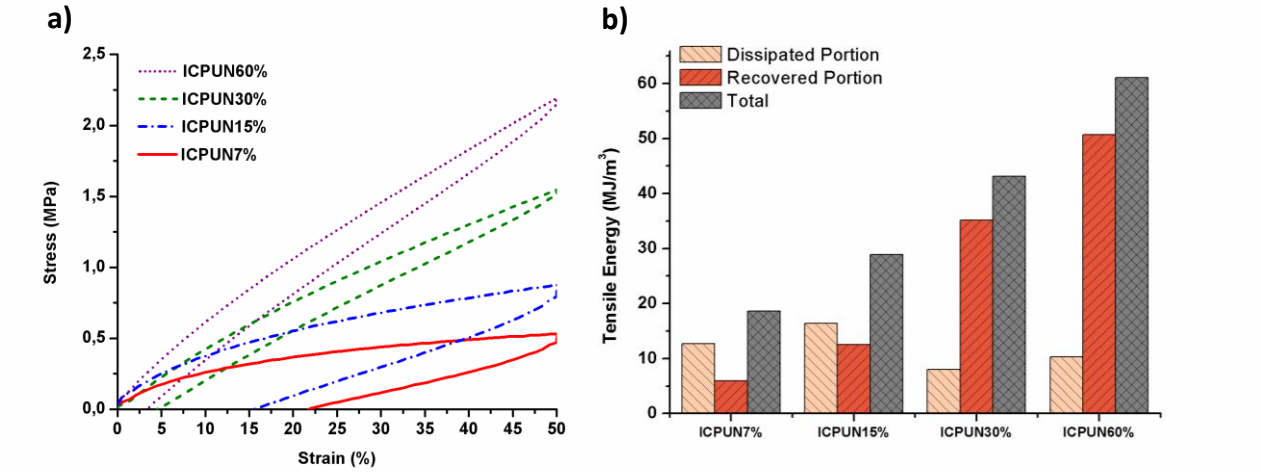

Figure 6.7. Loading-unloading curves at 50% strain (a) and total tensile energy, dissipated and recovered portion representation (b) of ICPUNs.

Further, loading-unloading response of ICPUNs was investigated at different strains 5, 10, 20, 40 and 80%. As an example, the loading-unloading curves of ICPUN15% and ICPUN30% are shown in Figure 6.8(a,b). As expected, hysteresis loops can be observed during loading-unloading cycles and the loops become larger when strain is raised. In Figure 6.8(c) are represented dissipated portion and total tensile energy for each strain deformation of ICPUN15%, it is shown that increasing strain decrease dissipation energy, the same phenomena can also observed in others ICPUNs. Moreover, the dissipation energy comparison between ICPUN15% and ICPUN30% when they are deformed at different strains is shown in the Figure 6.8(d) confirming the decrease of dissipation energy at higher covalent cross-link density and higher deformation of the sample.

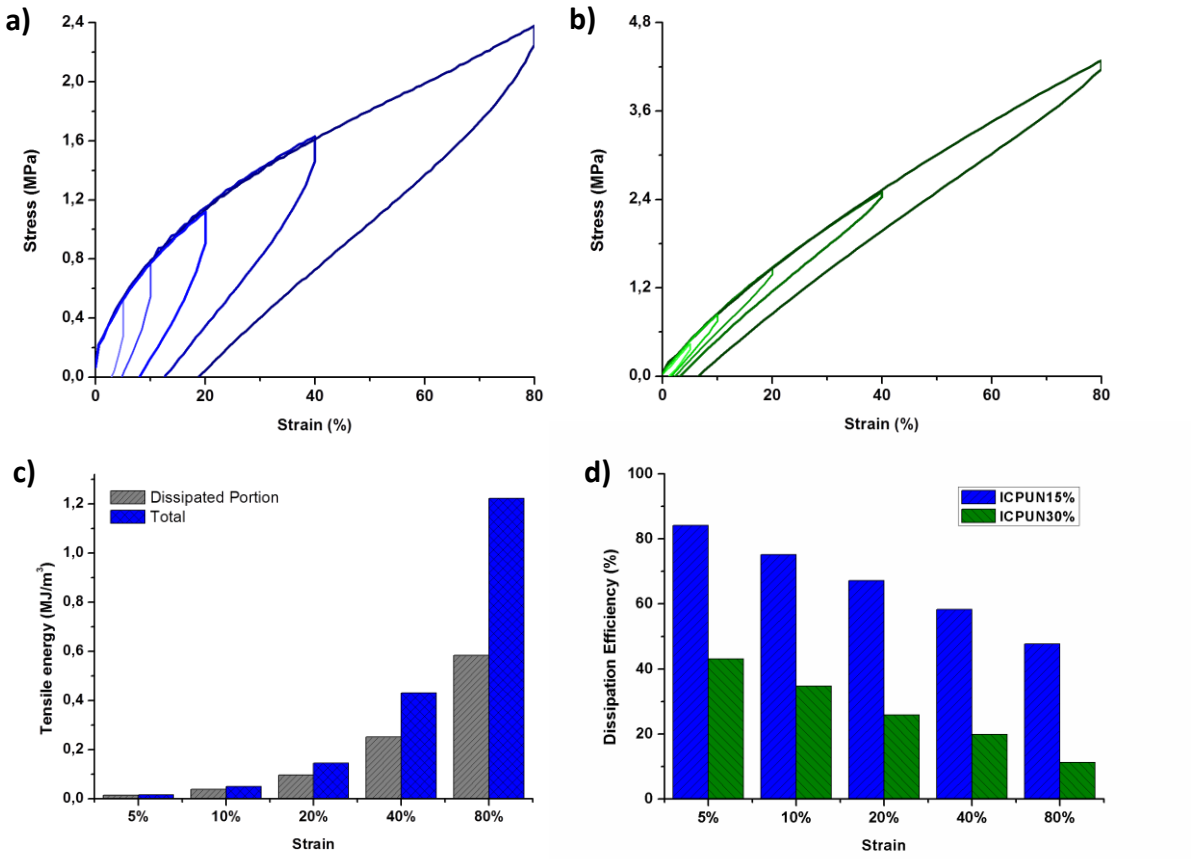

Figure 6.8. Loading-unloading curves at 5, 10, 20, 40 and 80% strain of ICPUN15%(a) and ICPUN3%(b) total toughness and dissipated portion of ICPUN15% (c) and comparison of dissipated efficiency between ICPUN15% and ICPUN30% (d).

In this case, the self-healing capability of ICPUNs was evaluated. Qualitative tests demonstrated the absence of self-healing behaviour at room temperature. Taking advantage of results presented in chapter 5, self-healing was investigated at 35 °C (Figure 6.13).

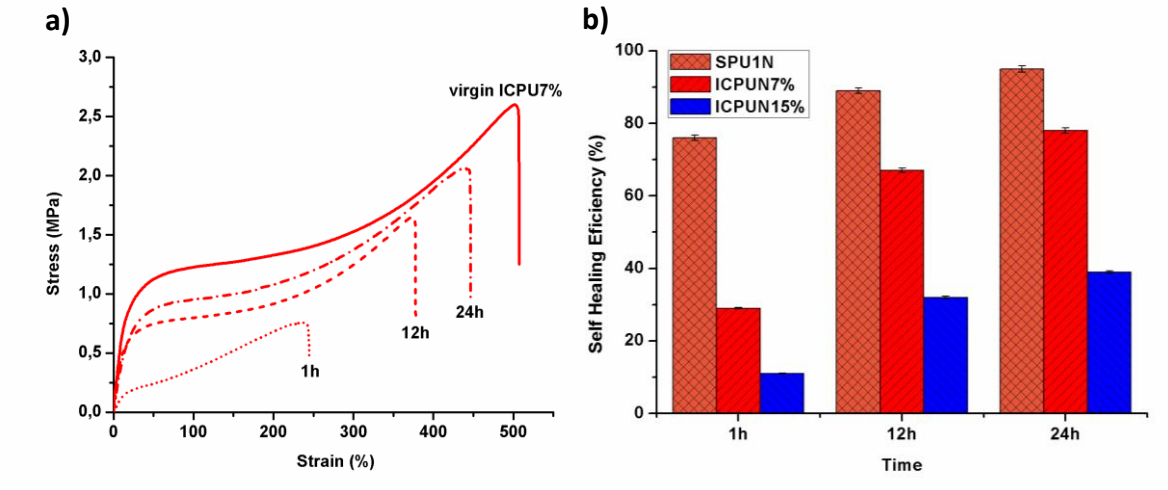

Figure 6.13. Mechanical properties of healed ICPUN7%(a) and self-healing efficiencies of SPU1N, ICPUN7% and ICPUN15% (b) as a function of healing time.

The stress–strain curves illustrate that the healing efficiency at 35 °C for ICPUN7% and ICPUN30% relies on the healing time. The sample SPU1N without covalent cross-links exhibits the fastest healing speed, recovering ~77% of its original strength after 1 h. A decrease in the healing efficiency was observed with the incorporation of covalent cross-links in the system. This can be attributed to the fact that irreversible covalent cross-links limit the mobility of polymer chains, thus resulting in the decrease in healing rate and efficiency. ICPU7% still possesses moderate self-healing capability, it recovering 67% of its original strength after healing for 12 h and 78% after 24 h. ICPU15% could only reach a healing efficiency of 39% after 24 h. The samples containing more than 15% of covalent cross-linking, ICPU30% and ICPU60%, did not exhibit self-healing properties at 35 °C. These results confirm the decrease of self-healing properties after incorporation of covalent cross-linking in the ICPUNs. The presence of major covalent cross-link restricts the mobility of PU chains making difficult the healing process by reformation of ionic hydrogen bonds in the interface of the damage specimen.

6.2.3. Shape-memory properties

The combination of covalent and non-covalent cross-links in ICPUNs was investigated in terms of shape-memory capacity. The shape-memory behaviour of ICPUNs was investigated by qualitative and quantitative measurements. ICPUN30% sample was selected for shape-memory qualitative investigation. Figure 6.9(A) shows a flat film sample that it was first healed at 65 °C for 15 min, subsequently lineal deformation was applied followed by cooling into an ice water bath for 2 min. When the film was removed from the bath, ICPUN30% could mantain a temporary shape (B) at room temperature. After that, the permanent shape could be fully recovered (C) after submerging the film into water bath at 65 °C for about twenty seconds. This methodology was repeated changing the type of deformation and the sample demonstrates an effective fixing and recovery capabilities. This qualitative demonstration confirms fixing process at room temperature thanks to the presence of a dynamic reversible network component, while the fast recovery verifies the relevancy of elastic mechanism from irreversible network component.

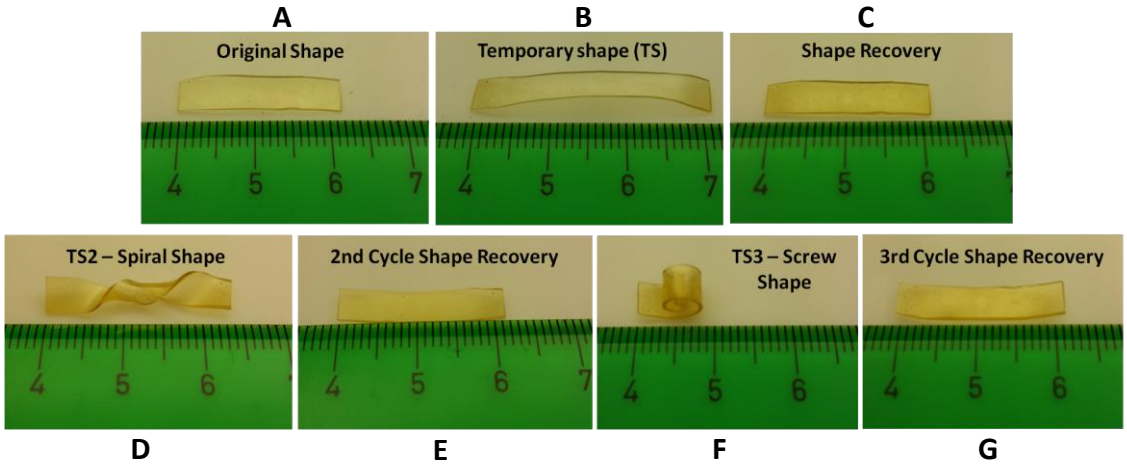

Figure 6.9. The ICPUN30% flat film (a) was lineal deformed around to give a temporary shape (b) at 65 °C, and its shape maintained at room temperature. The temporary shape was recovered (c) into original shape after heating at 65 °C. This process is repeated two times more with different temporary shapes: spiral (d) and screw (f).

For the quantitative demonstration the shape memory properties of ICPUNs films, a typical thermal one-way shape-memory cycle was used. The samples were first heated to 60 °C in the case of ICPUN7% and ICPUN15% or to 80 °C in the case of ICPUN30% and ICPUN60%, and a stress of 0.08 MPa or 0.9 MPa was respectively applied. Initial deforming conditions were selected taking advantage on the thermal and mechanical properties measured in the previous analysis, searching the major deformation before fracture. Then, the strain was fixed by cooling the sample to 20°C, after which the stress was removed. Shape recovery was achieved by reheating the sample to initial temperature (60 °C or 80 °C). Two main parameters define the quality of the shape memory material: the shape fixity (R_{fix}) and shape recovery (R_{rec}) were calculated using equations (1) and (2) below:

$$R_{fix} = \frac{\varepsilon}{\varepsilon_{load}} \times 100 \quad (1)$$

$$R_{rec} = \frac{(\varepsilon - \varepsilon_{rec})}{\varepsilon} \times 100 \quad (2)$$

Where ε_{load} represents the maximum strain under load, ε is the fixed strain after cooling and load removal, and ε_{rec} is the strain after recovery. In all samples were shown high strain fixity with values around 99%, and a recovery strain depending on the ICPUN and the initial deformation, the strain values are collected in the Table 6.3. Figure 6.10 shows the samples with the minor and the major percentage of covalent cross-linking content, ICPUN7% (a) and ICPUN60% (b), respectively

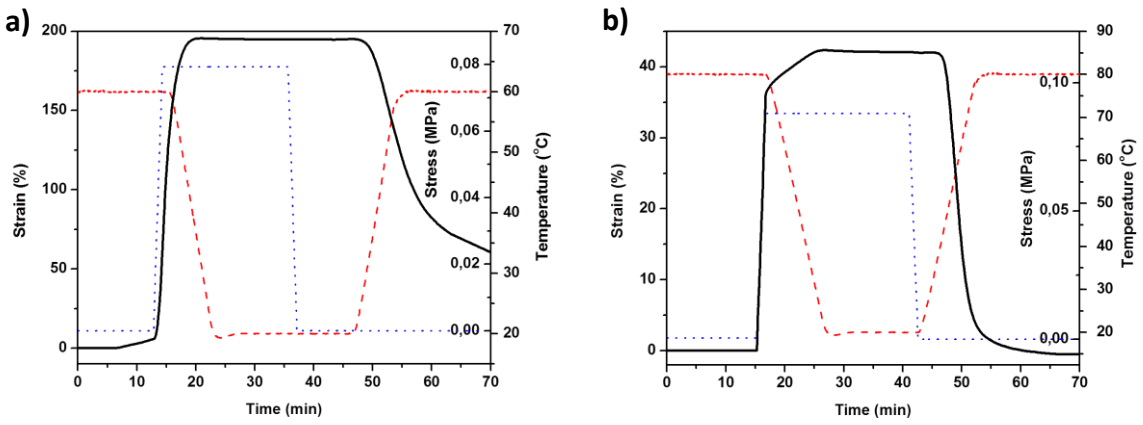

Figure 6.10. Dual shape-memory behaviour of ICPUN7%(a) and ICPUN60%(b).

Table 6.3. Dual-shape memory properties of ICPUNs.

Sample	S1	R_{fix} (S0-S1)	R_{rec} (s1-S0)
ICPUN7%	190%	99.8%	62.2%
ICPUN15%	120%	99.3%	70.7%
ICPUN30%	70%	98.4%	99.2%
ICPUN60%	45%	98.1%	99.8%

Similar shape memory capabilities were observed between ICPUN7% with ICPUN15% or between ICPUN30% with ICPUN60%. Minor presence of covalent cross-linking permits an increase in deformation and a good fixing strain, in detriment the recovery step. The reversibility of ionic hydrogen bonds in thermal conditions was thoroughly demonstrated in previous chapters, but in the SME can involve a handicap when the elastic mechanism is not efficient. In contrast, major presence of covalent cross-linking own a rapidly recovery but the deformation are limited due to the restricted mobility of chains. ICPUN30% and ICPUN60% after deformation, the physical network fixes the temporary shape by cooling, the new ionic hydrogen bonds formed prevent the recovery of permanent shape. Afterwards, when the temperature is increased, the ionic hydrogen bonds are broken and the elastic mechanism of covalent network, which has accumulated the tensile energy, permitted recover rapidly and efficiently the permanent shape.

To demonstrate that recovery efficiencies are in relation with the deformation and the dissipation tensile energy processes, three dual shape-memory cycles increasing performed stress for each cycle were carried out for the ICPUN15%. As can be observed in Figure 6.11(a), the increase of stress in the fixing step decreases the recovery efficiency. The values of the first plot about strain fixing demonstrate in all cycle to be major than 98% but the increase of the strain to fix the temporary form affects to the recovery value being for each cycle: 98% in first cycle, 95% in the second cycle and 72% in the third cycle. This phenomenon can be explained by increasing strain produce more breaking ionic hydrogen bonds in the dynamic network, as can be seen in Figure 6.8(c) the dissipated portion of total tensile energy is increased and the recovery process lost efficiency. On the contrary, in short deformations the number

non-covalent interactions broken are less but sufficient to fix the temporary shape and when the sample is heated the strain can be recovered totally.

The study of the dual shape-memory effect was completed by studying the reporductivility of the shape-memory behaviour. Figure 6.11(b) shows three successive c dual shape-memory cycles for ICPUN30%. The analysis show a lightly wear in the recovery value at 20 min as recovery time, in the first cycle recovery 99%, 97% in the second and 95% in the last cycle, in spite of is observed good cycle lifetime for the material.

Table 6.4. Cyclic dual-shape memory properties of ICPUN15% and ICPUN60%.

	ICPUN15%			ICPUN30%		
	Stress (MPa)	Rf	Rr	Stress (MPa)	Rf	Rr
Cycle1	0.02	99%	98%	0.07	99%	99%
Cycle2	0.03	99%	95%	0.07	99%	95%
Cycle3	0.06	99%	72%	0.07	99%	92%

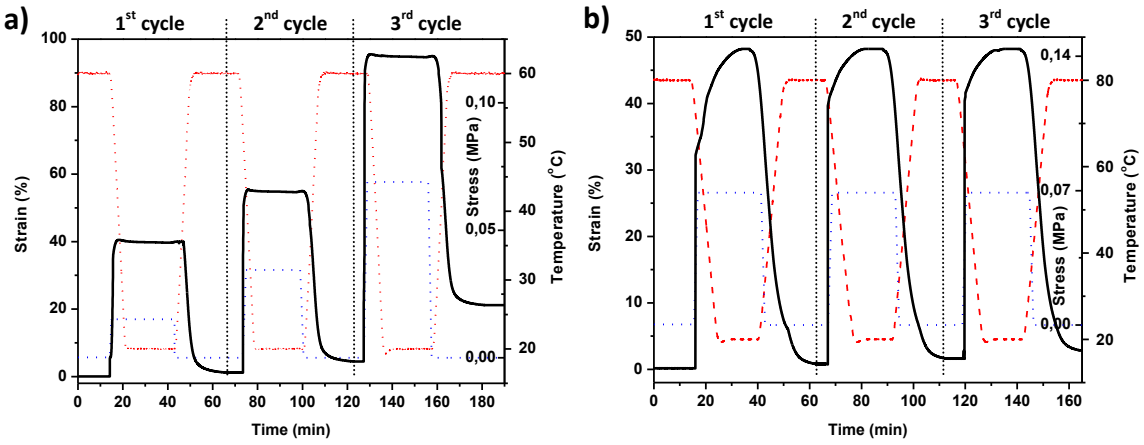

Figure 6.11. Cyclic dual shape-memory behaviour at different stress of ICPUN15%(a) and at same stress of ICPUN30%(b).

Triple-SMP are an important smart materials in SMP.[27,70] Triple-SMP can change shapes twice and can fix two metastable shapes in addition to its permanent shape. Usually the triple-SMP systems possess two well separated thermal transitions; ICPUNs, in contrast, only present one broad phase transition, as can be seen in thermo-mechanical analysis, that can be considered as multiple distinct transitions.

Figure 6.12 shows the triple-shape-memory effects of ICPUN30% (a) and ICPUN60% (b). On the previous analysis covalent cross-linking was responsible to the rapi recovery of the permanent shape but in this case where the principal requirement is to fix two temporary shapes and recovering them in programmed steps can be a drawback. The permanent shape (S0) was deformed at 80 °C and fixed at 40 °C to yield the first temporary shape (S1), which was further deformed at 40 °C and fixed at 10°C to yield the second temporary shape (S2). Upon reheating to 40 °C, the recovered first temporary shape ($S1_r$) was obtained. Further heating to 80 °C yielded the recovered permanent shape ($S0_r$).

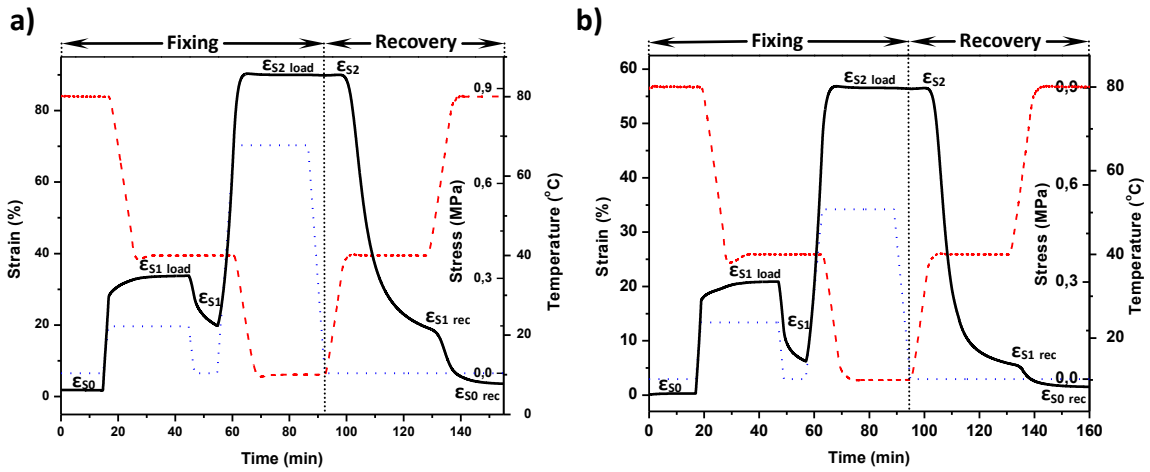

Figure 6.12. Triple shape-memory behaviour of ICPU3(a) and ICPU4(b).

Table 6.5. Triple-shape memory properties of ICPUN30% and ICPUN60%.

Sample	R_{fix} (S0-S1)	R_{fix} (S1-S2)	R_{rec} (S2-S1)	R_{rec} (s1-S0)
ICPUN30%	58.8%	99.7%	99.8%	94.3%
ICPUN60%	28.6%	99.9%	99.9%	83.4%

The triple-shape memory can be quantified by the percentage of shape fixation (R_f) and shape recovery (R_r). The values of these parameters are summarized in Table 4. The results demonstrate that the shape fixation ratio in the first stage is lower than in the second stage for both samples due to the higher fixing temperature and higher chain mobility. Similarly, the strain recovery in the first stage is considerably higher

than that in the second stage because the resulting recovery force in the first stage is considerably higher due to the lower temperature.

As observed previously for the dual-SME, the analysis shown that increasing the covalent cross-linking density complicate the fixation step of the first temporary shape due to the stress produced for the deformation of the restricted structure, but gives to system more recovery energy. In contrast, the major presence of ionic network helps to fix the form and increase the maximun of deformation but the recovery process is slower.

In summary, a novel thermo-reversible networks are constructed a combination of ionic hydrogen bonds and covalent cross-links using linear PU prepared from castor oil-derived diol. In the resultant materials, the covalent cross-links form a permanent network which can enhance the mechanical strength and maintain the shape of the polymers, while the dynamic ionic hydrogen bonds construct a reversible network which can increase the toughness and realize self-healing as well as the shape-memory function. By varying the covalent cross-linking density, the mechanical properties and the stimuli-responsive behaviour can be systematically tuned. This work demonstrates a simple and effective pathway to fabricate multifunctional polyurethanes with desired functions. This strategy can also be extended to exploring other types of dynamic non-covalent or covalent interactions to access a new range of multi-responsive biobased materials.

6.3. References

[1] R. Kempaiah, Z. Nie. From nature to synthetic systems: shape transformation in soft materials. *Journal of Materials Chemistry B*. **2014**, 2, 17, 2357-2368.

[2] R. V. Bellamkonda. Biomimetic materials: marine inspiration. *Natural Materials*. **2008**, 7, 347-8.

[3] W. M. Huang, Y. Zhao, C. C. Wang, Z. Ding, H. Purnawali, C. Tang, J. L. Zhang. Thermo/chemo-responsive shape memory effect in polymers: a sketch of working mechanisms, fundamentals and optimization. *Journal of Polymer Research*. **2012**, 19, 9, 1–34.

[4] F. Pilate, A. Toncheva, P. Dubois, J. M. Raquez. Shape-memory polymers for multiple applications in the materials world. *European Polymer Journal*. **2016**, 80, 268-294.

[5] Q. Zhao, H. J. Qi, T. Xie. Recent progress in shape memory polymer: new behavior, enabling materials, and mechanistic understanding. *Progress in Polymer Science*. **2015**, 49, 79–120.

[6] L. Sun, W. M. Huang, Z. Ding, Y. Zhao, C. C. Wang, H. Purnawali, C. Tang, Stimulus-responsive shape memory materials: a review. *Materials & Design*. **2012**, 33, 577–640.

[7] A. Lendlein. Smart biomaterials. *International Journal of Artificial Organs*. **2011**, 34, 8, 607.

[8] Z. Yuan, B. Ji, L. B. Wu. Synthesis and thermal induced shape memory properties of biodegradable segmented poly(ester-urethane)s. *Acta Polym Sin*. **2009**, 41, 2, 153-158.

[9] A. Lendlein, H. Jiang, O. Jünger, R. Langer. Light-induced shape-memory polymers. *Nature*. **2005**, 434, 7035, 879-882.

[10] J. Cho, J. W. Kim, Y. C. Jung, N. S. Goo. Electroactive shape-memory polyurethane composites incorporating carbon nanotubes. *Macromolecular Rapid Communications*. **2005**, 26, 5, 412-416.

[11] S. Chen, H. Yuan, H. Zhuo, S. Chen, H. Yang, Z. Ge, J. Liu. Development of liquid-crystalline shape-memory polyurethane composites based on polyurethane with semi-crystalline reversible phase and hexadecyloxybenzoic acid for self-healing applications. *Journal of Materials Chemistry C*. **2014**, 2, 21, 4203-4212.

[12] M. C. Serrano, G. A. Ameer. Recent Insights Into the biomedical applications of shape-memory polymers. *Macromolecular Bioscience*. **2012**, 12, 9, 1156-1171.

[13] S. Chen, J. Hu, Y. Liu, H. Liem, Y. Zhu, Y. Liu.. Effect of SSL and HSC on morphology and properties of PHA based SMPU synthesized by bulk polymerization method. *Journal of Polymer Science Part B: Polymer Physics*. **2007**, 45, 4, 444-454.

[14] Y. Wong, J. Kong, L. K. Widjaja, S. S. Venkatraman. Biomedical applications of shape-memory polymers: how practically useful are they?. *Science China Chemistry*. **2014**, 57, 4, 476-489.

[15] I. V. Ward Small, P. Singhal, T. S. Wilson, D. J. Maitland. Biomedical applications of thermally activated shape memory polymers. *Journal of Materials Chemistry*. **2010**, 20, 17, 3356-3366.

[16] S. J. Chen, J. L. Hu, S. G. Chen, C. L. Zhang. Study on the structure and morphology of supramolecular shape memory polyurethane containing pyridine moieties. *Smart Materials and Structures*. **2011**, 20, 65003.

[17] S. Chen, J. Hu, Y. Liu, H. Liem, Y. Zhu, Q. Meng. Effect of molecular weight on shape memory behavior in polyurethane films. *Polymer International*. **2007**, 56, 9, 1128-1134.

[18] P. Singhal, W. Small, E. Cosgriff-Hernandez, D. J. Maitland, T. S. Wilson. Low density biodegradable shape memory polyurethane foams for embolic biomedical applications. *Acta Biomaterialia*. **2014,** 10, 1, 67-76.

[19] M. C. Serrano, L. Carbajal, G. A. Ameer. Novel biodegradable shape-memory elastomers with drug-releasing capabilities. *Advanced Materials*. **2011**, 23, 19, 2211-2215.

[20] C. M. Yakacki, R. Shandas, C. Lanning, B. Rech, A. Eckstein, K. Gall. Unconstrained recovery characterization of shape-memory polymer networks for cardiovascular applications. *Biomaterials*. **2007**, 28, 14, 2255-2263.

[21] C. M. Yakacki, R. Shandas, D. Safranski, A. M. Ortega, K. Sassaman, K. Gall. Strong, Tailored, Biocompatible shape-memory polymer networks. *Advanced Functional Materials*. **2008**, 18, 16, 2428-2435.

[22] M. D. Hager, S. Bode, C. Weber, U. S. Schubert. Shape memory polymers: Past, present and future developments. *Progress in Polymer Science*. **2015**, 49, 3-33.

[23] F. Liu , M. W. Urban. Recent advances and challenges in designing stimuli-responsive polymers. *Progress in Polymer Science*. **2010**, 35, 3–23

[24] T. Xie. Recent advances in polymer shape memory. *Polymer*. **2011**, 52, 22, 4985-5000.

[25] K. K. Julich-Gruner, C. Löwenberg, A. T. Neffe, I. M. Beh, A. Lendlein. Recent trends in the chemistry of shape-memory polymers. *Macromolecular Chemistry and Physics*. **2013**, 214:527-36.

[26] H. Meng, G. Li. A review of stimuli-responsive shape memory polymer composites. *Polymer*. **2013**, 54, 2199–221.

[27] I. Bellin, S. Kelch, R. Langer, A. Lendlein. Polymeric triple-shape materials. *Proceedings of the National Academic of Science*. **2006**, 103, 48, 18043–18047.

[28] L. Wang, X. Yang, H. Chen, T. Gong, W. Li, G. Yang, S. Zhou. Design of triple-shape memory polyurethane with photo-cross-linking of cinnamon groups. *ACS Applied Materials & Interfaces*. **2013**, 5, 21, 10520–10528.

[29] L. Xiao, M. Wei, M. Zhan, J. Zhang, H. Xie, X. Deng, K. Yang, Y. Wang. Novel triple-shape PCU/PPDO interpenetrating polymer networks constructed by self-complementary quadruple hydrogen bonding and covalent bonding. *Polymer Chemistry*. **2014**, 5, 7, 2231–2241.

[30] Y. Luo, Y. Guo, X. Gao, B. G. Li, T. Xie. A general approach towards thermoplastic multishape-memory polymers via sequence structure design. *Advanced Materials*. **2013**, 25, 5, 743-748.

[31] Q. Zhao, M. Behl, A. Lendlein. Shape-memory polymers with multiple transitions: complex actively moving polymers. *Soft Matterials*. **2013**, 9:1744–55.

[32] C. Zeng, H. Seino, J. Ren, N. Yoshie. Polymers with multishape memory controlled by local glass transition temperature. *ACS Applied Materials & Interfaces*. **2014**, 6, 2753-8.

[33] T. Xie, X. Xiao, Y. T. Cheng. Revealing triple-shape memory effect by polymer bilayers. *Macromol. Rapid Communication.* **2009**. 30, 1823–1827.

[34] T. S. Kustandi, W. W. Loh, L. Shen, H. Y. Low. Reversible recovery of nanoimprintedpolymer structures. *Langmuir*. **2013**, 29, 10498–504.

[35] T. Pretsch. Triple-shape properties of a thermoresponsive poly(ester urethane). *Smart Materials and Structures*. **2009**, 19, 1, 015006.

[36] M. Bothe, K. Y. Mya, E. M. J. Lin, C. C. Yeo, X. Lu, C. He, T. Pretsch. Triple-shape properties of star-shaped POSS-polycaprolactone polyurethane networks. *Soft Matter*. **2012**, 8, 4, 965-972.

[37] Y. Bai, X. Zhang, Q. Wang, T. Wang. A tough shape memory polymer with triple-shape memory and two-way shape memory properties. *Journal of Materials Chemistry A*. **2014**, 2, 13, 4771-4778.

[38] L. Wang, X. Yang, H. Chen, G. Yang, T. Gong, W. Li, S. Zhou. Multi-stimuli sensitive shape memory poly (vinyl alcohol)-graft-polyurethane. *Polymer Chemistry*. **2013**, 4, 16, 4461-4468.

[39] K. Suchao-in, S. Chirachanchai. "Grafting to" as a novel and simple approach for triple-shape memory polymers. *ACS Applied Materials & Interfaces*. **2013**, 5, 15, 6850-6853.

[40] J. Li, T. Liu, S. Xia, Y. Pan, Z. Zheng, X. Ding, Y. Peng. A versatile approach to achieve quintuple-shape memory effect by semi-interpenetrating polymer networks containing broadened glass transition and crystalline segments. *Journal of Materials Chemistry*. **2011**, 21, 33, 12213-12217.

[41] I. Kolesov, O. Dolynchuk, H. J. Radusch. Shape-memory behavior of cross-linked semi-crystalline polymers and their blends. *Express Polymer Letters*. **2015**, 9, 3.

[42] C. Samuel, S. Barrau, J. M. Lefebvre, J. M. Raquez, P. Dubois. Designing multiple-shape memory polymers with miscible polymer blends: evidence and origins of a triple-shape memory effect for miscible PLLA/PMMA blends. *Macromolecules*. **2014**, 47, 19, 6791-6803.

[43] Z. Wang, J. Zhao, M. Chen, M. Yang, L. Tang, Z. M. Dang, X. Dong. Dually actuated triple shape memory polymers of cross-linked polycyclooctene–carbon nanotube/polyethylene nanocomposites. *ACS Applied Materials & Interfaces*. **2014**, 6, 22, 20051-20059.

[44] H. Meng, H. Mohamadian, M. Stubblefield, D. Jerro, S. Ibekwe, S. S. Pang, G. Li. Various shape memory effects of stimuli-responsive shape memory polymers. *Smart Materials and Structures*. **2013**, 22, 9, 93001.

[45] S. Chen, F. Mo, F. J. Stadler, S. Chen, Z. Ge, H. Zhuo. Development of zwitterionic copolymers with multi-shape memory effects and moisture-sensitive shape memory effects. *Journal of Materials Chemistry B*. **2015**, 3, 32, 6645-6655.

[46] J. Li, T. Liu, S. Xia, Y. Pan, Z. Zheng, X. Ding, Y. Peng. A versatile approach to achieve quintuple-shape memory effect by semi-interpenetrating polymer networks containing broadened glass transition and crystalline segments. *Journal of Materials Chemistry*. **2011**, 21, 12213–7.

[47] C. Zeng, H. Seino, J. Ren, N. Yoshie. Polymers with multishape memory controlled by local glass transition temperature. *ACS Applied Materials & Interfaces*. **2014**, 6, 2753-8.

[48] T. Xie. Tunable polymer multi-shape memory effect. *Nature*. **2010**, 464, 7286, 267-270.

[49] J. Li, T. Xie. Significant impact of thermo-mechanical conditions on polymer triple-shape memory effect. *Macromolecules*. **2010**, 44, 1, 175-180.

[50] D. Ratna, J. Karger-Kocsis. Recent advances in shape memory polymers and composites: a review. *Journal of Materials Science*. **2008**, 43, 1, 254-269.

[51] M. Behl, A. Lendlein. Actively moving polymers. *Soft Matter*. **2007**, 3, 1, 58-67.

[52] Z. Yuan, B. Ji, L. B. Wu. Synthesis and thermal induced shape memory properties of biodegradable segmented poly(ester-urethane)s. *Acta Polymerica Sinica*. **2009**, 41, 2, 153-158.

[53] B. S. Lee, B. C. Chun, Y. C. Chung, K. I. Sul, J. W. Cho. Structure and thermomechanical properties of polyurethane block copolymers with shape memory effect. *Macromolecules*. **2001**, 34, 18, 6431-6437.

[54] S. Zhang, Z. Yu, T. Govender, H. Luo, B. Li. A novel supramolecular shape memory material based on partial α-CD–PEG inclusion complex. *Polymer*. **2008**, 49, 15, 3205-3210.

[55] S. Chen, J. Hu, H. Zhuo, C. Yuen, L. Chan. Study on the thermal-induced shape memory effect of pyridine containing supra- molecular polyurethane. *Polymer*. **2010**, 51, 240-248.

[56] S. Chen, J. Hu, C. W. Yuen, L. Chan. Fourier transform infrared study of supramolecular polyurethane networks containing pyridine moieties for shape memory materials. *Polymer International*. **2010**, 59, 4, 529-538.

[57] Y. Zhu, J. Hu, Y. Liu. Shape memory effect of thermoplastic segmented polyurethanes with self-complementary quadruple hydrogen bonding in soft segments. *The European Physical Journal E*. **2009**, 28, 1, 3-10.

[58] K. Yu, T. Xie, J. Leng, Y. Ding, H. J. Qi. Mechanisms of multi-shape memory effects and associated energy release in shape memory polymers. *Soft Matter*. **2012**, 8, 20, 5687-5695.

[59] S. Chen, F. Mo, Y. Yang, F. J. Stadler, S. Chen, H. Yang, Z. Ge. Development of zwitterionic polyurethanes with multi-shape memory effects and self-healing properties. *Journal of Materials Chemistry A*. **2015**, 3, 6, 2924-2933.

[60] S. Chen, F. Mo, F. J. Stadler, S. Chen, Z. Ge, H. Zhuo. Development of zwitterionic copolymers with multi-shape memory effects and moisture-sensitive shape memory effects. *Journal of Materials Chemistry B*. **2015**, 3, 32, 6645-6655.

[61] S. Chen, Z. Mei, H. Ren, H. Zhuo, J. Liu, Z. Ge. Pyridine type zwitterionic polyurethane with both multi-shape memory effect and moisture-sensitive shape memory effect for smart biomedical application. *Polymer Chemistry*. **2016**, 7, 37, 5773-5782.

[62] L. Xiao, M. Wei, M. Zhan, J. Zhang, H. Xie, X. Deng, Y. Wang. Novel triple-shape PCU/PPDO interpenetrating polymer networks constructed by self-complementary quadruple hydrogen bonding and covalent bonding. *Polymer Chemistry*. **2014**, 5, 7, 2231-2241.

[63] T. Ware, K. Hearon, A. Lonnecker, K. L. Wooley, D. J. Maitland, W. Voit. Triple-shape memory polymers based on self-complementary hydrogen bonding. *Macromolecules*. **2012**, 45, 1062–9.

[64] Y. Pan, T. Liu, J. Li, Z. Zheng, X. Ding, Y. Peng. High modulus ratio shape-memory polymers achieved by combining hydrogen bonding with controlled crosslinking. *Journal of Polymer Science Part B: Polymer Physics*. **2011**, 49, 1241–5.

[65] D. Wang, J. Guo, H. Zhang, B. Cheng, H. Shen, N. Zhao, J. Xu. Intelligent rubber with tailored properties for self-healing and shape memory. *Journal of Materials Chemistry A*. **2016**, *3*, 24, 12864-12872.

[66] M. Comí, G. Lligadas, J. C. Ronda, M. Galià, V. Cádiz. Synthesis of castor-oil based polyurethanes bearing alkene/alkyne groups and subsequent thiol-ene/yne post-modification. *Polymer*. **2016**. 103, 163-170.

[67] D. K. Chattopadhyay, D. C. Webster. Thermal stability and flame retardancy of polyurethanes. *Progress in Polymer Science*. **2009**, 34, 10, 1068-1133.

[68] T. F. Garrison, M. R. Kessler, R. C. Larock. Effects of unsaturation and different ring-opening methods on the properties of vegetable oil-based polyurethane coatings. *Polymer*. **2014**, 55, 4, 1004-1011.

[69] R. Dolog, R. A. Weiss. Shape memory behavior of a polyethylene-based carboxylate ionomer. *Macromolecules*. **2013**, 46, 19, 7845-7852.

[70] M. Behl, A. Lendlein. Triple-shape polymers. *Journal of Materials Chemistry*. **2010**, 20, 17, 3335-3345.

Chapter 7

Experimental Part

Raw materials

Synthesis methods

Instrumentation

UNIVERSITAT ROVIRA I VIRGILI
AVANCES EN SISTEMAS INTERACTIVOS PARA PERSONAS CON PARÁLISIS CEREBRAL
Marc Comí Bonachí

7.1. Materials

The following chemicals were obtained from Aldrich and used as received: 10-undecen-1-ol, 3-chloroperoxybenzoic acid, N-allylmethylamine, N-methylpropargylamine, allylamine, propargyl chloride, tin(II) 2-ethylhexanoate (Aldrich), isophorone diisocyanate (IPDI), hexamethylene diisocyanate (HDI), octanoic acid, sebacic acid, suberic acid, succinic acid, citric acid, oxalic acid, thioglycerol (TG), 1,4-butadithiol, trimethylolpropane tris(3-mercaptopropionate)(TMMP), 3-tert-butyl-4-hydroxy-5-methylphenyl sulphide (Santonox®), boron trifluoride ethylamine complex and 2,2-dimethoxy-2-phenylacetophenone (DMPA). All solvents were purified by standard procedures.

7.2. Synthetic methods of monomers and polymers

7.2.1. Monomer synthesis

Synthesis of 10,11-epoxyundecan-1-ol

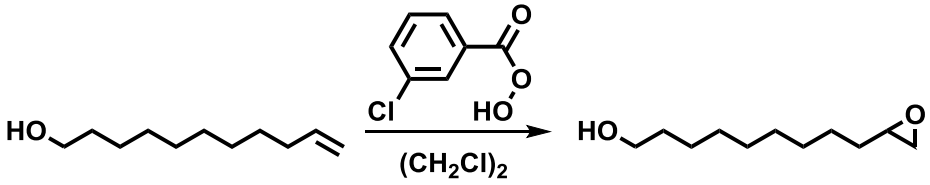

10-undecen-1-ol (17 g, 0.10 mol), 3-chloroperoxybenzoic acid (19 g, 0.11 mol), Santonox ($1x10^{-4}$ mol) as radical inhibitor, and 500 mL of 1,2-dichloroethane were placed into 1L two-necked round-bottom flask equipped with condenser and a teflon coated stirring bar. The reaction mixture was gently stirred and heated at 80°C for 1 h. The resulting yellow solution was cooled at room temperature and washed several times with 5% (w/w) $Na_2S_2O_3$ and 5% (w/w) NaOH solutions. The organic layer was dried over anhydrous $MgSO_4$, the solvent was removed in the rotary evaporator and the product was dried under vacuum at room temperature for 24 h. The resulting colourless oil was used without further purification in the next step. Yield 91%.

^{1}H NMR ($CDCl_3$, TMS, δ ppm): 3.61 (2H, t, -C<u>H</u>$_2$-OH), 2.90 (1H, m, CH in oxirane ring), 2.73 (1H, dd, , J_{cis} = 5.2 Hz, H cis in C<u>H</u>$_2$ of the oxirane ring), 2.45 (1H, dd, J_{trans} = 2.4 Hz, H trans in C<u>H</u>$_2$ of the oxirane ring) and 1.53-1.27 (16H, -CH_2-).

^{13}C NMR ($CDCl_3$, δ ppm): 66.77 (t), 59.27 (d), 56.79 (t), 34.80 (t), 32.75 (t), 29.75 (t), 29.50 (t), 29.47 (t), 29.38 (t), 25.72 (t) and 25.66 (t).

Synthesis of N-allylpropargylamine.

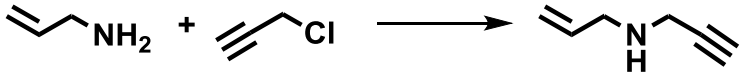

Propargyl chloride (7.00 g, 6.8 mL, 95 mmol) was added slowly to allylamine (38.00 g, 50 mL, 0.67 mol) into 100 mL round-bottom flask and the resulting solution was allowed to stir for a period of 48 h at 60°C. The reaction was then cooled at room temperature and then extracted several times with diethyl ether. The combined extracts were dried over $MgSO_4$, the solvent was removed in the rotary evaporator and the resulting oil was distilled at atmospheric pressure to obtain colourless oil. Yield (45%)

^{1}H NMR ($CDCl_3$, TMS, δ ppm): 5.42 (1H, m, CH_2=C<u>H</u>-), 5.04 (2H, m, C<u>H</u>$_2$=CH-), 3.36 (2H, dd, -C<u>H</u>$_2$-C≡CH), 3.19 (2H, dd, -C<u>H</u>$_2$-CH=CH_2) and 2.24 (1H, t, -C≡C<u>H</u>).

^{13}C NMR ($CDCl_3$, δ ppm): 135.25 (d), 117.76 (t), 78.47 (s), 73.45 (t), 56.47 (t) and 32.94 (t).

Synthesis of diols

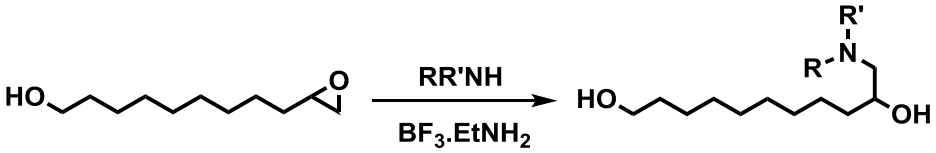

D1 : R = -CH_2CH=CH_2 ; R' = -CH_3
D2 : R = -CH_2C≡CH ; R' = -CH_3
D3 : R = -CH_2C≡CH ; R' = -CH_2CH=CH_2

A 25 mL round-bottom flask was charged with the corresponding amine (36 mmol), boron trifluoride ethylamine complex (1.8 mmol) and 10,11-epoxyundecan-1-ol (35 mmol). The mixture was stirred and heated at 80°C for 15h. The resulting oil was purified by column chromatography using silicagel and hexane/ethyl acetate 1/1 as eluent.

11-allylmethylaminoundecan-1,10-diol (D1). Colourless oil. Yield 91%.

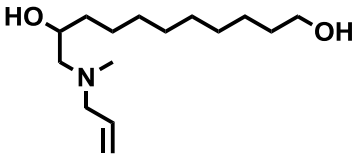

^{1}H NMR ($CDCl_3$, TMS, δ ppm): 5.82 (1H, m, CH_2=C<u>H</u>-), 5.14 (2H, m, C<u>H$_2$</u>=CH-), 3.62 (2H, t, C<u>H$_2$</u>-OH), 3.62 (1H, m, -C<u>H</u>-OH), 3.19 (1H, dd, -C<u>H$_2$</u>-CH=CH_2), 2.98 (1H, dd, -C<u>H$_2$</u>-CH=CH_2), 2.28 (2H, m, -N-C<u>H$_2$</u>-), 2.24 (3H, s, C<u>H$_3$</u>-N-) and 1.55-1.28 (16H, -CH_2-).

^{13}C NMR ($CDCl_3$, δ ppm): 135.25 (d), 117.76 (t), 66.81 (d), 63.03 (t), 62.89 (t), 60.98 (t), 41.91 (q), 34.88 (t), 32.75 (t), 29.74 (t), 29.50 (t), 29.47 (t), 29.39 (t), 25.72 (t), 25.63 (t).

11-methylpropargylaminoundecan-1,10-diol (D2). Yellow powder. Yield 90%.

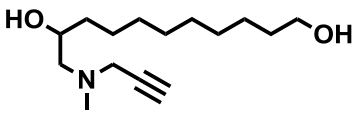

^{1}H NMR ($CDCl_3$, TMS, δ ppm: 3.62 (1H, m, C<u>H</u>-OH), 3.62 (2H, t, -C<u>H$_2$</u>-OH), 3.36 (2H, dd, -C<u>H$_2$</u>-C≡CH), 2.49 (1H, dd, -N-C<u>H$_2$</u>-), 2.34 (3H, s, C<u>H$_3$</u>-N-), 2.22 (1H, dd, -N-C<u>H$_2$</u>-), 2.24 (1H, t, CH≡C) and 1.55-1.28 (16H, -CH_2-).

^{13}C NMR ($CDCl_3$ δ ppm): 78.47 (s), 73.45 (d), 67.15 (d), 63.05 (t), 61.89 (t), 46.14 (t), 41.67 (q), 34.99 (t), 32.92 (t), 29.89 (t), 29.66 (t), 29.64 (t), 29.54 (t), 25.88 (t), 25.74 (t).

11-allylpropargylaminoundecan-1,10-diol (D3). Yellow oil. Yield 87%.

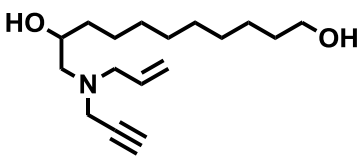

^{1}H NMR ($CDCl_3$, TMS, δ ppm): 5.78 (1H, m, CH_2=C<u>H</u>-), 5.19 (2H, m, C<u>H$_2$</u>=CH-), 3.61 (1H, t, C<u>H</u>-OH), 3.58 (2H, m, -C<u>H$_2$</u>-OH), 3.38 (2H, dd, -C<u>H$_2$</u>-C≡CH), 3.24 (1H, dd, -C<u>H$_2$</u>-CH=CH_2), 3.06 (1H, dd, -C<u>H$_2$</u>-CH=CH_2), 2.49 (1H, dd, -N-C<u>H$_2$</u>-), 2.26 (1H, dd, -N-C<u>H$_2$</u>-), 2.18 (1H, s, CH≡C) and 1.55-1.26 (16H, -CH_2-).

^{13}C NMR ($CDCl_3$, δ ppm): 134.91 (d), 118.46 (t), 78.21 (q), 73.19 (d), 66.90 (d), 62.74 (t), 59.29 (t), 41.83 (t), 34.75 (t), 32.73 (t), 29.70 (t), 29.49 (t), 29.46 (t), 29.38 (t), 25.72 (t), 25.57(t).

11-diethylaminoaminoundecan-1,10-diol (D4). Yellow oil. Yield 96%.

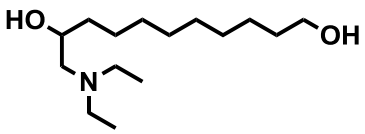

^{1}H NMR (CD_3OH, TMS, δ ppm): 3.63 (1H, m, C<u>H</u>-OH), 3.52 (2H, t, -C<u>H$_2$</u>-OH), 2.62 (1H, dq, J_{gem}= 14.4 Hz, J_{vic} = 7.6 Hz, N-C<u>H$_2$</u>-CH_3), 2.55 (1H, dq, J_{gem} = 14.4 Hz, J_{vic} = 7.6 Hz, N-C<u>H$_2$</u>-CH_3), 2.40 (1H, dd, J_{gem} = 19.9 Hz, J_{vic} = 13.8 Hz, N-C<u>H$_2$</u>-CH), 2.38 (1H, dd, J_{gem} = 19.9 Hz, J_{vic}= 13.8 Hz, N-C<u>H$_2$</u>-CH), 1.57-1.34 (18H, -C<u>H$_2$</u>-), 1,02 (6H, dd, -CH_2-C<u>H$_3$</u>).

^{13}C NMR (CD_3OH, δ ppm): 68.17 (d), 61.58 (t), 59.28 (t), 47.01 (t), 35.33 (t), 32.29 (t), 29.48 (t), 29.36 (t), 29.33 (t), 25.58 (t), 10.37 (q).

7.2.2. Polyurethane synthesis

Synthesis of polyurethanes from IPDI for thiol-ene/yne modification (PUD1-3)

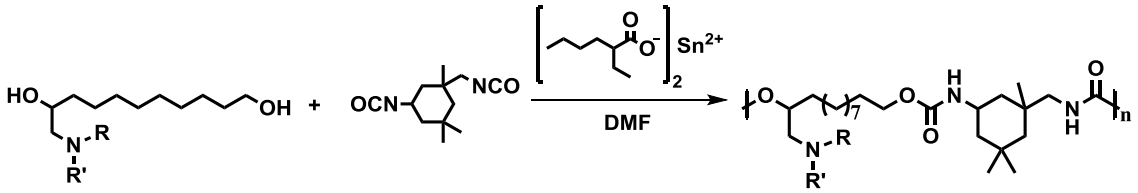

D1 : R = -$CH_2CH=CH_2$; R' = -CH_3
D2 : R = -$CH_2C\equiv CH$; R' = -CH_3
D3 : R = -$CH_2C\equiv CH$; R' = -$CH_2CH=CH_2$

D1-3 (1.84 mmonl) and tin (II) ethyl hexanoate (6 µL, 0.02 mmol) was placed in a 10 mL round-bottom flask equipped with a Teflon coated stirring bar and closed by septum. To the mixture were applied 6 cycles of vacuum/argon. Dried DMF (0.4 mL) was injected into the flask and the solution was stirred and heated at 60°C for 20 minutes. IPDI (0.4 mL, 1.84 mmol) was injected and the reaction mixture was left for 24 h. After this time, the solution was died with methanol (0.1 mL) and was precipitated into 250 mL of diethylether, filtered and dried under vacuum for 24h.

PUD1 Yield 93%.

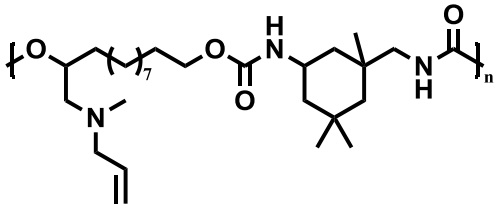

^{1}H NMR ($CDCl_3$, TMS, δ ppm): 5.81 (1H, m, CH_2=C<u>H</u>-), 5.13 (2H, m, C<u>H$_2$</u>=CH-) , 4.82 (1H, broad signal, CO-N<u>H</u>-CH_2-, Z-IPDI) , 4.81 (1H, m, C<u>H</u>-OCO-), 4.70 (1H, broad signal, CO-N<u>H</u>-CH_2-, E-IPDI), 4.50 (1H, broad signal, CO-N<u>H</u>-CH-), 4.03 (2H, t, -C<u>H$_2$</u>-OCO), 3.79 (1H, m, -C<u>H</u> ring), 3.24 (2H, d, -C<u>H$_2$</u>-NH-, E-IPDI), 3.00 (2H, d, C<u>H$_2$</u>-CH=CH_2), 2.91(2H, d, -C<u>H$_2$</u>-NH-, Z-IPDI), 2.49 (1H, m, N-C<u>H$_2$</u>-CH), 2.38 (1H, m, N-C<u>H$_2$</u>-CH), 2,26 (3H, s, -N-C<u>H$_3$</u>) and 1.79-0.63 (24H, -(C<u>H$_2$</u>)$_n$-C<u>H$_3$</u>).

^{13}C NMR ($CDCl_3$, δ ppm): 157.18 (s), 155.72 (s), 135.85 (d), 117.30 (t), 65.03 (t), 64.79 (t), 62.56 (t), 58.74 (t), 58.74 (t), 46.03 (t), 44.43 (t), 42.23 (s), 36.44 (t), 35.06 (q), 33,02 (t), 32.68 (d), 31.75 (t), 31.69 (t), 31.43 (t), 29.37 (t), 29.17 (t), 27.57 (t), 25.72 (t), 25.20 (s) and 23.21 (s).

PUD2 Yield 93%.

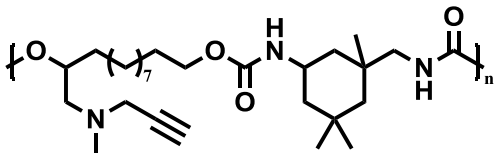

^{1}H NMR ($CDCl_3$, TMS δ ppm: 4,79 (1H, broad signal, CO-N<u>H</u>-CH_2-, Z-IPDI), 4.78 (1H, m, C<u>H</u>-OCO-), 4.71 (1H, broad signal, CO-N<u>H</u>-CH_2-, E-IPDI), 4,45 (1H, broad signal, CO-N<u>H</u>-CH-), 4,03 (2H, t, -C<u>H_2</u>-OCO), 3,79 (1H, m, -C<u>H</u> ring), 3.40 (2H, dd, C<u>H_2</u>-C≡CH), 3.29 (2H, d, -C<u>H_2</u>-NH-, E-IPDI)), 2.91 (2H, d, -C<u>H_2</u>-NH-, Z-IPDI), 2.49 (2H, d, N-C<u>H_2</u>-CH), 2.32 (3H, s, CH_3-N), 2.18 (1H, s, C<u>H</u>≡C-), and 1.71-0.86 (24H, -(C<u>H_2</u>)$_n$-C<u>H_3</u>).

^{13}C NMR ($CDCl_3$, δ ppm): 162.57 (s), 156.81 (s), 78.38 (s), 73.39 (d), 71.90 (t), 64.95 (t), 56.03 (t), 54.88 (t), 46.95 (d), 44.53 (t), 42.92 (t), 41.86 (q), 35.06 (q), 32.80 (t), 31.83 (t), 31.43 (t), 29.44 (t), 29.24 (t), 29.03 (t), 27.61 (t), 25.84 (t), 25.33 (s) and 23.22 (s).

PUD3 Yield 91%.

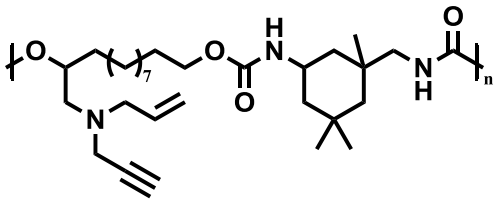

^{1}H NMR ($CDCl_3$, TMS, δ ppm): 5.81 (1H, m, CH_2=C<u>H</u>-), 5.12 (2H, m, C<u>H_2</u>=CH-) , 4.80 (1H, broad signal, CO-N<u>H</u>-CH_2-, Z-IPDI) , 4.79 (1H, m, C<u>H</u>-OCO-), 4.68 (1H, broad signal, CO-N<u>H</u>-CH_2-, E-IPDI), 4.48 (1H, broad signal, CO-N<u>H</u>-CH-), 4.01 (2H, t, -C<u>H_2</u>-OCO), 3.79 (1H, m, -C<u>H</u> ring), 3.35 (2H, dd, C<u>H_2</u>-C≡CH), 3.26 (2H, d, -C<u>H_2</u>-NH-, E-IPDI)), 2.95 (2H, d,-C<u>H_2</u>-NH-, Z-IPDI), 2.91 (2H, d, C<u>H_2</u>-CH=CH_2), 2.49 (2H, d, N-C<u>H_2</u>-CH), 2.21 (1H, s, C<u>H</u>≡C-), and 1.71-0.86 (24H, -(C<u>H_2</u>)$_n$-C<u>H_3</u>).

^{13}C NMR ($CDCl_3$, δ ppm): 157.18 (s), 155.72 (s), 134.89 (d), 118.45 (t), 78.20(s), 73.18(d), 66.89 (t), 66.83(t), 62.73 (t), 60.88(t), 59.27 (t), 56.62 (t), 56.08 (t), 41.83 (t), 32.72 (t), 29.70 (t), 29.49 (t), 29.48 (t), 29.45 (t), 29.38 (t), 25.72 (t), 20.26 (s) and 11.76 (s).

Synthesis of polyurethane from IPDI for acid-base modication (PUD4)

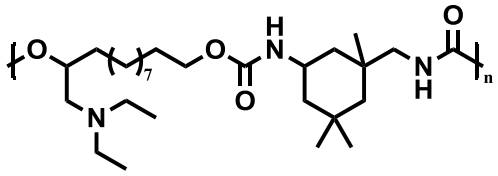

D4 (0.45 g, 1.84 mmol) and tin (II) ethyl hexanoate (6 µL, 0.02 mmol) was placed in a 10 mL round-bottom flask equipped with a Teflon coated stirring bar and closed by septum. To the mixture were applied 6 cycles of vacuum/argon. Dried THF (2 mL) was injected into the flask and the solution was stirred and heated at 60°C for 20 minutes. HDI (0.3 mL, 1.84 mmol) was injected and the reaction mixture was left for 4 h. Polymer was dried under vacuum during 24h. Yield 95%.

^{1}H NMR ($CDCl_3$, TMS, δ ppm): 4.82 (1H, broad signal, CO-N<u>H</u>-CH_2-, Z-IPDI) , 4.77 (1H, m, C<u>H</u>-OCO-), 4.54 (1H, broad signal, CO-N<u>H</u>-CH_2-), 4.00 (2H, t, -C<u>H</u>$_2$-OCO), 3.77 (1H, m, -C<u>H</u> ring), 3.23 (2H, d, -C<u>H</u>$_2$-NH-, E-IPDI)), 2.90 (2H, d,-C<u>H</u>$_2$-NH-, Z-IPDI), 2.52 (4H, q, C<u>H</u>$_2$-CH_3), 2.52 (1H, dd, N-C<u>H</u>$_2$-CH), 2.42 (1H, dd, N-C<u>H</u>$_2$-CH) and 1.71-0.86 (24H, -(C<u>H</u>$_2$)$_n$-C<u>H</u>$_3$).

^{13}C NMR ($CDCl_3$, δ ppm): 157.23 (s), 155.41 (s), 65.33 (t), 64.89 (t), 62.56 (t), 58.77 (t), 58.74 (t), 46.71 (t), 45.43 (t), 42.32 (s), 36.44 (t), 35.06 (q), 33,02 (t), 32.68 (d), 31.75 (t), 31.69 (t), 31.43 (t), 29.37 (t), 29.17 (t), 27.57 (t), 25.72 (t), 25.20 (s), 23.21 (s), 20.14 (t), 12.09 (q).

Synthesis of polyurethane from HDI for acid-base modication (PU1 and PU2)

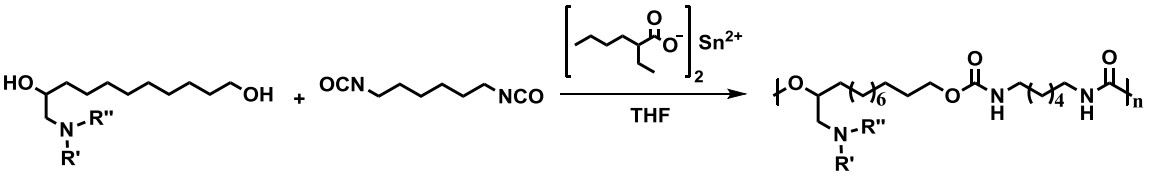

D1 : R = -$CH_2CH=CH_2$; R' = -CH_3
D4 : R = R' = -CH_2CH_3

PU1 : R = -$CH_2CH=CH_2$; R' = -CH_3
PU2 : R = R' = -CH_2CH_3

D1 or D4 (1.84 mmol) and tin (II) ethyl hexanoate (6 µL, 0.02 mmol) was placed in a 10 mL round-bottom flask equipped with a Teflon coated stirring bar and closed by septum. To the mixture were applied 6 cycles of vacuum/argon. Dried THF (2 mL) was injected into the flask and the solution was stirred and heated at 60°C for 20 minutes. HDI (0.3 mL, 1.84 mmol) was injected and the reaction mixture was left for 4 h.

PU1. Yield 96%

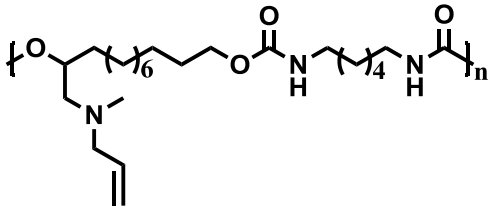

^{1}H NMR ($CDCl_3$, TMS, δ ppm): 5.81 (1H, m, CH_2=C<u>H</u>-), 5.13 (2H, m, C<u>H_2</u>=CH-), 4.84 (1H, m, C<u>H</u>-OCO-), 4.79 (2H, broad signal, CO-N<u>H</u>-CH_2-), 4.01 (2H, t, -C<u>H_2</u>-OCO), 3.13(2H, d, -C<u>H_2</u>-NH-), 3.03 (2H, d, C<u>H_2</u>-CH=CH_2), 2.52 (1H, m, N-C<u>H_2</u>-CH), 2.38 (1H, m, N-C<u>H_2</u>-CH), 2,26 (3H, s, -N-C<u>H_3</u>) and 1.66-1.18 (22H, -(C<u>H_2</u>)$_n$-).

^{13}C NMR ($CDCl_3$, δ ppm): 157.19 (s), 155.70 (s), 135.85 (d), 117.31 (t), 64.89 (t), 56.51 (t), 47.68 (t), 40.75 (t), 29.93 (t), 29.57 (d), 29.47 (t), 29.22 (t), 29.10 (t), 26.29 (t), 25.84 (t), 25.39 (t) and 23.21 (s).

PU2. Yield 96%

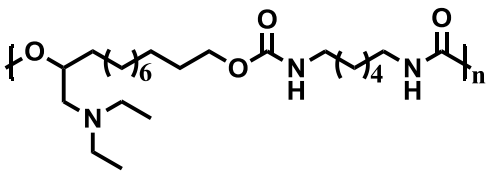

^{1}H NMR ($CDCl_3$, TMS, δ ppm): 4.78 (2H, broad signal, CO-N<u>H</u>-CH_2-) , 4.81 (1H, m, C<u>H</u>-OCO-), 4.00 (2H, t, -C<u>H_2</u>-OCO), 3.13(2H, d, -C<u>H_2</u>-NH-), 2.53 (1H, dd, N-C<u>H_2</u>-CH), 2.53 (4H, q, N-C<u>H_2</u>-CH_3) 2.42 (1H, dd, N-C<u>H_2</u>-CH), 1.58-0.25 (22H, -(C<u>H_2</u>)$_n$) and 0.96 (6H, t, N-CH_2-C<u>H_3</u>).

^{13}C NMR ($CDCl_3$, δ ppm): 156.60 (s), 72.82 (d), 64.87 (t), 56.52 (t), 47.69 (t), 40.74 (t), 29.94 (t), 29.57 (d), 29.46 (t), 29.25 (t), 29.05 (t), 26.31 (t), 25.85 (t), 25.39 (t) and 11.83 (q).

7.2.3. Polyurethane modification

Chapter 1: Synthesis of hydrophilic polyurethanes (PUD1-2OH, PUD2-4OH and PUD3-6OH)

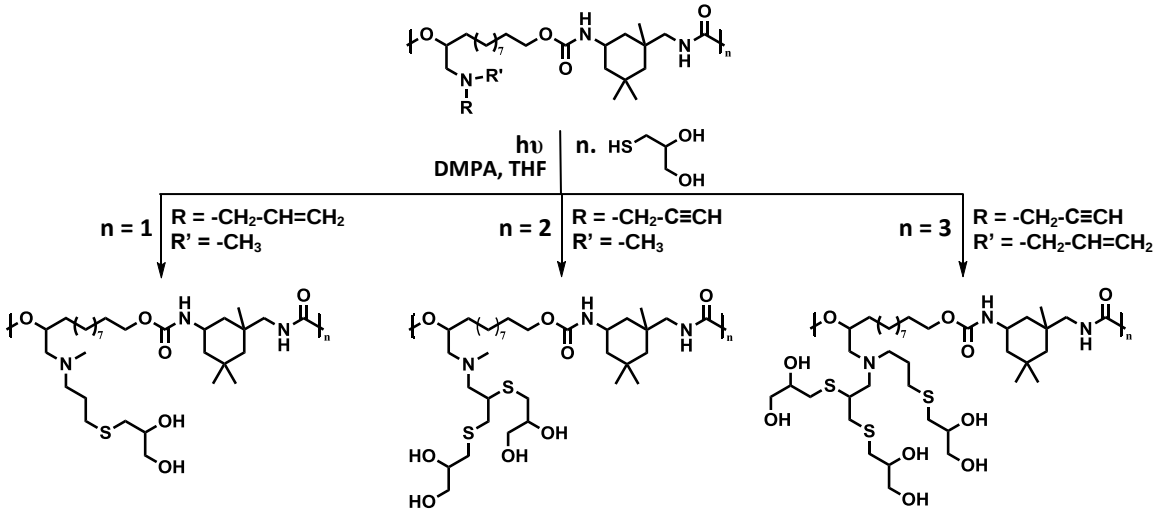

PUD1-3 (1 mmol) and 5% (w/w) DMPA was added to a 10mL round-bottom flask with a Teflon coated stirring bar and was closed by septum. The mixture was degassed six times and was purged with argon through a needle using a vacuum/argon line and using a syringe, 2mL of anhydrous THF and the appropriate amounts of thioglycerol (2 mmol for PUD1, 4 mmol for PUD2 and 6 mmol for PUD3) were added, and the components were dissolved. The reaction was stirred at room temperature under UV irradiation (365 nm) for 2 hours and the polymer was precipitated into cold water and

was washed with water three times. The polymer was dried under vacuum at 60°C during 24 hours.

Chapter 2: Synthesis of ionic biurethane (BIU)

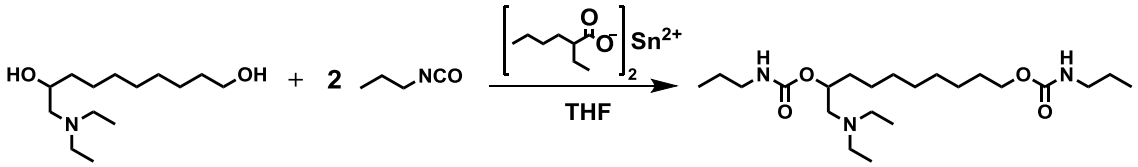

D4 (0.87 g, 2.10 mmol) and tin (II) ethyl hexanoate (6 µL, 0.02 mmol) was placed in a 10 mL round-bottom flask equipped with a Teflon coated stirring bar and closed by septum. To the mixture were applied 6 cycles of vacuum/argon. Dried THF (2 mL) was injected into the flask and the solution was stirred and heated at 60°C for 20 minutes. Propyl isocianate (0.2 mL, 2.1 mmol) was injected and the reaction mixture was left for 4 h. The resulting oil was purified by column chromatography using silicagel and hexane/ethyl acetate 1/1 as eluent. Yield 92%.

^{1}H NMR ($CDCl_3$, TMS, δ ppm): 4.77 (1H, broad signal, CO-N<u>H</u>-CH_2-), 4.69 (1H, m, C<u>H</u>-OCO-), 4.65 (1H, broad signal, CO-N<u>H</u>-CH_2-), 4.01 (2H, t, -C<u>H</u>$_2$-OCO), 3.16 (2H, d, -C<u>H</u>$_2$-NH-), 2.51 (4H, q, N-C<u>H</u>$_2$-CH_3), 2.51 (1H, dd, N-C<u>H</u>$_2$-CH), 2.41 (1H, dd, N-C<u>H</u>$_2$-CH), 1.68-1.16 (18H, -(C<u>H</u>$_2$)$_n$), 0.98 (6H, t, N-CH_2-C<u>H</u>$_3$) and 0.90 (6H, t, CH_2-CH_2-C<u>H</u>$_3$).

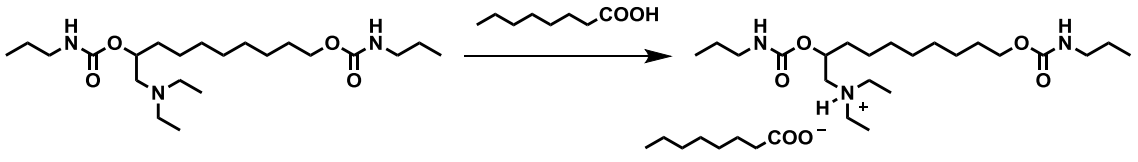

BIU (1g, 2,4 mmol) was mixed with octanoic acid (0.35 g, 2.4 mmol) at room temperature for 2h. The solvent was removed with vacuum at room temperature.

^{1}H NMR ($CDCl_3$, TMS, δ ppm): 8.63 (1H, broad signal, $^+$N-H), 4.87 (1H, m, CH-OCO-), 4.64 (2H, broad signal, CO-NH-CH_2-), 4.02 (2H, t, -CH_2-OCO), 3.17 (2H, d, -CH_2-NH-), 2.80-2.60 (6H, N-CH_2-CH and N-CH_2-CH_3), 2.26 (2H, t, -CH_2-COO^-), 1.67-1.17 (28H, -$(CH_2)_n$), 1.06 (6H, t, N-CH_2-CH_3) and 0.95-0.80 (9H, t, CH_2-CH_2-CH_3).

Chapter 2 and chapter 3: Synthesis of ionic polyurethanes (SIPU1, SIPU2, SIPU3, SIPU4, SPUN1, SPUN2, SPUN3, SPUN4 and SPUN5)

The reaction was stoped with MeOH (0.02 mL) at room temperature for 1h. Di or tricarboxylic acid were added (9.2 mmol for diacid and 6.1 mmol for citric acid). The mixture was left for 2h. The solution was extracted with syringe and in Teflon plate was put. The polymer was dried under vacuum at 40°C for 24h.

SIPUs

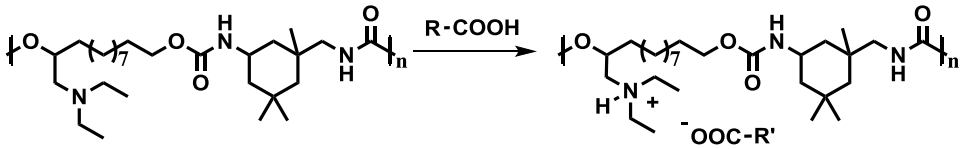

SIPU1 : R' = -$(CH_2)_6$-CH_3
SIPU2 : R' = -$(CH_2)_8$-COO^-
SIPU3 : R' = -$(CH_2)_4$-COO^-

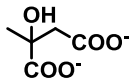

SIPU1

^{1}H NMR ($CDCl_3$, TMS, δ ppm): 4.82 (1H, broad signal, CO-NH-CH_2-, Z-IPDI) , 4.77 (1H, m, CH-OCO-), 4.54 (1H, broad signal, CO-NH-CH_2-), 4.00 (2H, t, -CH_2-OCO), 3.77 (1H, m, -CH ring), 3.23 (2H, d, -CH_2-NH-, E-IPDI)), 2.90 (2H, d,-CH_2-NH-, Z-IPDI), 2.75 (4H, q, CH_2-CH_3), 2.81 (1H, dd, N-CH_2-CH), 2.63 (1H, dd, N-CH_2-CH) and 1.71-0.86 (24H, -$(CH_2)_n$-CH_3).

SIPU2

^{1}H NMR ($CDCl_3$, TMS, δ ppm): 4.82 (1H, broad signal, CO-NH-CH_2-, Z-IPDI) , 4.77 (1H, m, CH-OCO-), 4.54 (1H, broad signal, CO-NH-CH_2-), 4.00 (2H, t, -CH_2-OCO), 3.77 (1H, m, -CH ring), 3.23 (2H, d, -CH_2-NH-, E-IPDI)), 2.90 (2H, d,-CH_2-NH-, Z-IPDI), 2.73 (4H, q, CH_2-

CH_3), 2.75 (1H, dd, N-C$\underline{H}_2$-CH), 2.62 (1H, dd, N-C$\underline{H}_2$-CH) and 1.71-0.86 (24H, -(C$\underline{H}_2$)$_n$-C$\underline{H}_3$).

SIPU3

^{1}H NMR ($CDCl_3$, TMS, δ ppm): 4.82 (1H, broad signal, CO-N$\underline{H}$-CH_2-, Z-IPDI) , 4.77 (1H, m, C$\underline{H}$-OCO-), 4.54 (1H, broad signal, CO-N$\underline{H}$-CH_2-), 4.00 (2H, t, -C$\underline{H}_2$-OCO), 3.77 (1H, m, -C$\underline{H}$ ring), 3.23 (2H, d, -C$\underline{H}_2$-NH-, E-IPDI)), 2.90 (2H, d,-C$\underline{H}_2$-NH-, Z-IPDI), 2.82 (4H, q, C$\underline{H}_2$-CH_3), 2.85 (1H, dd, N-C$\underline{H}_2$-CH), 2.68 (1H, dd, N-C$\underline{H}_2$-CH) and 1.71-0.86 (24H, -(C$\underline{H}_2$)$_n$-C$\underline{H}_3$).

SIPU4

^{1}H NMR ($CDCl_3$, TMS, δ ppm): 4.82 (1H, broad signal, CO-N$\underline{H}$-CH_2-, Z-IPDI) , 4.77 (1H, m, C$\underline{H}$-OCO-), 4.54 (1H, broad signal, CO-N$\underline{H}$-CH_2-), 4.00 (2H, t, -C$\underline{H}_2$-OCO), 3.77 (1H, m, -C$\underline{H}$ ring), 3.23 (2H, d, -C$\underline{H}_2$-NH-, E-IPDI)), 2.90 (2H, d,-C$\underline{H}_2$-NH-, Z-IPDI), 2.75 (4H, q, C$\underline{H}_2$-CH_3), 2.82 (1H, dd, N-C$\underline{H}_2$-CH), 2.65 (1H, dd, N-C$\underline{H}_2$-CH) and 1.71-0.86 (24H, -(C$\underline{H}_2$)$_n$-C$\underline{H}_3$).

SPUNs

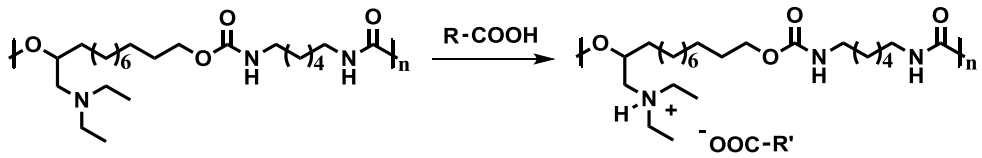

SPUN1 : R' = -$(CH_2)_8$-COO^-
SPUN2 : R' = -$(CH_2)_4$-COO^-
SPUN3 : R' = -$(CH_2)_2$-COO^-
SPUN4 : R' = 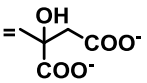
SPUN5 : R' = -COO^-

SPUN1

^{1}H NMR ($CDCl_3$, TMS, δ ppm): 6.59 (1H, broad signal, $^+$N-$\underline{H}$), 5.02 (2H, broad signal, CO-N$\underline{H}$-CH_2-) , 4.82 (1H, m, C$\underline{H}$-OCO-), 4.01 (2H, t, -C$\underline{H}_2$-OCO), 3.12(2H, d, -C$\underline{H}_2$-NH-),

2.85-2.39 (6H, N-C<u>H</u>$_2$-CH and N-C<u>H</u>$_2$-CH$_3$), 2.21 (2H, t, -CH$_2$-COO$^-$), 1.58-0.25 (24H, -(C<u>H</u>$_2$)$_n$) and 1,04 (6H, t, N-CH$_2$-C<u>H</u>$_3$).

SPUN2

^{1}H NMR (CDCl$_3$, TMS, δ ppm): 6.59 (1H, broad signal, $^+$N-<u>H</u>), 5.12 (2H, broad signal, CO-N<u>H</u>-CH$_2$-) , 4.84 (1H, m, C<u>H</u>-OCO-), 4.01 (2H, t, -C<u>H</u>$_2$-OCO), 3.13(2H, d, -C<u>H</u>$_2$-NH-), 2.85-2.39 (6H, N-C<u>H</u>$_2$-CH and N-C<u>H</u>$_2$-CH$_3$), 2.25 (2H, t, -CH$_2$-COO$^-$), 1.58-0.25 (24H, -(C<u>H</u>$_2$)$_n$) and 0.96 (6H, t, N-CH$_2$-C<u>H</u>$_3$).

SPUN3

^{1}H NMR (CDCl$_3$, TMS, δ ppm): 6.61 (1H, broad signal, $^+$N-<u>H</u>), 5.01 (2H, broad signal, CO-N<u>H</u>-CH$_2$-) , 4.89 (1H, m, C<u>H</u>-OCO-), 4.01 (2H, t, -C<u>H</u>$_2$-OCO), 3.12(2H, d, -C<u>H</u>$_2$-NH-), 2.80-2.61 (6H, N-C<u>H</u>$_2$-CH and N-C<u>H</u>$_2$-CH$_3$), 2.54 (2H, s, -CH$_2$-COO$^-$), 1.58-0.25 (24H, -(C<u>H</u>$_2$)$_n$) and 1,05 (6H, t, N-CH$_2$-C<u>H</u>$_3$).

SPUN4

^{1}H NMR (CDCl$_3$, TMS, δ ppm): 6.59 (1H, broad signal, $^+$N-<u>H</u>), 5.02 (2H, broad signal, CO-N<u>H</u>-CH$_2$-) , 4.82 (1H, m, C<u>H</u>-OCO-), 4.01 (2H, t, -C<u>H</u>$_2$-OCO), 3.12(2H, d, -C<u>H</u>$_2$-NH-), 2.85-2.39 (6H, N-C<u>H</u>$_2$-CH and N-C<u>H</u>$_2$-CH$_3$), 2.21 (2H, t, -CH$_2$-COO$^-$), 1.58-0.25 (24H, -(C<u>H</u>$_2$)$_n$) and 1,04 (6H, t, N-CH$_2$-C<u>H</u>$_3$).

SPUN5

^{1}H NMR (CDCl$_3$, TMS, δ ppm): 6.56 (1H, broad signal, $^+$N-<u>H</u>), 5.93 (2H, broad signal, CO-N<u>H</u>-CH$_2$-) , 4.85 (1H, m, C<u>H</u>-OCO-), 4.01 (2H, t, -C<u>H</u>$_2$-OCO), 3.12(2H, d, -C<u>H</u>$_2$-NH-), 2.90-2.49 (6H, N-C<u>H</u>$_2$-CH and N-C<u>H</u>$_2$-CH$_3$), 2.21 (2H, t, -CH$_2$-COO$^-$), 1.58-0.25 (24H, -(C<u>H</u>$_2$)$_n$) and 1,04 (6H, t, N-CH$_2$-C<u>H</u>$_3$).

Chapter 3: Synthesis of covalent polyurethane networks (CPU)

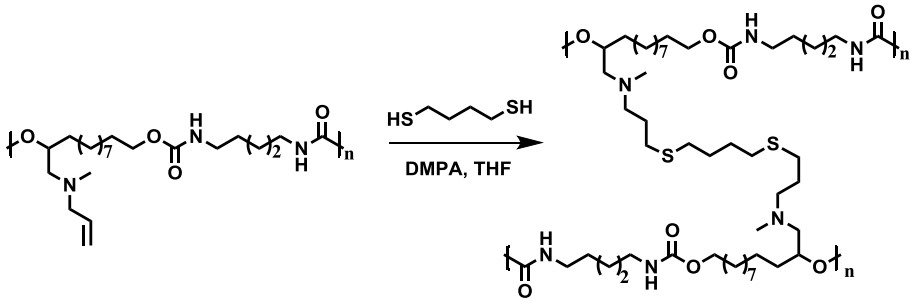

The reaction of PU1 was stoped with MeOH (0.02 mL) at room temperature for 1h. DMPA 1% (w/w) respect the diol weight and 1,4-butadithiol (0,21 mL, 1,84 mmol) were added. The solution stirred at room temperature for 1 hour. The THF was dried by solution casting method at room temperature during 12 hours in dark conditions. The film was reacted under UV irradiation (365 nm) for 1.5 hours. Film was dried at 40 °C during 24h.

Chapter 4: Synthesis of covalent/ionic polyurethanes networks (ICPUN)

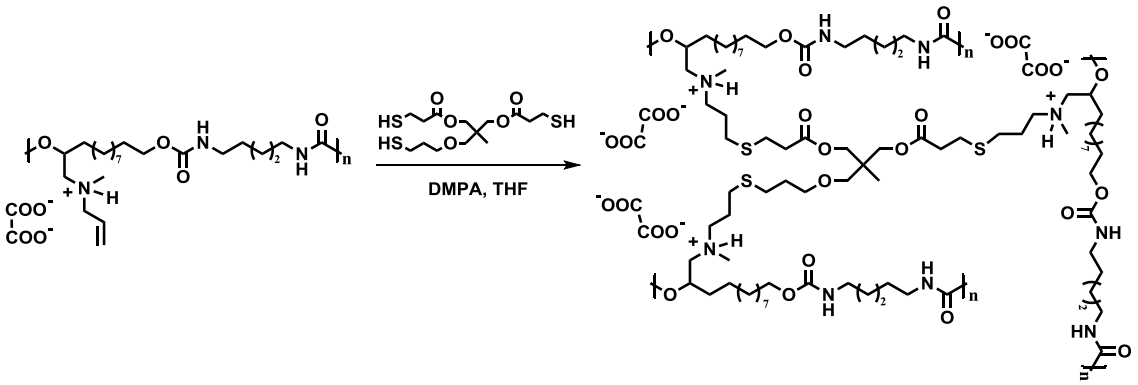

PU1 was mixed in THF solution with DMPA 1% (w/w) respects the diol weight and different molar percentage: 7, 15, 30 and 60% of TMMP were added. The solution stirred at room temperature for 1 hour. The THF was dried by solution casting method on a Petri dish at room temperature during 48 hours in dark conditions. The film was reacted under UV irradiation (365 nm) for 2.5 hours and dried at 40 °C during 24h.

7.3. Instrumentation

Nuclear Magnetic Ressonance (NMR) analysis

^{1}H NMR (400 MHz) and ^{13}C NMR (100.6 MHz) spectra were recorded using a Varian Gemini 400 spectrometer. Spectra were recorded at room temperature using 15-25 mg of sample, in $CDCl_3$ or CD_3OD as solvent. Chemical shifts were reported in ppm relative to TMS as internal standards.

Fourier Transform Infrared Spectroscopy (FT-IR)

FTIR spectra were recorded on a Bomem Michelson MB 100 FTIR spectrophotometer with a resolution of 4 cm^{-1} in the absorbance mode. An attenuated total reflection (ATR) device with thermal control and a diamond crystal (Golden Gate heated single-reflection diamond ATR, Specac-Tknokroma) was used.

Raman spectroscopy

Raman spectra were recorded on a RENISHAW-INVIA spectrometer. A laser of wavelength 785 nm line filtered at 10% of its nominal power was used. Each spectrum was obtained by accumulation of two spectra recorded from 800 to 3200 cm^{-1} over 120 s.

Size Exclusion Chromatography (SEC)

Size exclusion chromatography (SEC) analysis in DMF with 0.025 M of LiCl was carried out with an Agilent 1200 series system equipped with three serial columns (PLgel 3µm MIXED-E, PLgel 5µm MIXED-D and PLgel 5µm MIXED-C from Polymer Laboratories) and an Shimatzu RID-6A refractive-index detector working at 60 °C at a flow rate of 1.0 mL/min. The calibration curves for SEC analysis were obtained with polystyrene (PS) standards.

Differential Scanning Calorimetry (DSC)

Calorimetric studies were carried out on a Mettler DSC821 differential scanning calorimeter. Samples were accurately weighed (5.5 ± 0.5 mg) and sealed in hermetic aluminium pans. Dry nitrogen gas was purged into the DSC cell at a flow rate of 100 mL/min. DSC analysis was carried out in three cycles two of heating and one of cooling from -50°C to 100°C, from 100°C to -50°C and finally from -50°C to 100°C at scanning rate of 10°C/min.

Thermogravimetric Analysis (TGA)

Thermal stability studies were carried out on a Mettler TGA/SDTA851e/LF/1100 with N2 as purge gas at a flow rate of 100 mL/min. The studies were performed in the 30–600°C temperature range at a scan rate of 10°C/min. Samples of 10 ± 0.5 mg in a ceramic pans were used.

Dinamomechanical and thermal Analysis (DMTA)

Mechanical properties were measured using a dynamic mechanical thermal analysis (DMTA) apparatus TA DMA 2928 in the controlled force-tension Film mode. The tensile essays were performed on rectangular films (20 x 5 x 0.5 mm^3) measuring the strain while applying a ramp of 3N/min at 20-150°C. Preload forces of 0.01 N and soak time of 5 min were used.

Shape memory behavior testing the temperature-induced shape-memory behaviors were determined with cyclic thermo-mechanical analysis in accordance with. All samples were dried at 100°C in vacuo for 24h and cut in rectangular pieces of approximately 10mm×5.0mm×0.5mm. The test setups:

1) For dual-shape-memory cycles: (1) heating to T_g+20-25°C (based on DMA) and equilibrated for 20 min; (2) uniaxially stretching to strain (ε_{load}) by ramping force from 0.001 N to 0.1 or 0.4 N at a rate of 0.05 or 0.2 N/min respectively; (3) fixing the strain (ε) by quickly cooling to T_g-20-25°C with a rate of -5°C/min, followed by equilibration for 20 min; (4) unloading external force 0N at a rate of 0.05 or 0.2 N/min; (5) reheating to Tg+20-25°C at a rate of 5°C/min and followed by equilibration for 20min; the recovery strain (ε_{rec}) is finally recorded.

2) For triple-shape-memory cycles: (1) heating to ca. Tg+25°C (based on DMA) and equilibrated for 20 min; (2) uniaxially stretching by ramping force from 0.001 N to 0.3 N at a rate of 0.15 N/min; (3) fixing the strain by quickly cooling to Tg-10 °C with q=-10°C/min, followed by equilibration for 20 min; (4) unloading external force 0N at a rate of 0.15 N/min, followed by equilibration for 8 min; (5) uniaxially stretching by ramping force from 0.001 N to 1.5 N at a rate of 0.25 N/min; (6) further fixing the strain by quickly cooling to Tg-30°C with with a rate of =-5 °C/min, followed by equilibration for 20 min; (7) unloading external force 0N at a rate of 0.25 N/min; (8) reheating to T_g-10°C at a rate of 5 °C/min and followed by equilibration for 20 min; (9) reheating to ca. Tg+20°C at a rate of 5°C/min and followed by equilibration for 20min.

Calculations of shape memory behaviors For dual-shape memory effect, the shape fixity (R_{fix}) and shape recovery (R_{rec}) were calculated using equations (1) and (2) below:

$$R_{fix} = \frac{\varepsilon}{\varepsilon_{load}} \times 100 \quad (1)$$

$$R_{rec} = \frac{(\varepsilon - \varepsilon_{rec})}{\varepsilon} \times 100 \quad (2)$$

Where ε_{load} represents the maximum strain under load, ε is the fixed strain after cooling and load removal, and ε_{rec} is the strain after recovery. Equations (1) and (2) are expanded to equations (3) and (4) to calculate R_{fix} and R_{rec} for triple-shape memory effect.

$$R_{fix}(X \rightarrow Y) = \frac{(\varepsilon_y - \varepsilon_x)}{(\varepsilon_{y,\ load} - \varepsilon_x)} \times 100 \quad (3)$$

$$R_{rec}(Y \rightarrow X) = \frac{(\varepsilon_y - \varepsilon_{x,\ rec})}{(\varepsilon_y - \varepsilon_x)} \times 100 \quad (4)$$

Where X and Y denote two different shapes, respectively, $\varepsilon_{y,\ load}$ represents the maximum strain under load, ε_y and ε_x are fixed strain after cooling and load removal, and $\varepsilon_{y,\ rec}$ is the strain after recovery.

Rheological analysis

Small amplitude oscillatory flow experiments were carried out on a Thermo-Haake Rheostress I viscoelastometer, using a parallel plate geometry. The testing protocol consisted of temperature sweeps to determine G' and G'' on heating cycles at an angular frequency of 6.28 rad/s and temperature intervals defined for each sample. Cooling cycles were also carried out, to test the reversibility of the rheological process. The temperature ramp rate was 5 °C/min. Angular frequency sweeps were also performed at constant strain amplitude in isothermal experiments at the temperatures reflected in the text. The strain value was selected when that both moduli G and G" were obtained in the linear viscoelastic regime.

The electrical conductivity was determined using the Dielectric Analysis option (DETA) of the ARES Rheometer (TA Instruments) coupled to an Agilent E4980 Bridge (Agilent). Electrodes were 20 mm diameter stainless steel plates and the measurements were performed on samples of 1 mm thickness. Temperature sweeps were carried out in the temperature range from 0 °C to 130 °C using a voltage of 1 V. Test were performed using frequency at 6,28 rad/s. Dielectric data were recorded as a function of the frequency *(ν)*. The real part of the conductivity, *σ' (ν)* is calculated from the imaginary part of the dielectric constant *ε''(ν)* through the relation using equation (5) :

$$\sigma'(\upsilon) = 2\pi\upsilon\varepsilon_0\varepsilon''(\upsilon) \quad (5)$$

Where ε_0=8.8510-12 F/m is de vacuum permittivity. The variation of the conductivity with frequency is described by the Universal Dynamic response. The dielectric conductivity value calculated from the frequency independent conductivity associated to the low frequency regime accounts for the ionic conductivity.

Mechanical Analysis

Tensile tests were performed with an Instron dynamometer (model 5942, USA) on specimen of 45 x 5 x 2 mm^3 length. Distance between the rips of about 30 mm at a crosshead rate of 10 or 100 mm/min and at room temperature.

Specimens for self-healing tests were prepared following two steps. In the first step the measured specimen was cut into two parts at the middle. In the second step the two parts were recombined into a Teflon mould and were remained for different times at room temperature. The self-healing efficiency was calculated using equation (6) as:

$$\eta_{SH} = \frac{U_T^{healed}}{U_T^{virgin}} \times 100 \qquad (6)$$

Where, U_T = area underneath the stress–strain (σ–ε) curve = $\sigma \times \varepsilon$.

Specimens for recycling tests were obtained from used specimen who was cut in different parts and then the parts were put into Teflon mould under pressure at 40°C for 2h. The obtained specimen was analysed following the mentioned tensile method.

The loading-unloading tests were carried out at a loading and unloading rate of 100 mm/min. The final of loading test was fixed with different strains and the final of unloading test was selected when the stress was near 0 MPa. The hysteresis energy, ΔU_i , in the ith loading–unloading cycle is defined by equation (6) as:

$$\Delta U_i = \oint \sigma \, d\varepsilon \qquad (7)$$

where σ is stress, and ε is strain. The energy loss coefficient, η, measures how efficiently a material dissipates energy and is calculated with equation (8) as:

$$\eta = \frac{\Delta U_i}{U_i} \qquad U_i = \int_0^{\sigma_{max}} \sigma \, d\varepsilon \qquad (8)$$

where U_i is the elastic energy stored in the materials when it is loaded elastically to a stress σmax in the ith cycle.

Environmental Scanning Electron Microscopy (ESEM)

Environmental scanning electron microscopy (ESEM) images were obtained with a FEI QUANTA 600 instrument using an accelerating potential of 10 KV.

Contact Angle

The contact angle of deionised water against polymer surfaces was measured by the water drop method (3μL) at 25°C, using the OCA15EC contact angle setup (Neurtek Instruments).

Chapter 8

Conclusions

UNIVERSITAT ROVIRA I VIRGILI
AVANCES EN SISTEMAS INTERACTIVOS PARA PERSONAS CON PARÁLISIS CEREBRAL
Marc Comí Bonachí

In this Thesis has been demonstrated that fatty acids derived from castor oil are efficient raw materials for the preparation of side-chain functionalized polyurethanes (PU)s with improved properties. Moreover, the use of click chemistry thiol-ene/yne coupling and acid-base reactions were successful methodologies to modify these functionalized PUs with a wide range of compositions and displaying diverse behaviour.

The conclusions of this research are summarized as follows:

- Ring-opening reaction of fatty acid-derived epoxide with secondary amines allows the straightforward preparation of tertiary amine-, alkene- and/or alkyne-containing diols.
- The polymerization of functional diols with isophorone diisocyanate or hexamethylene diisocyanate leads to allyl- and propargyl- functionalized PUs.
- Photoinitiated thiol-ene/yne coupling reaction is an efficient process to post-polymerization modification of alkene/yne side-chain PUs with thioglycerol to obtain PUs with enhanced hydrophilicity.
- Acid-base reaction is a simple approach to synthesize supramolecular PUs by interaction between tertiary amino-side chain PU and carboxylic acids.
- Supramolecular PUs have been characterized to determine their chemical structure and their thermal and mechanical properties, concluding that supramolecular PUs exhibit tuneable properties depending on the acid functionality and the chain length of carboxylic acid.
- Supramolecular PUs networks display good energy dissipation mechanism, shape-regeneration property, recycling/reshaping capability and inherent self-healing ability , which can be seen as upgrade of their sustainability
- The combination of covalent and non-covalent approaches leads to dually cross-linked networks. These materials exhibit different thermal and mechanical properties depending on the covalent cross-link content. Moreover, these materials present effective shape-memory properties.

Appendix A: List of abbreviations

ADMET	Acyclic diene metathesis polymerization
ATR	Attenuated total reflection
BDT	1,4-butandithiol
$CDCl_3$	Deuterated chloroform
DMF	N,N'-dimethylformamide
DMSO	Dimethyl sulfoxide
DMPA	2,2-dimethoxy-2-phenylacetophenone
DMTA	Dynamic mechanical thermal analysis
DSC	Differential scanning calorimetry
ΔU_i	Hysteresis energy
E'	Storage modulus
E''	Loss Modulus
ε	Strain
ε_{load}	Maximun strain under load
ε_{rec}	Recovery strain
ESEM	Environmental scanning electron microscopy
FTIR	Fourier transform infrared spectroscopy
G'	Elastic moduli
G''	Viscous moduli
GPC	Gel permeation chromatography
HDI	Hexamethylene diisocyanate
HSQC	Heteronuclear single quantum coherence spectroscopy
ICPUN	Ionic-covalent polyurethane network
IPDI	Isophorone diisocyanate
MDEA	Methyldiethanolamine

MDI	4,4'-Methylenebis(phenyl isocyanate)
M_n	Number average molecular weight
M_w	Weight average molecular weight
NMR	Nuclear magnetic resonance
PU	Polyurethane
R_{fix}	Shape fixity
ROMP	Ring-opening metathesis polymerization
R_{rec}	Shape recovery
SEC	Size exclusion chromatography
SIPU	Supramolecular ionic polyurethane
SME	Shape memory effect
SPUN	Supramolecular polyurethane network
$T_{5\%}$	Temperature of 5% weight loss
TDI	Toluene diisocyanate
TG	Thioglycerol
T_g	Glass transition temperature
TGA	Therogravimetric analysis
THF	Tetrahydrofuran
T_{max}	Temperature of maximum weight loss
TMMP	Trimethylolpropane tris(3-mercaptopropionate)
TMS	Tetramethylsilane
T_{nl}	Network-liquid transition temperature
TPU	Thermoplastic polyurethane
U_T	Area underneath the stress-strain curve

Appendix B: List of Publications

Title: Synthesis of castor-oil based polyurethanes bearing alkene/alkyne groups and subsequent thiol-ene/yne post-modification.

Authors: M. Comí, G. Lligadas, J. C. Ronda, M. Galià, V. Cádiz.

Ref.: Polymer, 2016, 103, 163-170.

Title: Carboxylic acid ionic modification of castor-oil based polyurethanes bearing amine groups. Correlation between chemical structure and physical properties.

Authors: M. Comí, M. Fernandez, A. Santamaria, G. Lligadas, J. C. Ronda, M. Galià, V. Cádiz.

Ref.: Polymer 2017. Under revisión.

Title: Post-synthetic non-covalent crosslinked polyurethanes as self-healing elastomers from renewable resources.

Authors: M. Comí, G. Lligadas, J. C. Ronda, M. Galià, V. Cádiz.

Ref.: Submited to European Polymer Journal

Title: Biobased polyurethanes wit shape-memory properties through covalent and non-covalent aproaches.

Authors: M. Comí, G. Lligadas, J. C. Ronda, M. Galià, V. Cádiz.

Ref.: To be submitted

Appendix C: Meeting contributions

Authors: M. Comí, G. Lligadas, J. C. Ronda, M. Galià, V. Cádiz.

Poster presentation: Functional Polyurethanes with Modulable Properties from Vegetable Oils Derivates

XIII Reunión del Grupo Especializado en Polímeros (GEP), Girona (Spain), 7-10 September, 2014.

Authors: M. Comí, M. Fernandez, G. Lligadas, J. C. Ronda, M. Galià, V. Cádiz.

Poster presentation: Functional Polyurethanes from Vegetable Oils Derivates with Modulable Properties.

Fourth International Symposium FronTiers in Polymers Science, Riva de Garda (Italy), 11-14 May, 2015

Authors: M. Comí, G. Lligadas, J. C. Ronda, M. Galià, V. Cádiz.

Poster send: Castor Oil-Derived Polyurethanes Engineered by Dynamic Crosslinks for Self-Healing

46th IUPAC World Polymer Congress (MACRO), Istambul (Turkey), 17-20 July, 2016.

Authors: M. Comí, G. Lligadas, J. C. Ronda, M. Galià, V. Cádiz.

Poster presentation: Castor Oil-Based Polyurethanes with Allyl and Propargyl Side Groups and Subsequent Thiol-Ene/Yne Post-Modification

XIV Reunión del Grupo Especializado en Polímeros (GEP), Burgos (Spain), 5-8 September, 2016.

Authors: M. Comí, G. Lligadas, J. C. Ronda, M. Galià, V. Cádiz.

Oral Communication: Castor Oil-Derived Polyurethanes Engineered by Dynamic Crosslinks for Self-Healing

XIV Reunión del Grupo Especializado en Polímeros (GEP), Burgos (Spain), 5-8 September, 2016.